

Westinghouse Non-Proprietary Class 3

WCAP-7832-A



**EVALUATION OF STEAM
GENERATOR TUBE,
TUBE SHEET AND DIVIDER
PLATE UNDER COMBINED
LOCA PLUS
SSE CONDITIONS**

Westinghouse Electric Company LLC



EVALUATION OF STEAM
GENERATOR TUBE, TUBE SHEET
AND DIVIDER PLATE UNDER COMBINED
LOCA PLUS SSE CONDITIONS

APRIL 1978

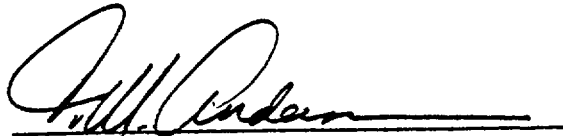
P. De Rosa

W. Rinne

H. W. Massie, Jr.

P. Mitchell

APPROVED:


T. M. Anderson, Manager
Nuclear Safety Department

© 1978 Westinghouse Electric Corp.

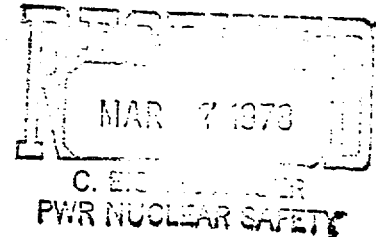
Westinghouse Electric Corporation
PWR Systems Division
P. O. Box 355
Pittsburgh, Pennsylvania 15230



UNITED STATES
NUCLEAR REGULATORY COMMISSION
WASHINGTON, D. C. 20555

MAR 2 1978

Mr. C. Eicheldinger, Manager
Nuclear Safety Department
Westinghouse Electric Corporation
P. O. Box 355
Pittsburgh, Pennsylvania 15230



Dear Mr. Eicheldinger:

SUBJECT: SAFETY EVALUATION OF WCAP-7832

The Nuclear Regulatory Commission staff has completed its review of Westinghouse Electric Corporation report WCAP-7832 entitled "Evaluation of Steam Generator Tube, Tube Sheet, and Divider Plate Under Combined LOCA Plus SSE Condition." Our safety evaluation is enclosed.

As a result of our review we have concluded that for the Model D and Series 51 Westinghouse steam generators, the maximum stresses in new tube bundles, tube sheets and divider plates for combined seismic and LOCA loads (except pipe ruptures in steam generator compartments) are less than limiting stresses in ASME Boiler and Pressure Vessel Code, Section III, Appendix F, and are therefore acceptable. The exclusion of loads caused by reactor coolant pipe rupture in steam generator compartments must be justified in individual applications. We have also concluded that service-exposed tubes containing defects caused by localized corrosion near the tube sheet will maintain their integrity during combined seismic and LOCA loading provided the remaining wall thickness for tubes thinned by wastage is at least 72% of the original nominal wall thickness and the length of through-wall cracks is less than the critical crack length. In Model D steam generators, the critical crack length is 0.64 inches for tubes with nominal wall thickness and 0.38 inches for tubes with 72% of the nominal wall thickness when subjected to maximum expected pressure differential of 1485 psi. The acceptability of larger defects or other types of defects in service-exposed steam generators, such as denting in tubes, wastage and cracks at support plates, and cracks in tube U-bends must be determined by further analyses or experiments within the guidelines of Regulatory Guide 1.121, "Bases for Plugging Degraded Steam Generator Tubes."

The use of the BLODWN-2 computer code for obtaining the primary side pressure response in the steam generator was reviewed. The BLODWN-2 code is acceptable for this use provided (1) the code is modified to use the correct sonic velocity and the correct radial transport distance in the pressure vessel lower plenum, and (2) a break opening time of 1 millisecond is used.

MAR 2 1978

Mr. C. Eicheldinger, Manager

-2-

Accordingly, WCAP-7832 is acceptable for referencing to support the above conclusions. We do not intend to repeat our review of WCAP-7832 when it appears as a reference in a particular license application except to assure that the steam generator design and tube defects are similar to those described in this report.

In accordance with established procedure, we request that within three months of receiving this letter, you issue a revised version of WCAP-7832 to include this acceptance letter and additional information submitted during the review.

Sincerely,

Dennis P. Allison

John F. Stolz, Chief
Light Water Reactors Branch No. 1
Division of Project Management

Enclosure:
As stated

cc: D. Rawlins

ENCLOSURE
TOPICAL REPORT EVALUATION

MAR 2 1978

Report No: WCAP7832
Report Title: Evaluation of Steam Generator Tube, Tube Sheet and Divider
Plate Under Combined LOCA plus SSE Conditions.
Report Date: Dec. 1973
Supplement 1: Oct. 1974
Supplement 2: Dec. 1975
Originating Organization: Westinghouse Electric Corp.

SUMMARY OF TOPICAL REPORT

This report describes the structural analysis of tubes, tubesheet and divider plate of 51-Series and Model D Westinghouse steam generators when subjected to combined LOCA and SSE loading. The objective of this analysis was to demonstrate that the maximum stresses in these components fall within ASME B & PV Code Section III allowable limits when subjected to these loading conditions.

The hydraulic forces acting on these components consisted of two types:

1. Forces on the steam-generator internals due to rupture of a main coolant pipe. The pipe break used for this analysis was a double ended coolant pipe rupture, located in the crossover leg immediately outside the steam generator coolant outlet nozzle. These forces were derived from pressure-time histories calculated by the computer program BLODWN-2.
2. Forces on the internals due to motion of the steam generator caused by the LOCA forces acting on the entire reactor coolant system. The program SATAN-V is used to calculate the pressure-time histories at various points in the broken and unbroken loops, which are then used as input into the program STHRUST from which the system external force-histories are calculated. These histories are then introduced

into the programs FIXFM and WESTDYN-7 which calculate the dynamic response (displacement histories) of the reactor coolant system. The displacement history of the steam-generator is then applied to a model of the generator which includes the tube bundle, tube sheet and divider plate, from which the internal force histories acting on these elements are obtained.

The SSE loads are specified by an envelope of the floor response spectra at elevations in the reactor containment building corresponding to the upper and lower supports on the steam generator. The peak spectral acceleration was specified as 2.75 g's using damping of 1%. Both horizontal and vertical earthquake motion were assured in the analysis.

Following is a description of the analysis of the three components.

1. Analysis of the tube bundle.

This analysis was performed by subjecting a model of the largest radius tube in the bundle to the loading described above, plus dead-weight. The analysis used the computer program STASYS which performs static and dynamic analysis of elastic beam type structures. The tube was assumed to have experienced thinning of 3 mils due to erosion after 40 years of service (this does not include the local corrosion due to sludge deposits and local chemical hydraulic interaction).

The largest primary membrane stress intensity is based on the highest pressure difference (internal minus external), which exists before the dynamic loading is applied. The largest primary-membrane-plus-primary-bending stress intensity was calculated by superimposing

MAR 2 1978

absolutely the combined LOCA effects and the SSE effect. Both intensities were found to be below the limits for elastic system analysis prescribed by the ASME Section III Appendix F criteria. The largest effect was determined to be due to the variation of internal pressure. The effect due to the system motion was shown to be much smaller while the effect due to SSE was found to be of a secondary nature (about 10% of the total effect). Other loads were also included in the analysis such as fluid centrifugal forces and fluid friction in the U-tube region. These were found to be negligible. Likewise, effects due to flow induced vibration were also found to be negligible.

Other effects which influence tube integrity were also investigated as follows:

- a. The critical crack length for non-thinned D-Series tubes was calculated as .64 in., based on a high ductility fracture mechanics method developed at the Battelle Memorial Institute, and a maximum expected pressure differential of 1485 psi. For maximum uniformly thinned tubes the critical length was calculated as .38 in. when subjected to the same pressure differential.
- b. A parametric study was performed to determine the margins of uniform tube wall thinning due to degradation which could be tolerated without exceeding Faulted Condition stress limits. For D-Series tubing of .75 in. nominal diameter and .036 in. minimum thickness a decrease to a minimum wall thickness of .026 in. was found to be tolerable. For 51-Series tubing of .875 in. nominal diameter

MAR 2 1978

and .050 nominal wall thickness the minimum wall thickness was found to be .021 in.

c, The external collapse pressure for straight tubes of nominal wall thickness was investigated analytically and experimentally. For D-Series tubing at 600° F and maximum allowable 5% ovality this pressure was determined to exceed by 23% the maximum differential pressure existing across the tubes subsequent to blowdown.

2. Tube sheet analysis

The analysis of the Model D tube sheet under the LOCA loading was performed by using the computer program ANSYS. The model used was a three dimensional finite element elastic model of the channel head, divider plate, tube sheet and stud barrel. The pressure loading which was applied to this model originated from the hydraulic analysis described above. The maximum pressure differential was amplified by a load factor of 2, and applied statically to the model. The maximum primary membrane and primary membrane-plus-bending stresses were found to be well below the Appendix F allowables for elastic system/elastic component analysis. Stresses due to steam generator movement and SSE were also found to be negligible.

3. Divider plate analysis

Based on the results of the tube sheet analysis the only significant loading condition which was applied to the divider plate was the internal pressure time history. The analysis was performed by using a finite difference, large deformation elastic-plastic dynamic

MAR 2 1978

computer program called PETROS-III. The calculated results show that the maximum primary-membrane stress intensity was lower than the value prescribed by Appendix F for inelastic component analysis.

The review was conducted by surveying the references and the background information of some of the computer programs mentioned in the report. A number of short confirmatory calculations of tube behavior under internal pressure and bending, and of crack propagation in tubes with thin wall axial cracks were also performed. They were found to support specific conclusions in the report.

The applicant was also requested to submit additional references which supported the analytical methods and results described in the report. These were examined and found to be acceptable.

The BLODWN-2 computer code was reviewed by the NRC during the evaluation of the Westinghouse MULTIFLEX* computer code. The Topical Report Evaluation on MULTIFLEX was issued on June 17, 1977 (Reference 1). MULTIFLEX is an extension of the BLODWN-2 code and includes the effects of fluid-structure interactions.

The modeling of the PWR primary system presented in WCAP-7832 is the same as that reviewed in MULTIFLEX. The modeling of the steam generator primary side features was approved at that time.

During the review of the Multiflex code, two changes were required to the BLODWN-2 and modeling portions of the analysis. These changes carry over to the use of the BLODWN-2 code for this application. These changes are (1) the use of the correct sonic velocity and (2) the use of the correct radial transport distance in the pressure vessel lower plenum. These

*WCAP-8708, "MULTIFLEX, A FORTRAN IV Computer Program for Analyzing Thermal-Hydraulic-Structure System Dynamics."

changes should be included for future analyses, for completeness. These changes will not have a significant effect on the pressure response in the steam generator. In addition to these changes, the break model is limited to either a full, complete double-ended guillotine failure or a simple slot rupture. A break opening time of one milisecond is required for a licensing calculation.

REGULATORY POSITION

We find this report and subsequent supplements acceptable as a reference to support conclusions that tubes thinned by localized wastage or containing smaller-than-critical-length thru-wall cracks will withstand LOCA plus SSE loads, provided the wall thickness of the tube is at least 72% of its original nominal thickness. This value is conservative because of assumptions used in the analysis. Use of lesser wall thicknesses should be justified by more refined analysis, which should be performed within the guidelines of R. G. 1.121, or experiment. These tubes may also contain longitudinal thru-wall cracks of a length which should not be exceeded to satisfy safety requirements under these loading conditions. For Model D tubes critical crack lengths are .64 inches for healthy tubes and .38 inches for uniformly thinned tubes, when subjected to maximum expected pressure differential of 1485 psi.

The report does not discuss various specific forms of degradation encountered since its submittal, such as denting, wastage and cracks in the support plates, and cracks in the U-bends. It is, therefore, deemed insufficient to determine the safety of these tubes with these forms of degradation. Furthermore, it is not applicable to later models of steam generators which incorporate quare-foil tube support design.

MAR 2 1978

Finally, we find acceptable the methods of analysis used for determining the safety of the tube sheet and divider plate when subjected to LOCA and SSE, and the conclusions derived from these analyses.

The use of the BLODWN-2 computer code, subject to the modification and restrictions as outlined above, is acceptable for the evaluation of the steam generator tube, tube sheet and divider plate under combined LOCA plus SSE conditions. Reference 1 presents a detailed evaluation of the BLODWN-2 code.

References

1. Letter from J. F. Stolz to C. Eicheldinger, "Topical Report Evaluation of Westinghouse WCAP-8708 (P) and WCAP-8709 (NP)," June 17, 1977.

TABLE OF CONTENTS

<u>Section</u>	<u>Title</u>	<u>Page</u>
<u>ABSTRACT</u>		
<u>1.0</u>	<u>INTRODUCTION</u>	1.1-1
1.1	<u>PURPOSE OF REPORT</u>	1.1-1
1.2	<u>APPLICABILITY</u>	1.1-1
1.3	<u>DESCRIPTION OF STEAM GENERATOR</u>	1.1-1
1.4	<u>LOADING ASSUMPTIONS</u>	1.1-1
<u>2.0</u>	<u>DETERMINATION OF INPUT LOADS</u>	2.1-1
2.1	<u>HYDRAULIC FORCES ON INTERNALS</u>	2.1-1
2.1.1	DETAILED STEAM GENERATOR NODING MODEL	2.1-2
2.1.2	TYPICAL PRESSURE-TIME HISTORIES	2.1-2
2.2	<u>EXTERNAL RESPONSE OF STEAM GENERATOR CAUSED BY LOCA FORCES</u>	2.2-1
2.2.1	HYDRAULIC MODELING OF LOCA EXTERNAL FORCES	2.2-2
2.3	<u>SEISMIC LOADS</u>	2.3-1
2.3.1	METHOD OF DYNAMIC SEISMIC ANALYSIS	2.3-1
2.4	<u>DESCRIPTION OF COMPUTER CODES</u>	2.4-1
2.4.1	BLODWN-2 CODE	2.4-1
2.4.2	SATAN-V CODE	2.4-2
2.4.3	STHRUST CODE	2.4-2
2.4.4	FIXFM CODE	2.4-3
2.4.5	WESTDYN-7 CODE	2.4-3
2.4.6	SEISMIC ANALYSIS PROGRAM	2.4-4
<u>3.0</u>	<u>RESULTS OF ANALYSIS</u>	3.1-1
3.1	<u>TUBE ANALYSIS</u>	3.1-1
3.1.1	DISCUSSION OF LOADING	3.1-1
3.1.2	LOADS ON TUBES	3.1-2
3.1.2.1	<u>Assumptions</u>	3.1-2
3.1.2.2	<u>Secondary Blowdown Effects</u>	3.1-4

TABLE OF CONTENTS (Continued)

<u>Section</u>	<u>Title</u>	<u>Page</u>
	3.1.3 STRESS LIMITS	3.1-6
	3.1.4 RESULTS FOR A HEALTHY TUBE	3.1-6
	3.1.4.1 Combined Stresses for All Loads	3.1-6
	3.1.4.2 Stresses Due to Individual Loads	3.1-8
	3.1.5 PERMISSIBLE CRACK LENGTHS FOR A NORMAL TUBE	3.1-9
	3.1.6 TUBE THINNING	3.1-14
	3.1.7 EXTERNAL PRESSURE EFFECTS	3.1-15
3.2	<u>TUBE SHEET ANALYSIS</u>	3.2-1
	3.2.1 DISCUSSION OF LOADING	3.2-1
	3.2.2 COMPUTATIONAL MODEL	3.2-2
	3.2.3 STRESS LIMITS	3.2-3
	3.2.4 RESULTS	3.2-5
	3.2.4.1 <u>Effects of Individual Loads on</u> <u>Tubesheet</u>	3.2-5
3.3	<u>DIVIDER PLATE ANALYSIS</u>	3.3-1
	3.3.1 APPLIED LOAD	3.3-1
	3.3.2 STRUCTURAL MODEL	3.3-1
	3.3.3 MATERIAL PROPERTIES	3.3-1
	3.3.4 RESULTS OF ANALYSIS	3.3-2
<u>4.0</u>	<u>CONCLUSIONS</u>	4.0-1
<u>5.0</u>	<u>REFERENCES</u>	5.0-1

LIST OF TABLES

<u>Table</u>	<u>Title</u>
1.3-1	Steam Generator Design Data and Dimensions
3.1-1	SSE Stresses in Steam Generator Tubes
3.1-2	Stresses Due to Tube Thinning
3.2-1	DBE Tubesheet Accelerations

LIST OF FIGURES

<u>Figure</u>	<u>Title</u>
1.3-1	Steam Generator Nomenclature
1.3-2	Model D Steam Generator Dimensions
2.1-1	Piping Network Representation of Four Loop Plant Reactor Vessel Inlet Annulus Region
2.1-2	Representation of Three Intact Loops for 4-Loop Reactor Coolant System BLODWN Model
2.1-3	Broken Loop Representation with Cross-over Leg Rupture for BLODWN Model
2.1-4	BLODWN Steam Generator Model
2.1-5	Average Radius U-Tube Model
2.1-6	Largest Radius U-Tube Model
2.1-7	BLODWN-2 Channel Head Model
2.1-8	Pressure History of Location Node 1
2.1-9	Pressure History of Location Node 4
2.1-10	Pressure History of Location Node 10
2.1-11	Pressure History of Location Node 16
2.1-12	Pressure History of Location Node 19
2.2-1	Reactor Coolant System, SATAN Model
2.2-2	STHRUST Reactor Coolant System Model
2.2-3	Reactor Coolant Loop Model
2.2-4	LOCA Displacement History Imposed on Tube Model, X Direction
2.2-5	LOCA Displacement History Imposed on Tube Model, Y Direction
2.2-6	LOCA Displacement History Imposed on Tube Model, Z Direction
2.3-1	Horizontal Response Spectrum Curve
2.3-2	Seismic Model of Steam Generator

LIST OF FIGURES (Continued)

<u>Figure</u>	<u>Title</u>
3.1-1	Model D Steam Generator U-Tube Configuration
3.1-2	STASYS Tube Model - Elastic Pipe Elements Model D Steam Generator Largest Tube
3.1-3	Maximum Stress Intensity on Tube Outer Wall Node Location 1 - Total LOCA Effect
3.1-4	Maximum Stress Intensity on Tube Outer Wall Node Location 3 - Total LOCA Effect
3.1-5	Maximum Stress Intensity on Tube Outer Wall Node Location 4 - Total LOCA Effect
3.1-6	Maximum Stress Intensity on Tube Outer Wall Node Location 6 - Total LOCA Effect
3.1-7	Maximum Stress Intensity on Tube Outer Wall Node Location 8 - Total LOCA Effect
3.1-8	Maximum Stress Intensity on Tube Outer Wall Node Location 10 - Total LOCA Effect
3.1-9	Maximum Stress Intensity on Tube Outer Wall Node Location 12 - Total LOCA Effect
3.1-10	Maximum Stress Intensity on Tube Outer Wall Node Location 14 - Total LOCA Effect
3.1-11	Maximum Stress Intensity on Tube Outer Wall Node Location 16 - Total LOCA Effect
3.1-12	Maximum Stress Intensity on Tube Outer Wall Node Location 17 - Total LOCA Effect
3.1-13	Stresses at Node Location 4 Due to LOCA Pressure History
3.1-14	Stresses at Node Location 8 Due to LOCA Pressure History
3.1-15	Stresses at Node Location 10 Due to LOCA Pressure History
3.1-16	Stresses at Node Location 12 Due to LOCA Pressure History
3.1-17	Stresses at Node Location 16 Due to LOCA Pressure History
3.1-18	In-Plane Displacements of Node Location 5 Due to LOCA Pressure History

LIST OF FIGURES (Continued)

<u>Figure</u>	<u>Title</u>
3.1-19	In-Plane Displacements of Node Location 7 Due to LOCA Pressure History
3.1-20	In-Plane Displacements of Node Location 10 Due to LOCA Pressure History
3.1-21	In-Plane Displacements of Node Location 13 Due to LOCA Pressure History
3.1-22	In-Plane Displacements of Node Location 15 Due to LOCA Pressure History
3.1-23	Stresses at Node Location 4 Due to LOCA Displacement History on Steam Generator
3.1-24	Stresses at Node Location 7 Due to LOCA Displacement History on Steam Generator
3.1-25	Stresses at Node Location 10 Due to LOCA Displacement History on Steam Generator
3.1-26	Stresses at Node Location 13 Due to LOCA Displacement History on Steam Generator
3.1-27	Stresses at Node Location 15 Due to LOCA Displacement History on Steam Generator
3.1-28	In-Plane Displacements of Node Location 5 Due to LOCA Displacement History on Steam Generator
3.1-29	In-Plane Displacements of Node Location 7 Due to LOCA Displacement History on Steam Generator
3.1-30	In-Plane Displacements of Node Location 10 Due to LOCA Displacement History on Steam Generator
3.1-31	In-Plane Displacements of Node Location 13 Due to LOCA Displacement History on Steam Generator
3.1-32	In-Plane Displacements of Node Location 15 Due to LOCA Displacement History on Steam Generator
3.1-33	Out-of-Plane Displacements of Node Location 6 Due to LOCA Displacement History on Steam Generator
3.1-34	Out-of-Plane Displacements of Node Location 7 Due to LOCA Displacement History on Steam Generator

LIST OF FIGURES (Continued)

<u>Figure</u>	<u>Title</u>
3.1-35	Out-of-Plane Displacements of Node Location 9 Due to LOCA Displacement History on Steam Generator
3.1-36	Out-of-Plane Displacements of Node Location 10 Due to LOCA Displacement History on Steam Generator
3.1-37	Out-of-Plane Displacements of Node Location 11 Due to LOCA Displacement History on Steam Generator
3.1-38	Out-of-Plane Displacements of Node Location 13 Due to LOCA Displacement History on Steam Generator
3.1-39	Out-of-Plane Displacements of Node Location 14 Due to LOCA Displacement History on Steam Generator
3.1-40	Tube Rotation in the Vicinity of Tubesheet
3.1-41	Relationship between λ and Stress Magnification Factor M
3.1-42	Stresses at Node Location 4 Due to LOCA Pressure History, Tube Wall Thickness 26 mils
3.1-43	Stresses at Node Location 7 Due to LOCA Pressure History, Tube Wall Thickness 26 mils
3.1-44	Stresses at Node Location 10 Due to LOCA Pressure History, Tube Wall Thickness 26 mils
3.1-45	Stresses at Node Location 13 Due to LOCA Pressure History, Tube Wall Thickness 26 mils
3.1-46	Stresses at Node Location 16 Due to LOCA Pressure History, Tube Wall Thickness 26 mils
3.1-47	Stresses at Node Location 4 Due to LOCA Displacement History on Steam Generator, Tube Wall Thickness 26 mils
3.1-48	Stresses at Node Location 7 Due to LOCA Displacement History on Steam Generator, Tube Wall Thickness 26 mils
3.1-49	Stresses at Node Location 10 Due to LOCA Displacement History on Steam Generator, Tube Wall Thickness 26 mils
3.1-50	Stresses at Node Location 13 Due to LOCA Displacement History on Steam Generator, Tube Wall Thickness 26 mils
3.1-51	Stresses at Node Location 16 Due to LOCA Displacement History on Steam Generator, Tube Wall Thickness 26 mils
3.1-52	Maximum Stress Intensity on Tube Outer Wall Node Location 16 - Total LOCA Effect, Tube Wall Thickness 26 mils

LIST OF FIGURES (Continued)

<u>Figure</u>	<u>Title</u>
3.2-1	Pressure History at Tubesheet During LOCA
3.2-2	Pressure Loads Due to LOCA
3.2-3	Channel Head, Tubesheet and Divider Plate Assembly
3.2-4	Tube Sheet - Channel Head - Stub Barrel Assembly Dimensions
3.2-5	3-D ANSYS Model of (1) Divider Plate, (2&3) Tubesheet, (4) Channel Head and (5) Stub Barrel
3.2-6	Node Points, Divider Plate Portion of 3-D ANSYS Model
3.2-7	Elements, Divider Plate Portion of 3-D ANSYS Model
3.2-8	Tubesheet Properties, 3-D ANSYS Model
3.2-9	Node Points, Tubesheet Portion of 3-D ANSYS Model
3.2-10	Elements, Tubesheet Portion of 3-D ANSYS Model
3.2-11	Node Points, Channel Head Portion of 3-D ANSYS Model
3.2-12	Elements, Channel Head Portion of 3-D ANSYS Model
3.2-13	Stub Barrel Portion of 3-D ANSYS Model
3.2-14	Tubesheet deflection Due to LOCA Along Diameter Perpendicular to Divider Plate Relative to Tubesheet Center
3.2-15	Tubesheet Perpendicular Displacement
3.2-16	Tubesheet Equivalent Plate Stresses Radial Stress Perpendicular to Divider Plate Along Diameter
3.2-17	Radii on Which Ligament Stresses Were Calculated
3.3-1	Pressure Difference Across Divider Plate
3.3-2	Smoothed Pressure History Across Divider Plate
3.3-3	Divider Plate - Finite Difference Mesh Model
3.3-4	Engineering Stress-Strain Curves for Inconel at 600°F
3.3-5	True Stress-Strain Curve for Inconel at 600°F
3.3-6	Adjusted True Stress - Strain Curve for Inconel at 600°F

LIST OF FIGURES (Continued)

<u>Figure</u>	<u>Title</u>
3.3-7	Maximum Membrane Stress at Tubesheet Line
3.3-8	Membrane Stress History at Point of Maximum Deflection on Divider Plate
3.3-9	Displacement History of Point of Maximum Deflection, in the Center of the Divider Plate
3.3-10	Displacement Contours at Maximum Pressure Differential, For Divider Plate

ABSTRACT

This report gives details of the stress analysis performed on the tubes, tubesheet and divider plate components of current Westinghouse steam generators when subjected to combined Loss-of-Coolant-Accident (LOCA) and Safe Shutdown Earthquake (SSE) loads. The analysis indicates that the stresses in the components studied are within ASME Boiler and Pressure Vessel Code, Section III allowable limits.

1.0 INTRODUCTION

1.1 PURPOSE OF REPORT

This report evaluates the structural adequacy of the primary side internals, specifically the tubes, tubesheet and divider plate of the current Westinghouse steam generator, when subjected to combined LOCA and SSE loadings.

1.2 APPLICABILITY

The results of the analysis, due to combined LOCA and SSE conditions, as presented in this report, are applicable to those Westinghouse plants having 51 Series and Model D steam generators. The seismic response spectrum used in the analysis represents a SSE level for a typical plant. Evaluation of the stresses for plants in excessively high seismic areas could be performed, if necessary, on a case by case basis. However, it should be noted that the stress contributions due to seismic loading amounted to about 10% of that due to LOCA loading in the case of the U-tube, for example, and the report shows that there is ample margin to accommodate additional seismic stresses. For the tubesheet and divider plate the seismic stresses were found to be negligible.

1.3 DESCRIPTION OF STEAM GENERATOR

The design is a vertical shell and U-tube evaporator with integral moisture separating equipment. The reactor coolant flows through inverted U-tubes, entering and leaving through nozzles located in the hemispherical bottom head (channel head) of the steam generator. The head is divided into inlet and outlet chambers by a vertical divider plate extending from the head to the tube sheet. The primary and secondary volumes of the steam generator are separated by the tubes and tubesheet. The tubesheet is a thick, perforated circular plate which connects the shell and the channel head and to which the ends of the U-tubes are attached. The tube bundle is supported at intervals by horizontal support plates, which are ported to permit flow of the steam-water mixture.

The steam generator produces steam by transferring heat from the reactor coolant water to a subcooled mixture. The subcooled mixture is formed by the mixing of saturated recirculating fluid and feedwater. The feedwater enters the lower shell region and flows directly into a preheater section where it is heated almost to saturation temperature before entering the boiler section. Subsequently, water-steam mixture flows upward through the tube bundle and into the steam drum section. A set of centrifugal moisture separators, located above the tube bundle, removes most of the entrained water from the steam.

Steam dryers are employed to increase the steam quality to a minimum of 99.75 percent (0.25 percent moisture). The separated moisture recirculates through the annulus formed by the shell and tube bundle wrapper.

Manways are provided for access to both sides of the channel head. The upper shell has two bolted and gasketed access openings for inspection and maintenance of the dryers, which can be disassembled and removed through the opening.

The steam generator shell is constructed of manganese-molybdenum steel plate, (ASME SA-533). The channel head is a low alloy steel casting (ASME SA-216) and the tubesheet is a manganese-molybdenum steel plate, (ASME SA-508). The interior surfaces of the channel head and nozzles are clad with austenitic stainless steel. The lower surface of the tubesheet, in contact with the reactor coolant, is clad with Inconel. The divider plate in the channel head is an Inconel (ASME SB-168) plate.

The 51 Series have 3388 U-Tubes of 0.875 in S.O.D. and 0.050 ins. nominal wall thickness; the steam generator has 4674 U-tubes of 0.75 inches O.D. and 0.043 inches nominal wall thickness. The tube material is Inconel (ASME SB-163).

Figure 1.3-1 depicts the Model D unit and illustrates the nomenclature used throughout the report and Figure 1.3-2 presents the dimensions of the unit. Table 1.3-1 lists the Model D design data and dimensions.

1.4 LOADING ASSUMPTIONS

This stress analysis required various dynamic load inputs. These were:

1. LOCA hydraulic loads on the steam generator primary side internals, in the form of pressure-time histories.
2. LOCA induced reactor coolant loop forces, transmitted to the steam generator supports (external shaking effects).
3. Response of the steam generator due to SSE accelerations.

Model D tube dimensions were used to determine load inputs for item 1. However, since Model D steam generator support designs have not been finalized at the time of writing, load inputs for the last two items were derived from support configurations of a typical plant having 51 series steam generators. Typical plant layouts using either model of steam generator are such that the differences are considered insignificant.

TABLE 1.3-1

MODEL D STEAM GENERATOR DESIGN DATA AND DIMENSIONS

<u>Parameter</u>		<u>Model D</u>
Primary Coolant Flow,	10^6 lb/hr	34.6
Steam Flow,	10^6 lb/hr	3.79
Coolant Inlet Temp.,	°F	618.5
Coolant Outlet Temp.,	°F	557.2
Coolant Average Temp.,	°F	587.9
Primary Pressure drop,	psi	30.8
Primary Design Pressure,	psig	2485
Primary Operating Pressure,	psig	2250
Feedwater Temperature,	°F	440
Secondary Design Pressure,	psig	1185
Tube O.D.,	in.	0.75
Tube wall thickness,	in.	0.043
Number of tubes		4674
Heat Transfer Surface,	ft ²	48,000
Circulation Ratio		2.4

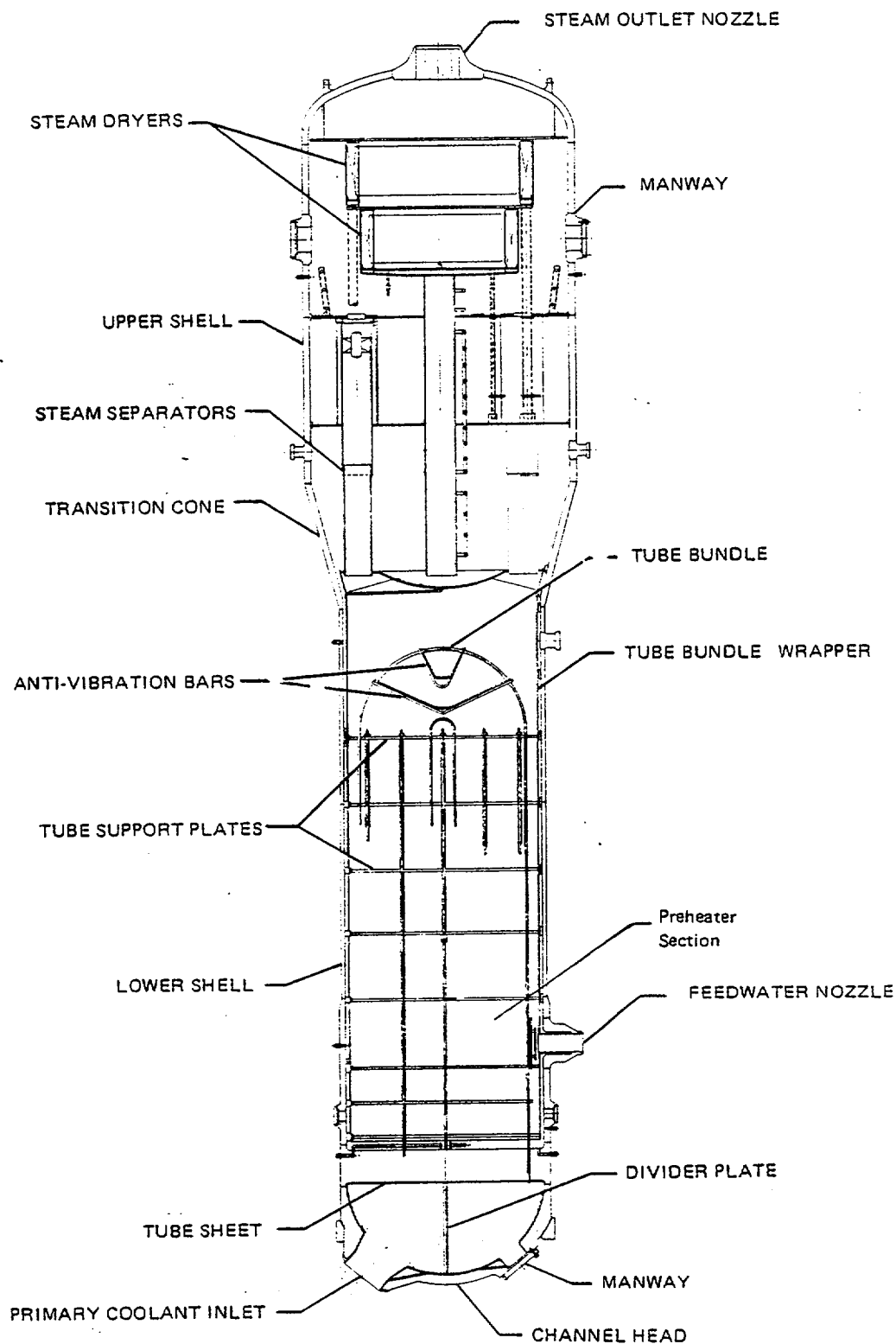
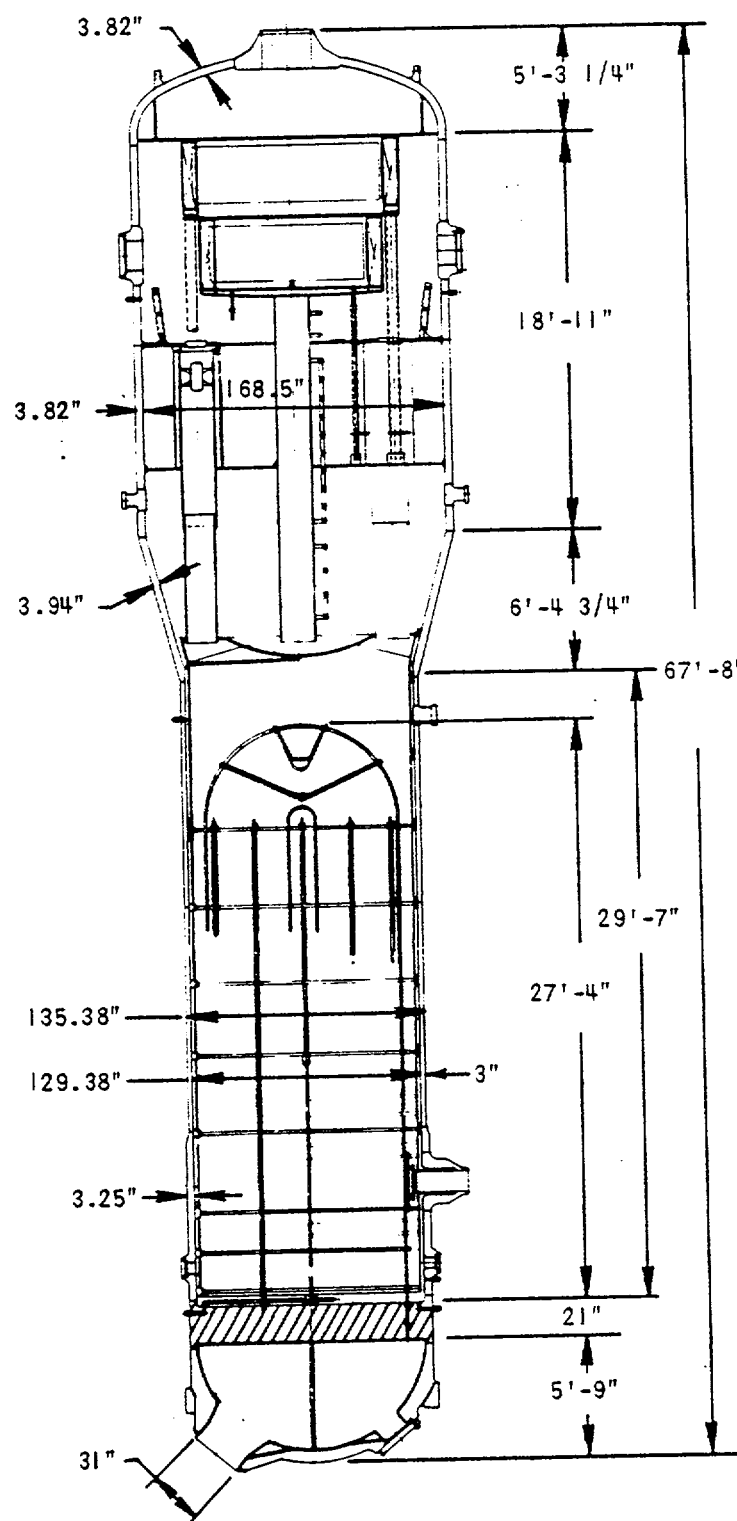


Figure 1.3-1 Steam Generator Nomenclature



MODEL D STEAM GENERATOR

Figure 1.3-2 Model D Steam
Generator
Dimensions

2.0 DETERMINATION OF INPUT LOADS

The stress analysis of the steam generator tubes, tubesheet and divider plate, under the faulted condition of combined LOCA plus SSE loads, requires various transient hydraulic and dynamic structural load inputs. These are:

1. The hydraulic forces (pressure-time history of the primary coolant fluid) on the steam generator internals due to a rupture of a main coolant pipe. The pipe break used for this analysis was a double ended coolant pipe rupture, located in the crossover leg immediately outside the steam generator coolant outlet nozzle.
2. The resultant displacement history of the steam generator supports due to the forces caused by the LOCA.
3. Acceleration of the steam generator due to the SSE.

The mathematical models and analytical techniques to determine these inputs are described in this chapter.

2.1 HYDRAULIC FORCES ON INTERNALS

The pressure-time history inside the steam generator primary side is calculated by the BLOWN-2^[1] computer code. This code can evaluate the pressure and velocity transients for a maximum of 2400 locations (120 equivalent pipes, each subdivided 20 times), in the Reactor Cooling System (RCS), resulting in a detailed hydraulic description, needed for this analysis. Figures 2.1-1 through 2.1-3 present a typical BLOWN-2 model of a four loop plant. Figure 2.1-1 presents a typical model of the piping network representing the reactor vessel inlet annulus (downcomer) region. Figure 2.1-2 shows how the three intact loops are combined, using appropriate scaling laws (from pipes #54 to #63), which are then assumed to separate near the end of the cold leg, so that the correct inlet conditions into the downcomer region is modeled. Figure 2.1-3 presents a model of the broken

loop. The inlet pipes of the broken loop and the intact loops are shown attached to the vessel annulus in Figure 2.1-1.

The broken loop steam generator is modeled with 5 equivalent pipes; one for each of the steam generator plenums and 3 for the steam generator tubes. Figure 2.1-4 presents the BLOWDN-2 model of the broken loop steam generator described above. Pipes 8-12 in Figure 2.1-4 are equivalent to pipes 67-71 presented in the typical 4 loop BLOWDN-2 model presented in Figure 2.1-3. Pipes 8 through 12 are subdivided into 69 nodes. BLOWDN-2 circulates the pressure-time history for each of these nodes, resulting in a detailed description of the pressure wave traveling through the steam generator tubes after initiation of LOCA.

As a result of LOCA, several loading phenomena occur in the steam generator. Following LOCA, a rapid decay of the primary coolant pressure occurs which initiates a rarefaction wave through the steam generator primary side. The magnitude and rise time of this wave is important for determining the induced stresses in the steam generator internals.

Following the rarefaction wave, a quasi-steady blowdown flow is established in the steam generator. This flow creates further hydraulic loading phenomena which act on the steam generator tubes; centrifugal fluid forces in the bend region of the tubes and frictional forces throughout the tube length.

The steam generator tubes length is a relatively important parameter for determining the effect of the rarefaction wave on the steam generator primary side internals. Since the rarefaction wave travels at the speed of sound (~ 3000 ft/sec), the length determines the travel time through the tube. Pipes 9-11 in Figure 2.1-4 represent all tubes in the steam generator lumped together using the appropriate scaling laws. The length of the tube, (i.e. the sum of the lengths of pipes 9 to 11) is equal to the average length of all the tubes (see Figure 2.1-5), hence representing the behavior of an average rarefaction wave through all the tubes. This "average tube" analysis is believed appropriate for analysis, of the tube

sheet and divider plate, since these components should experience an average rarefaction wave, due to the combined effects of the pressure wave traveling through all the tubes.

For the U-tube analysis, a 'largest tube' model was also examined. The length of the steam generator tubes in the BLODWN-2 model (Figure 2.1-6) was set equal to the length of the largest tube. This was a mechanistic approach, since the BLODWN-2 model lumps together all the tubes, to approximate the rarefaction waves traveling through the largest tube. It was determined that the 'largest tube' case was the most conservative assumption for the U-tube analysis. (See Section 3.1 for details of the tube analysis).

2.1.1 DETAILED STEAM GENERATOR NODING MODEL

For purposes of the detailed stress analysis (described later), specific pressure locations, or nodes, were required in the steam generator BLODWN-2 model (Figure 2.1-4). Figures 2.1-5 shows the region of the tube in the U-bend region, for the representative 'average tube' down to the elevation of the second tube support plate, which is divided into 19 nodes. Figure 2.1-6 presents the similar model for the 'largest tube'. The inlet and outlet plenums (channel head section), are also subdivided into several nodes. Figure 2.1-7 presents the nodes used specifically in the stress analysis. The model for the inlet and outlet plenums are identical for the 'average tube' and 'largest tube' analysis. Hence Figures 2.1-5 and 2.1-7 represent the specific pressure locations used for the 'average tube' analysis (for tube sheet and divider plate stress analysis). Figures 2.1-6 and 2.1-7 represent the specific pressure locations used for the 'largest tube' analysis (U-tube stress analysis only).

2.1.2 TYPICAL PRESSURE-TIME HISTORIES

Figures 2.1-8 to 2.1-12 present pressure-time histories generated from the BLODWN-2 analysis at selected nodes, for application in the U-tube analysis.

Figure 3.2-1 shows the pressure-time histories in the lower inlet and outlet plenums, for use in the tube sheet stress evaluation.

Figure 3.3-1 shows the pressure-time history for the divider plate analysis.

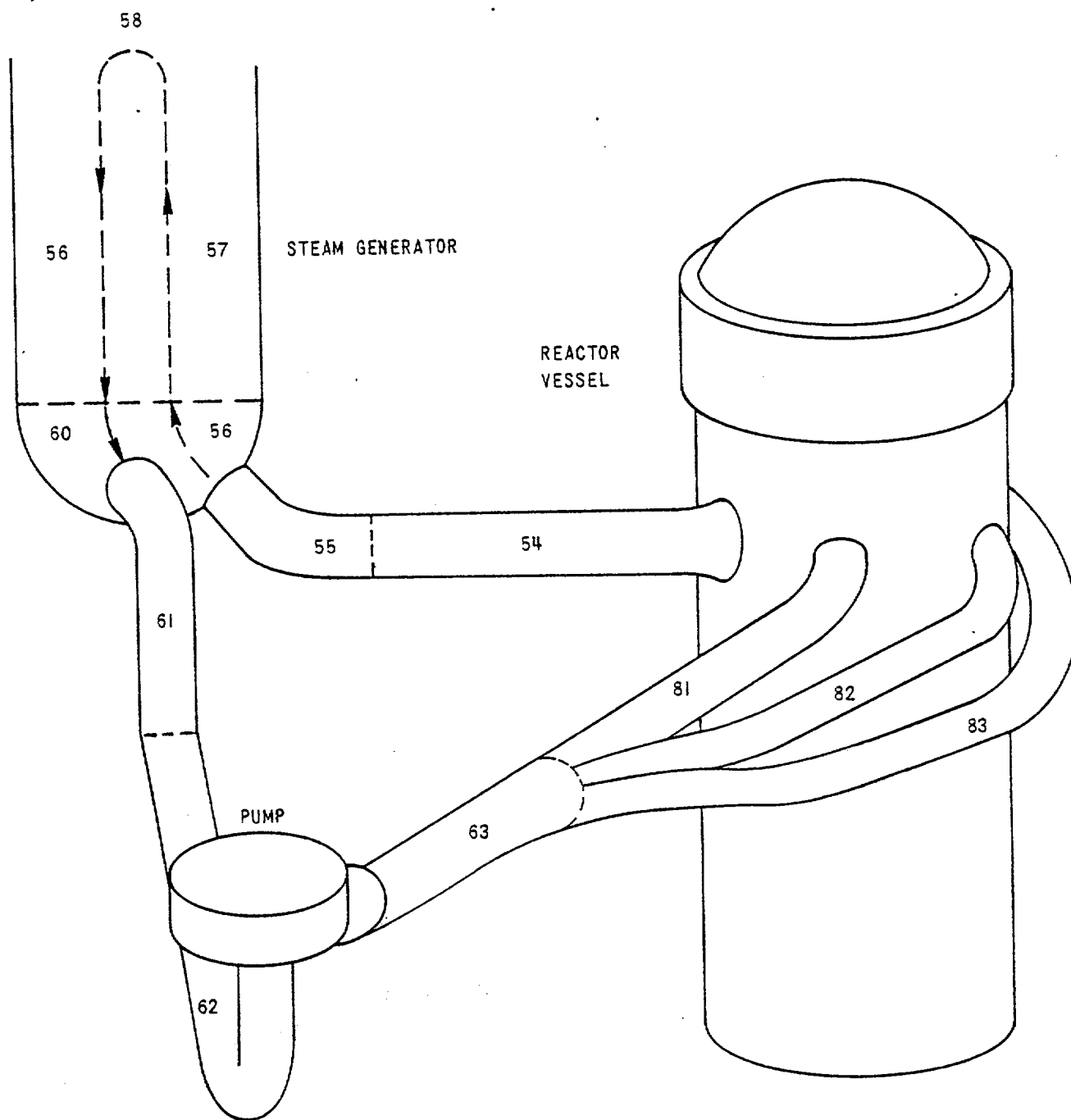


Figure 2.1-2 Representation of Three Intact Loops for
4-Loop Reactor Coolant System BLOWN Model

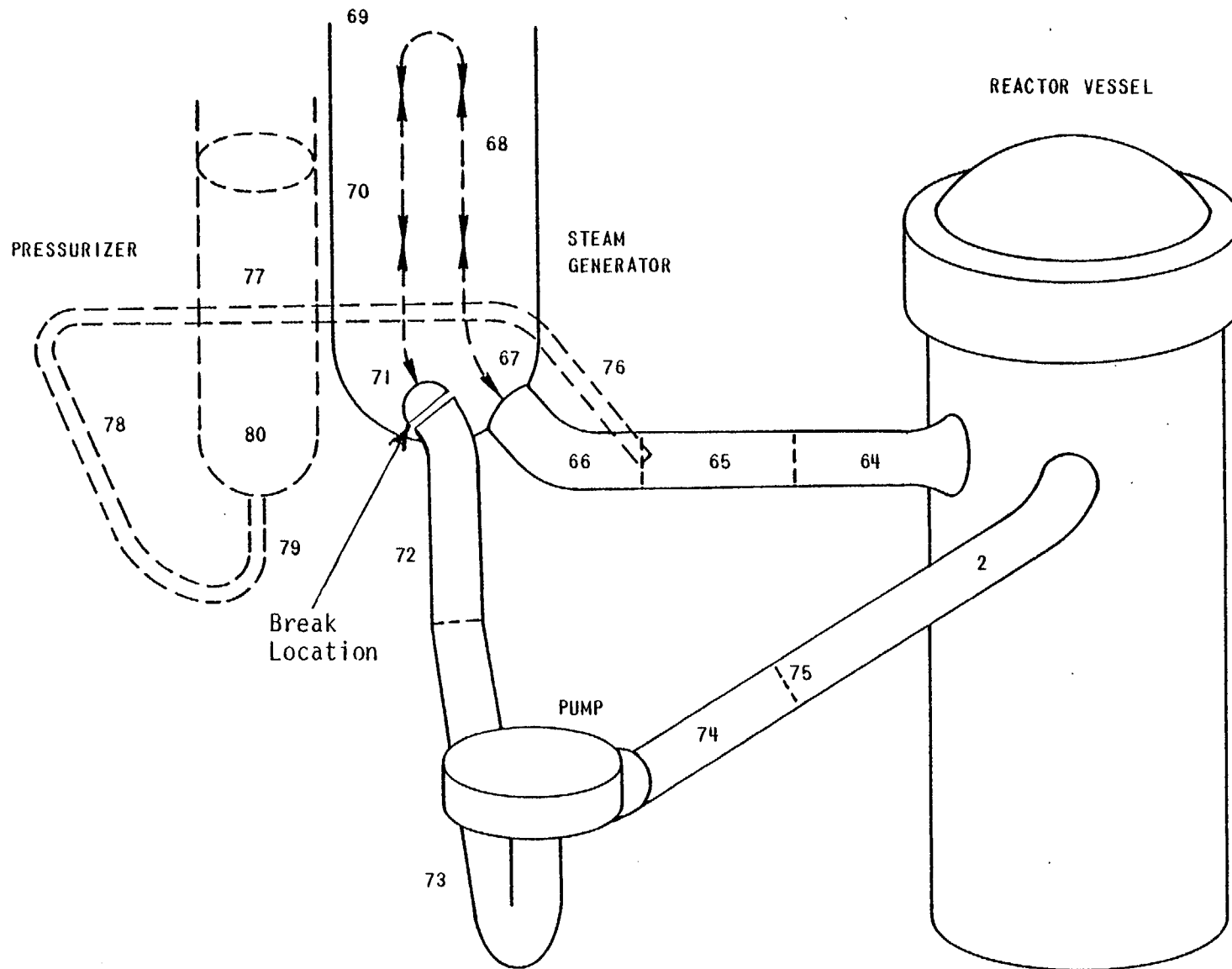
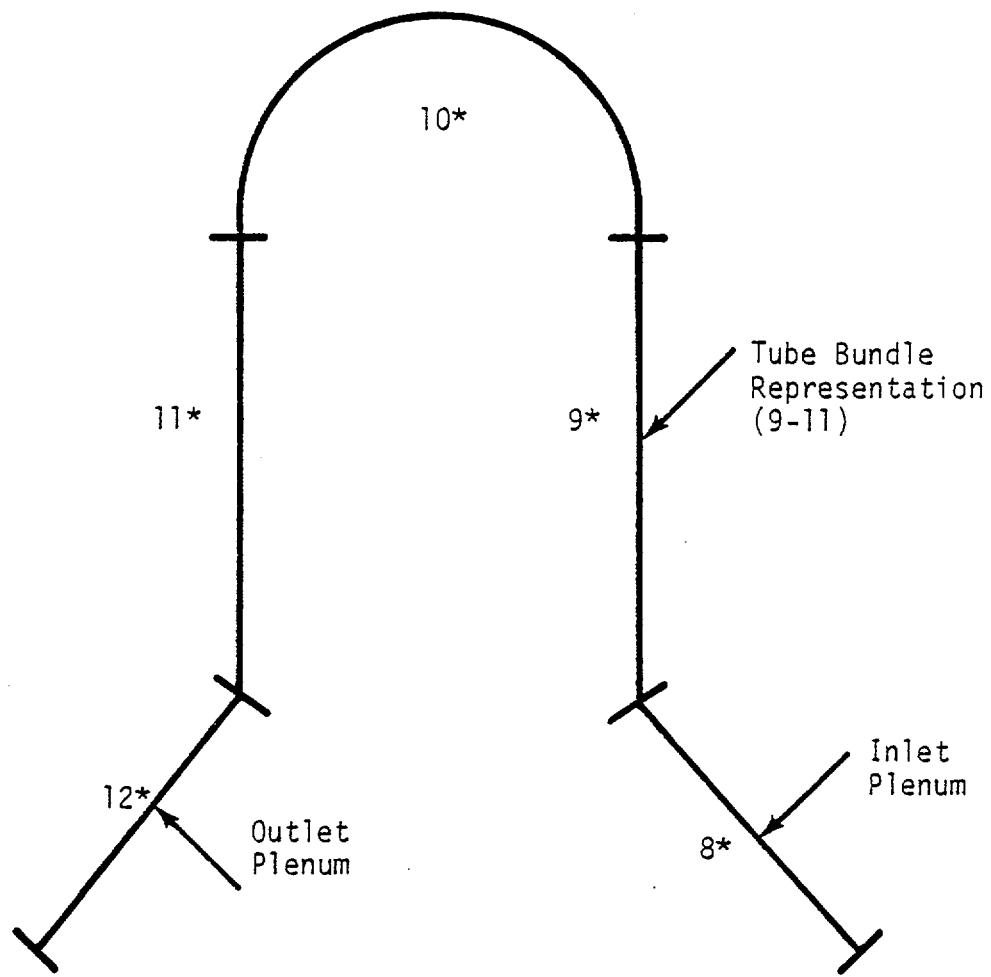


Figure 2.1-3 Broken Loop Representation with, Cross-over
Leg Rupture for BLOWDOWN Model



* These equivalent "pipes" are further subdivided into nodes;
See Figures 2.1-5 and 2.1-6.

Figure 2.1-4 BLOWN Steam Generator Model

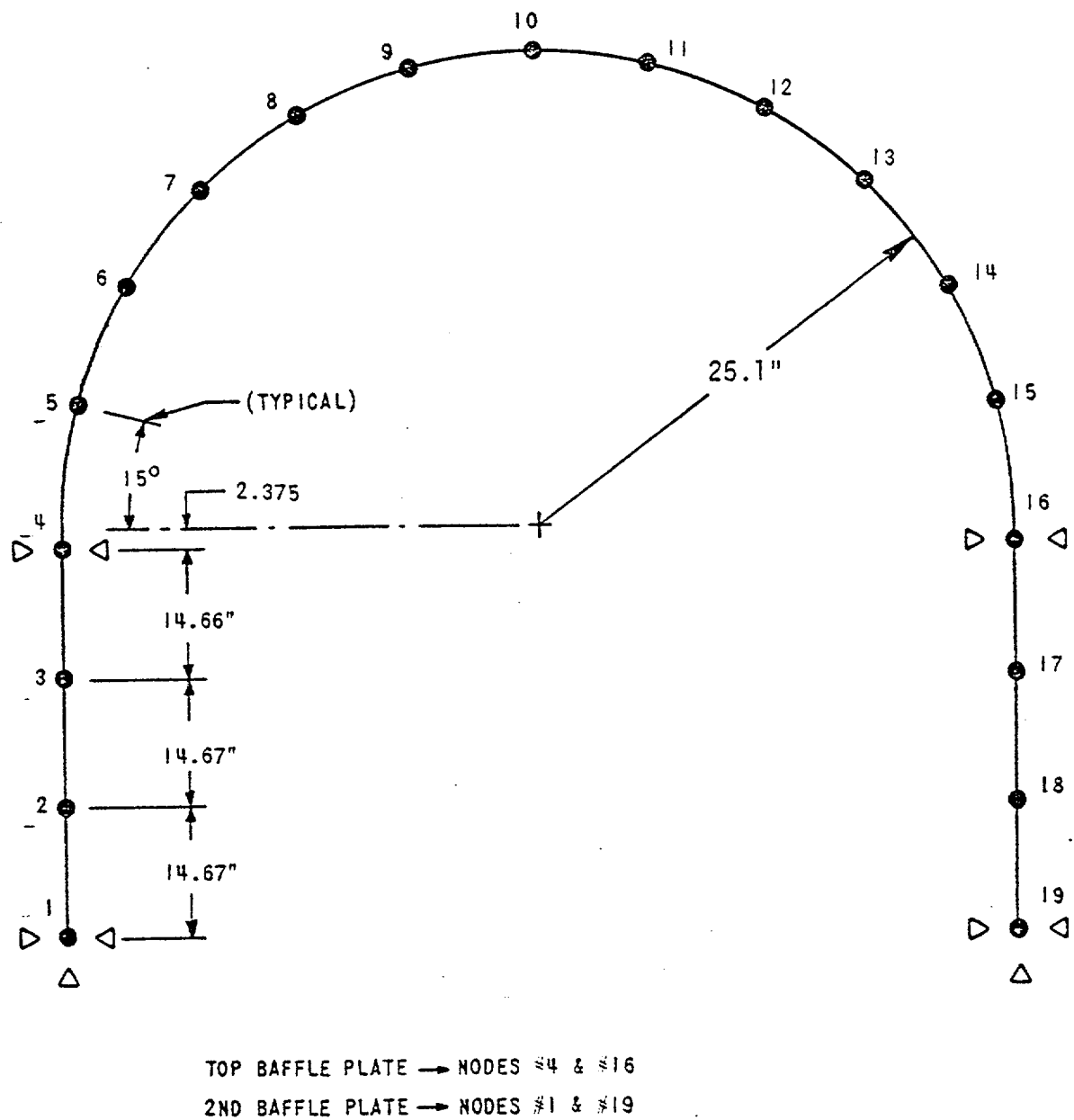


Figure 2.1-5 Average Radius U-Tube Model -- used for determining tubesheet and divider plate pressure-time histories

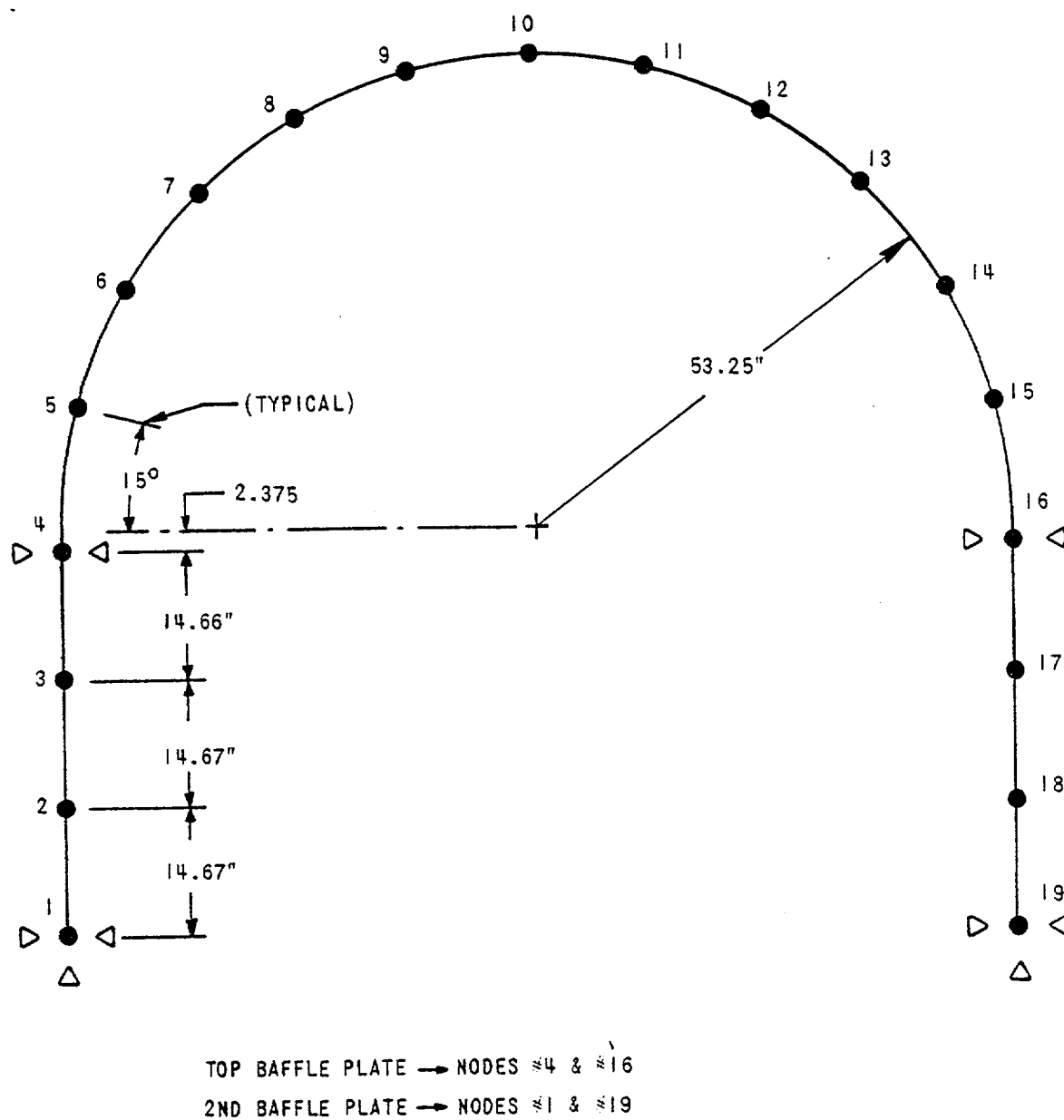


Figure 2.1-6 Largest Radius U-Tube Model -- used for determining tube pressure-time history

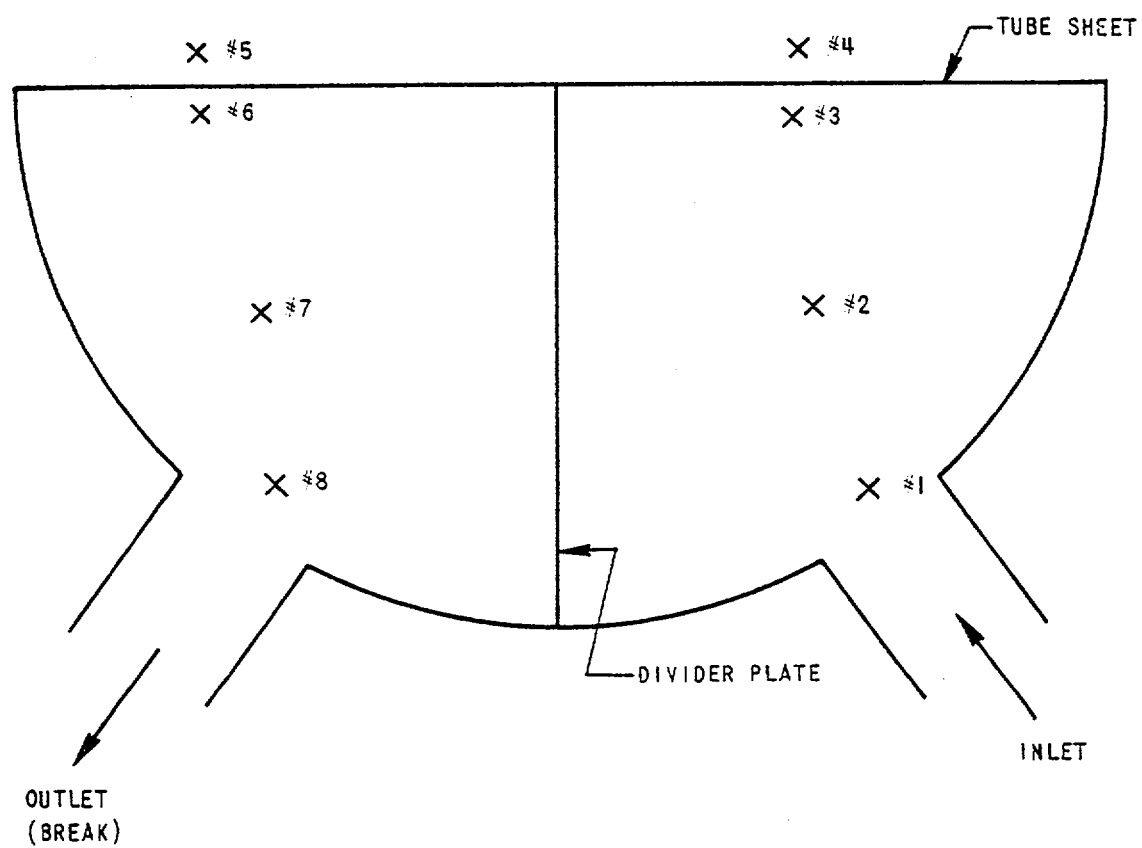
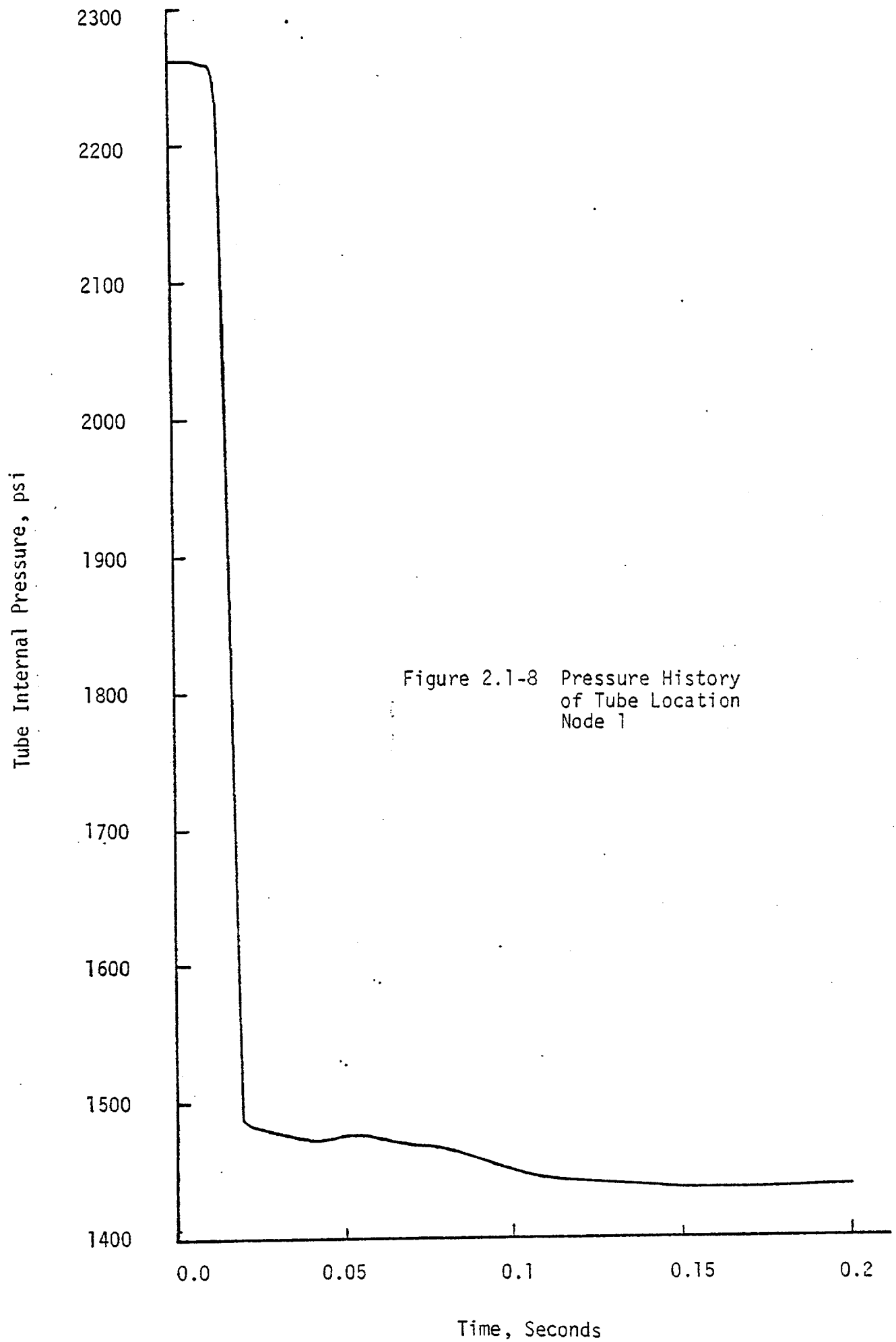


Figure 2.1-7 BLODWN-2 Channel Head Model



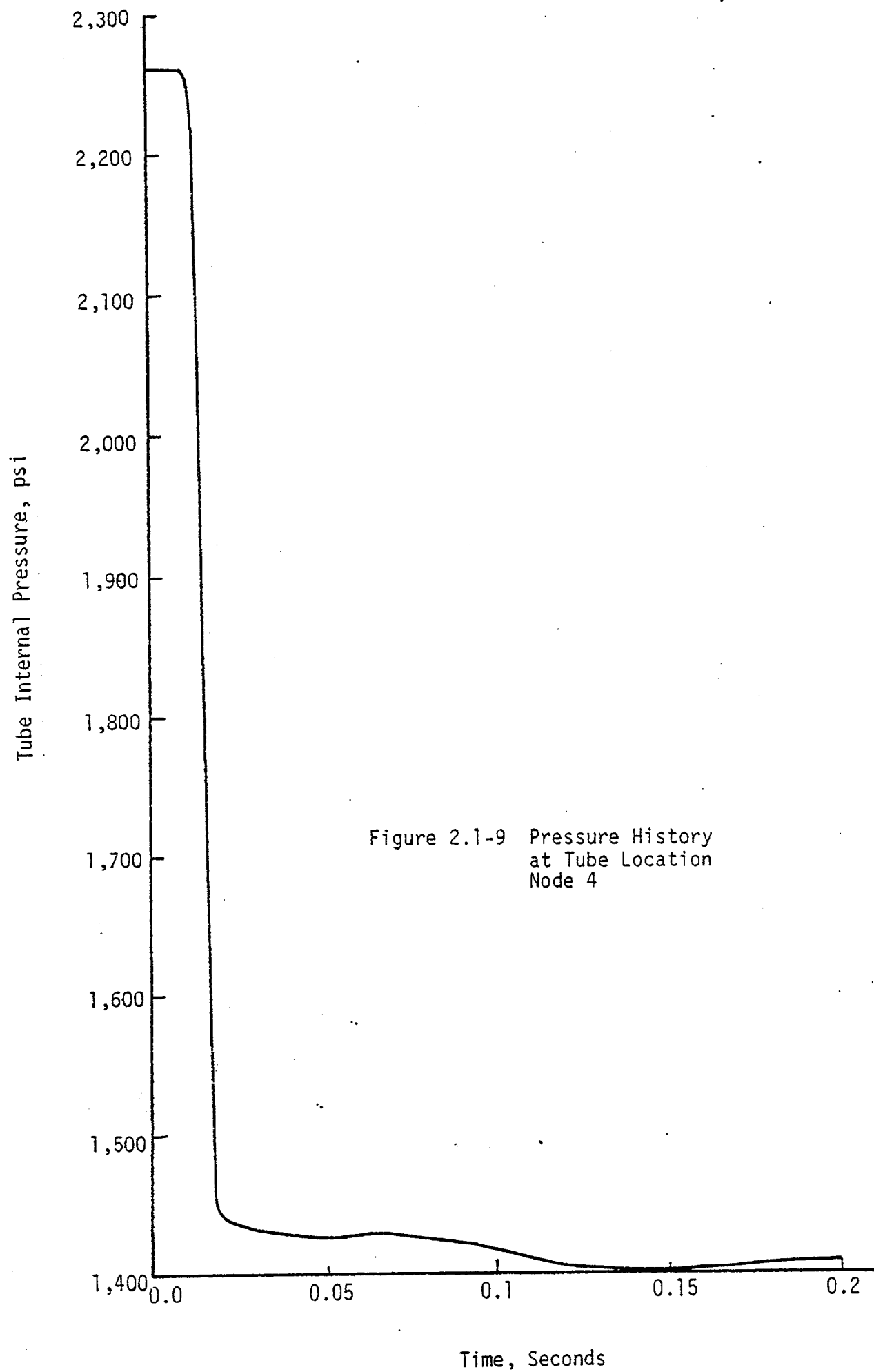


Figure 2.1-9 Pressure History
at Tube Location
Node 4

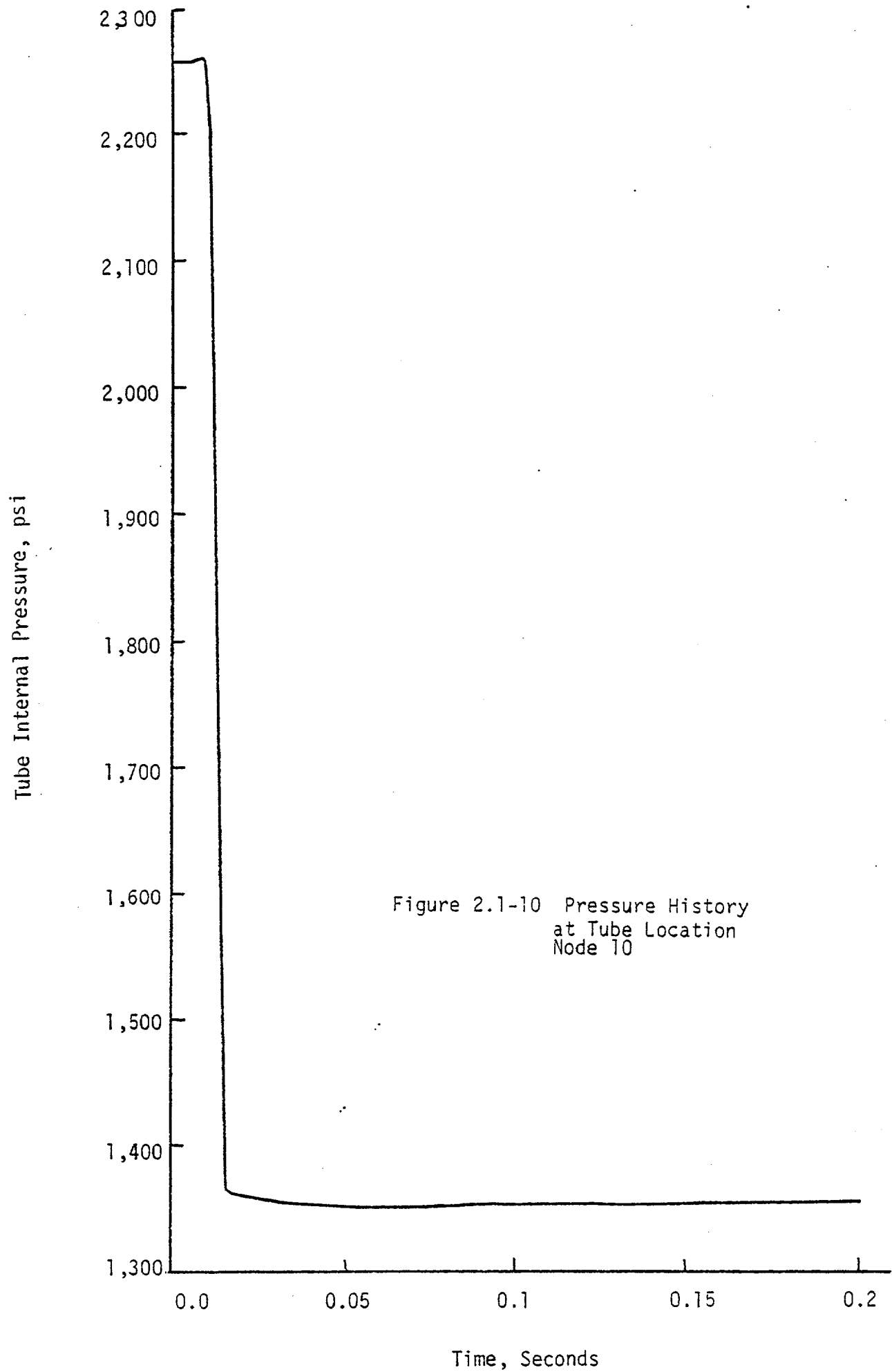


Figure 2.1-10 Pressure History
at Tube Location
Node 10

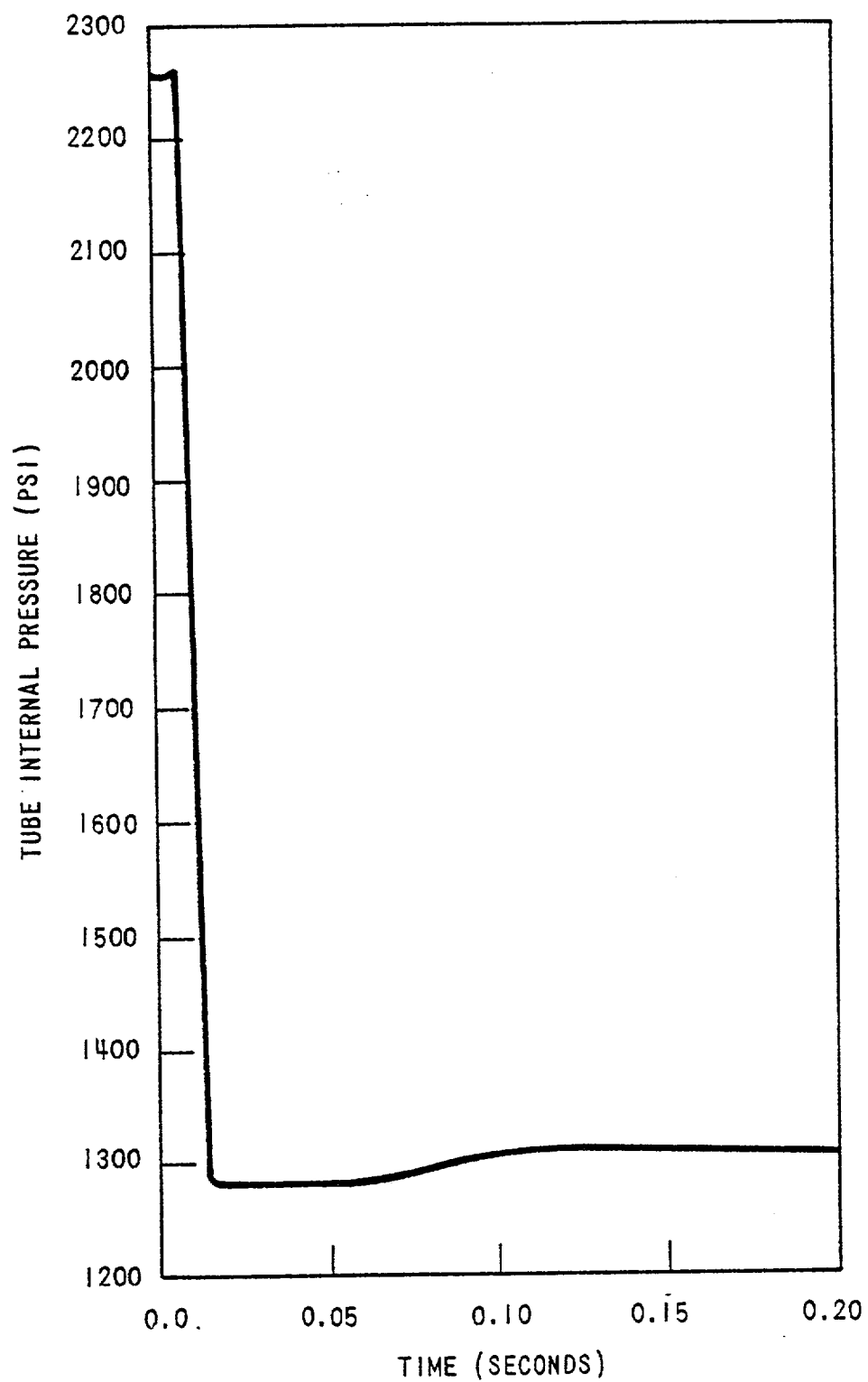
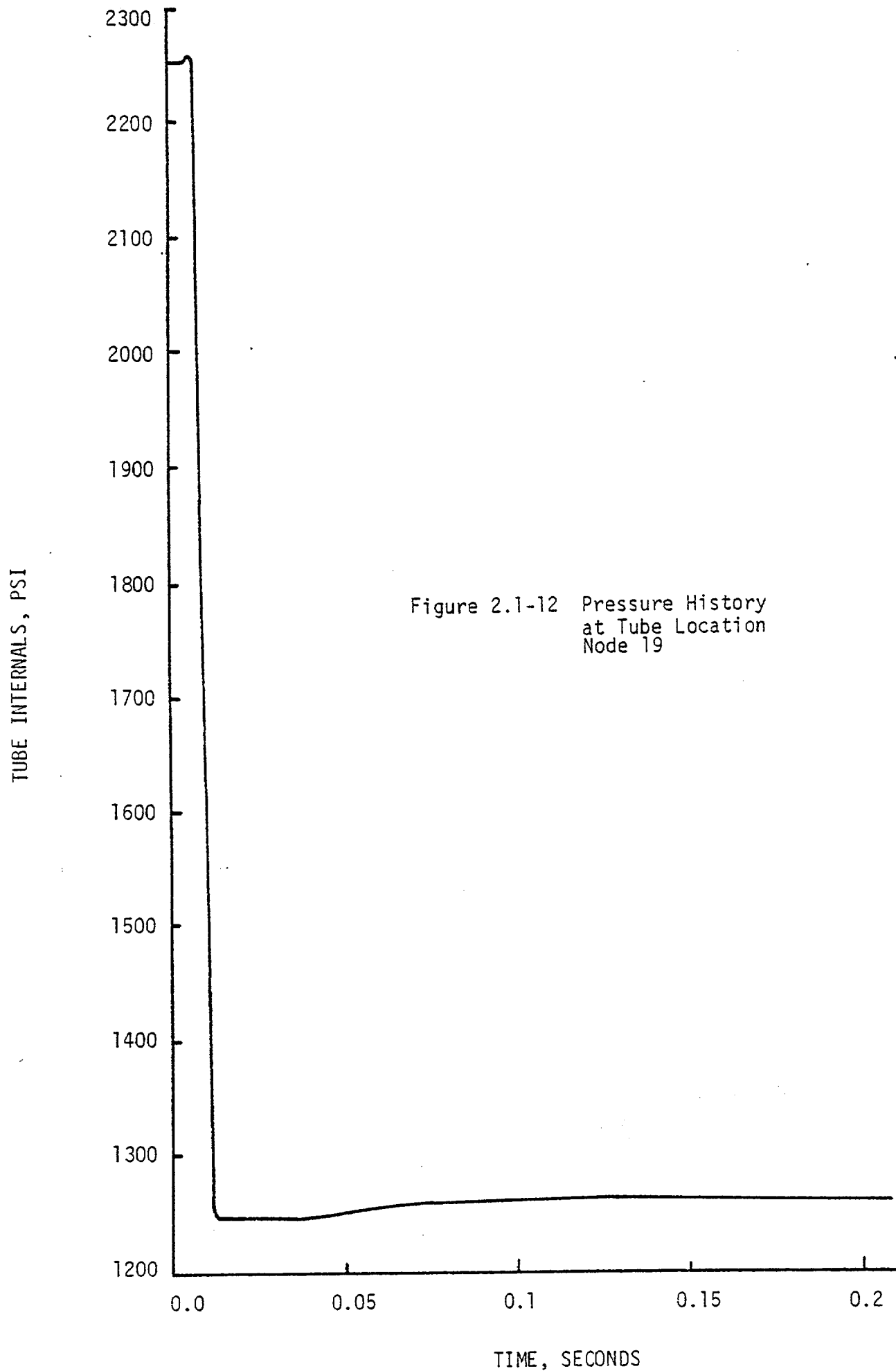


Figure 2.1-11 Pressure History at Tube Location Node 16



2.2 EXTERNAL RESPONSE OF THE STEAM GENERATOR CAUSED BY LOCA FORCES

Deflections of the steam generator caused by LOCA shaking forces were also obtained, for input to the structural response model. Since the Model D will not be in service until 1976, loop support configurations were not available. Consequently, a typical support design from a plant using 51 Series units was used for this analysis.

Typical plant loop layouts for either model of steam generator are similar and the small differences between the two designs are not expected to affect the validity of this assumption significantly. The similarities between the two models may be summarized as follows:

- 1) The pressure vessel shells are almost identical in overall dimensions, thicknesses and materials.
- 2) The channel head configuration, including the divider plate in the lower plenum, nozzle geometry and layout, are identical.
- 3) The Model D has more tubes, but of a smaller diameter than the 51 Series.
- 4) The tubesheets are the same thickness with very similar ligament efficiencies.
- 5) The feedwater inlet nozzle on the Model D has been relocated to a position above the tubesheet. The feedwater nozzle on the 51 Series is located in the upper shell section. However, it has been determined that the stiffness of the feedwater line piping has a negligible effect upon the response of the steam generator.
- 6) The moisture separation equipment is significantly modified in the D Series unit.
- 7) Design and operational characteristics are very similar.

Determination of the external shaking forces are described in Sections 2.2.1 and 2.2.2.

2.2.1 HYDRAULIC MODELING OF LOCA EXTERNAL FORCES ON THE STEAM GENERATOR

The Reactor Coolant Loop hydraulic forcing functions are calculated in a two step process, using the SATAN-V^[2] computer code to generate pressure and flow time histories, which are used as input into the STHRUST code for the calculation of the hydraulic forces on the reactor coolant loops. The hydraulic model, for a typical four loop plant, shown in Figure 2.2-1 divides the Reactor Coolant System into 68 elements (control volumes). Appropriate scaling laws are used to combine the three intact loops represented by the larger of the two loops depicted in Figure 2.2-1. SATAN-V calculates pressure and flow time histories for all 68 elements, which are used as input into the STHRUST code to generate forcing functions as several pre-specified points in the Reactor Coolant Loops, both the intact and broken loops. The locations of the calculated forcing functions are shown in Figure 2.2-2.

The next step involves the use of the FIXFM computer program which determines the time-history response of the Reactor Coolant Loop to LOCA loads. The input to this program consists of the natural frequencies, normal modes, applied forces and nonlinear elements. These inputs are generated by the WESTDYN-7 program.

Figure 2.2-3 presents the model used for calculation of the dynamic response of the loops. The SATAN-V, STHRUST, FIXFM and WESTDYN-7 codes are described in Section 2.4.

The shaking effect was generated as displacement histories in the three principal axes, to be applied to the U-tube model at the upper support points. Figures 2.2-4 through 2.2-6 give these applied displacement histories.

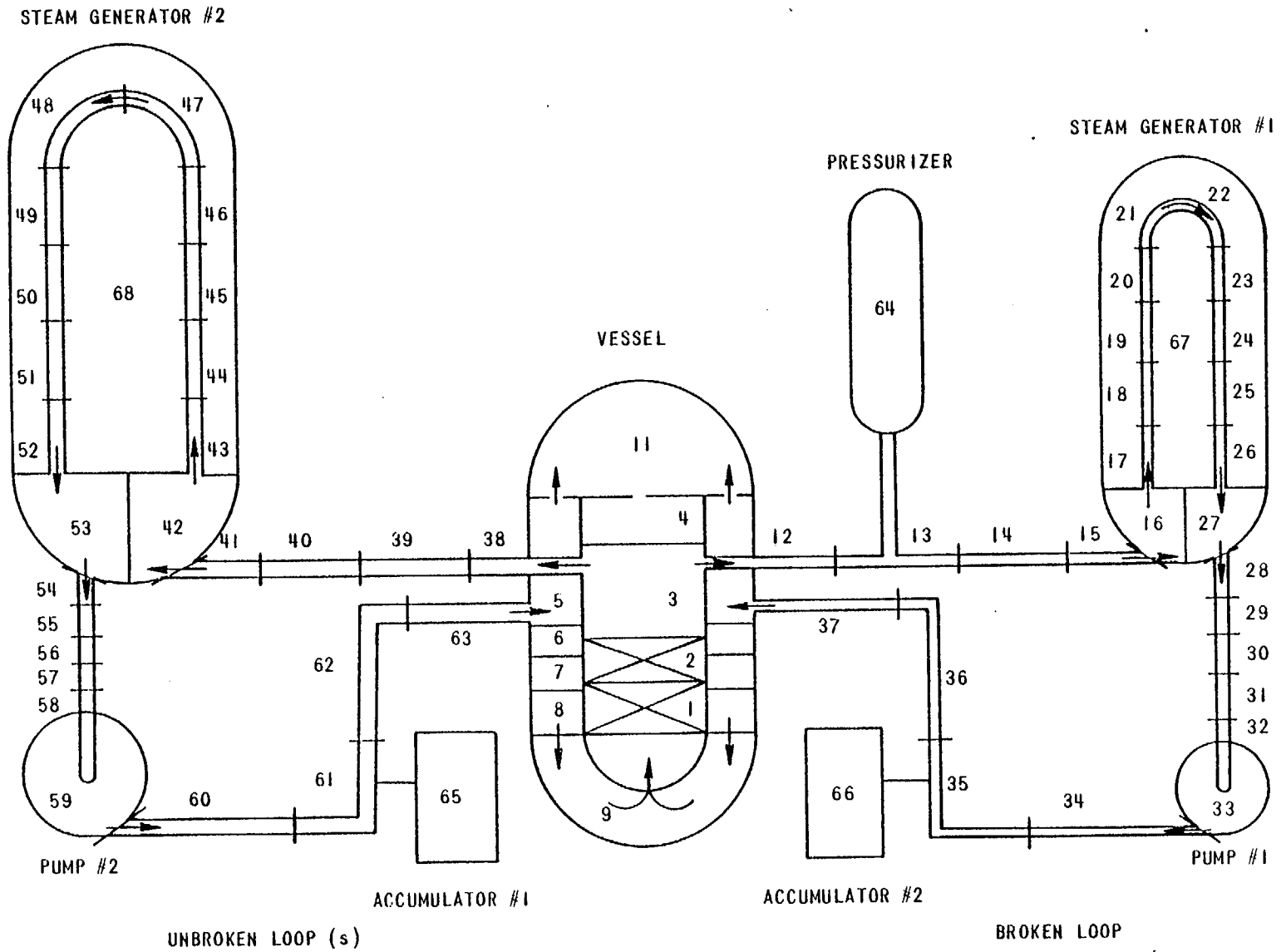


Figure 2.2-1 Four Loop Reactor Coolant System, Satan Model

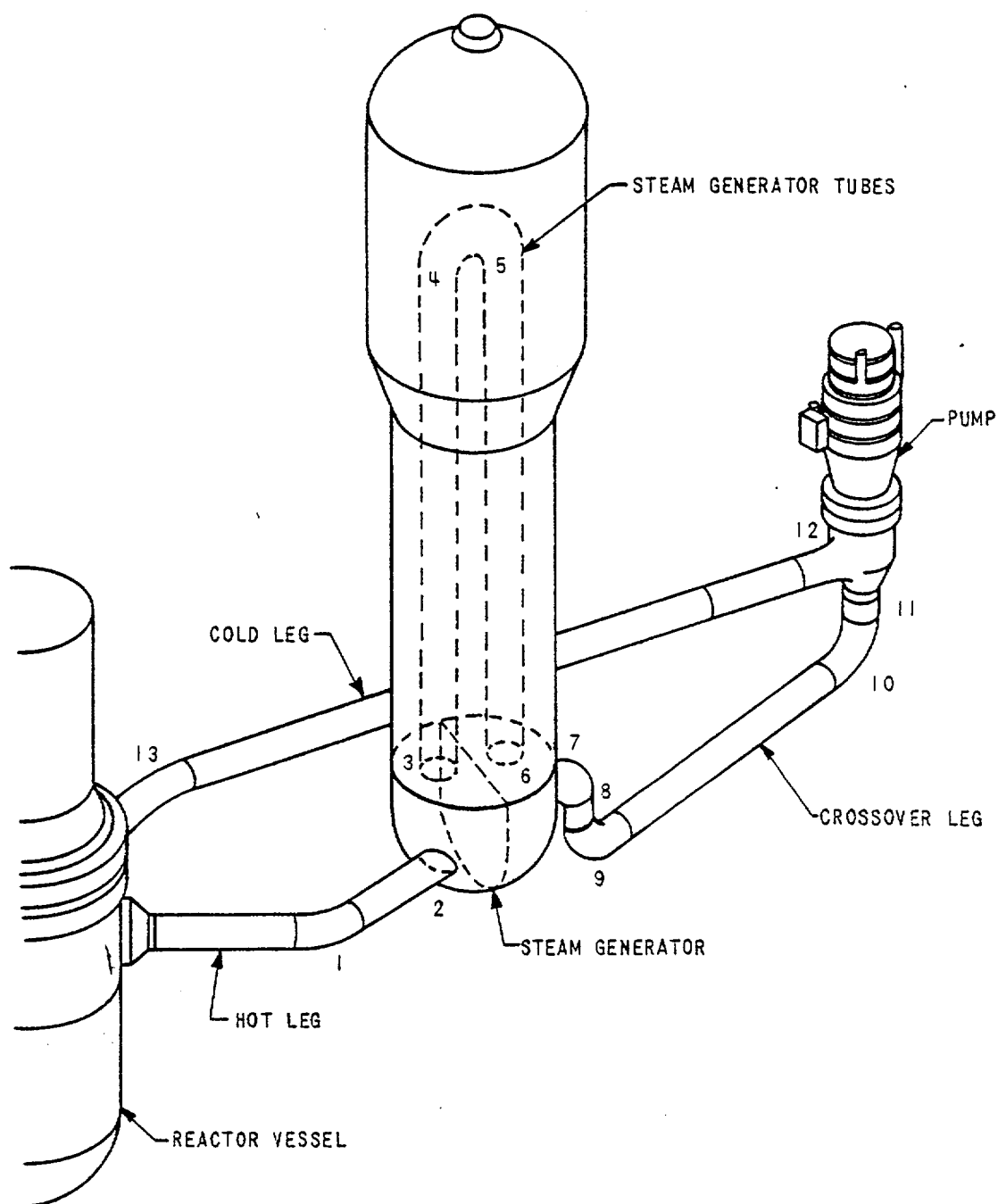


Figure 2.2-2 STHRUST Reactor Coolant Loop Model Showing Hydraulic Force Locations

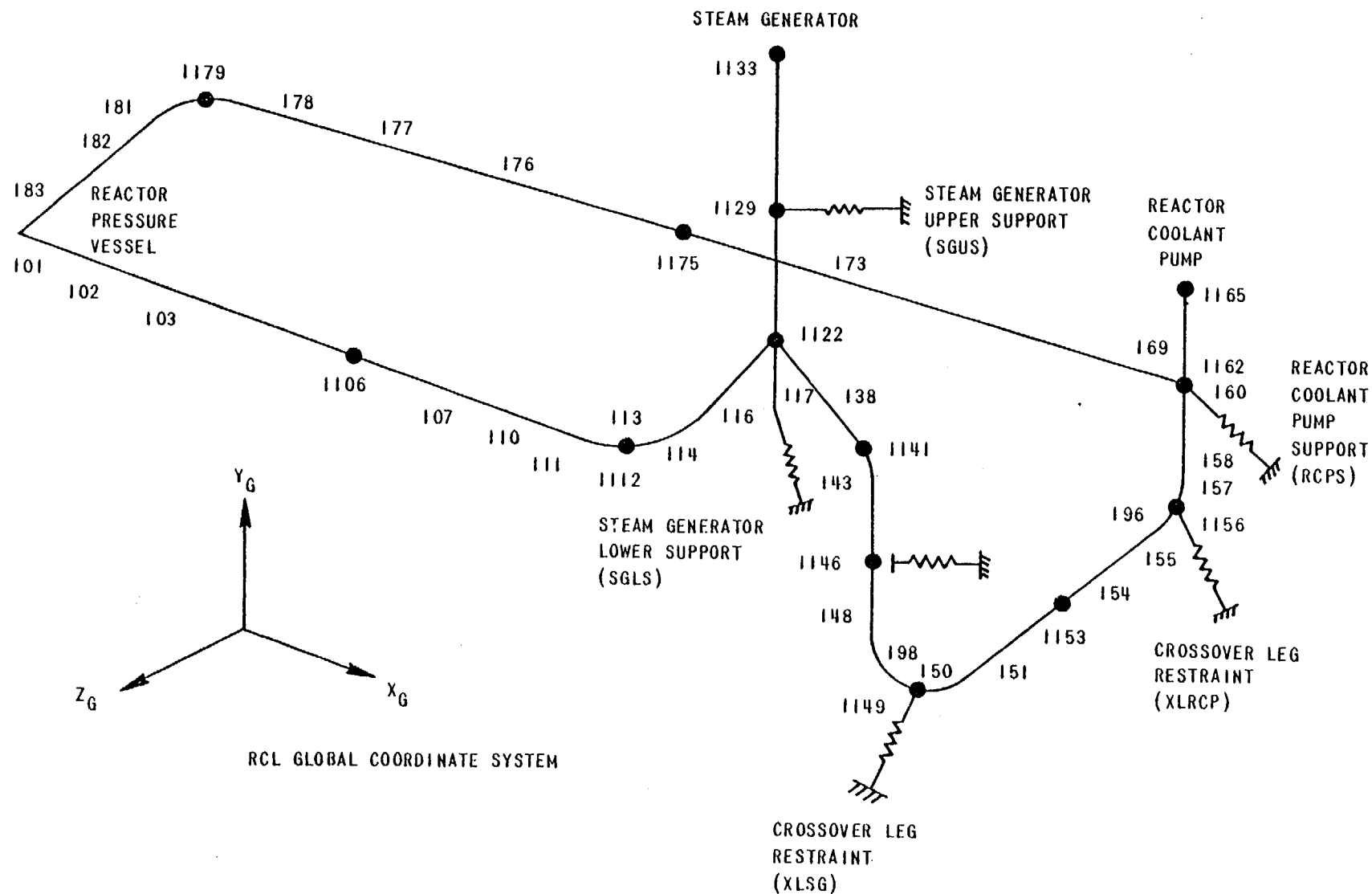


Figure 2.2-3 Reactor Coolant Loop FIXFM Model

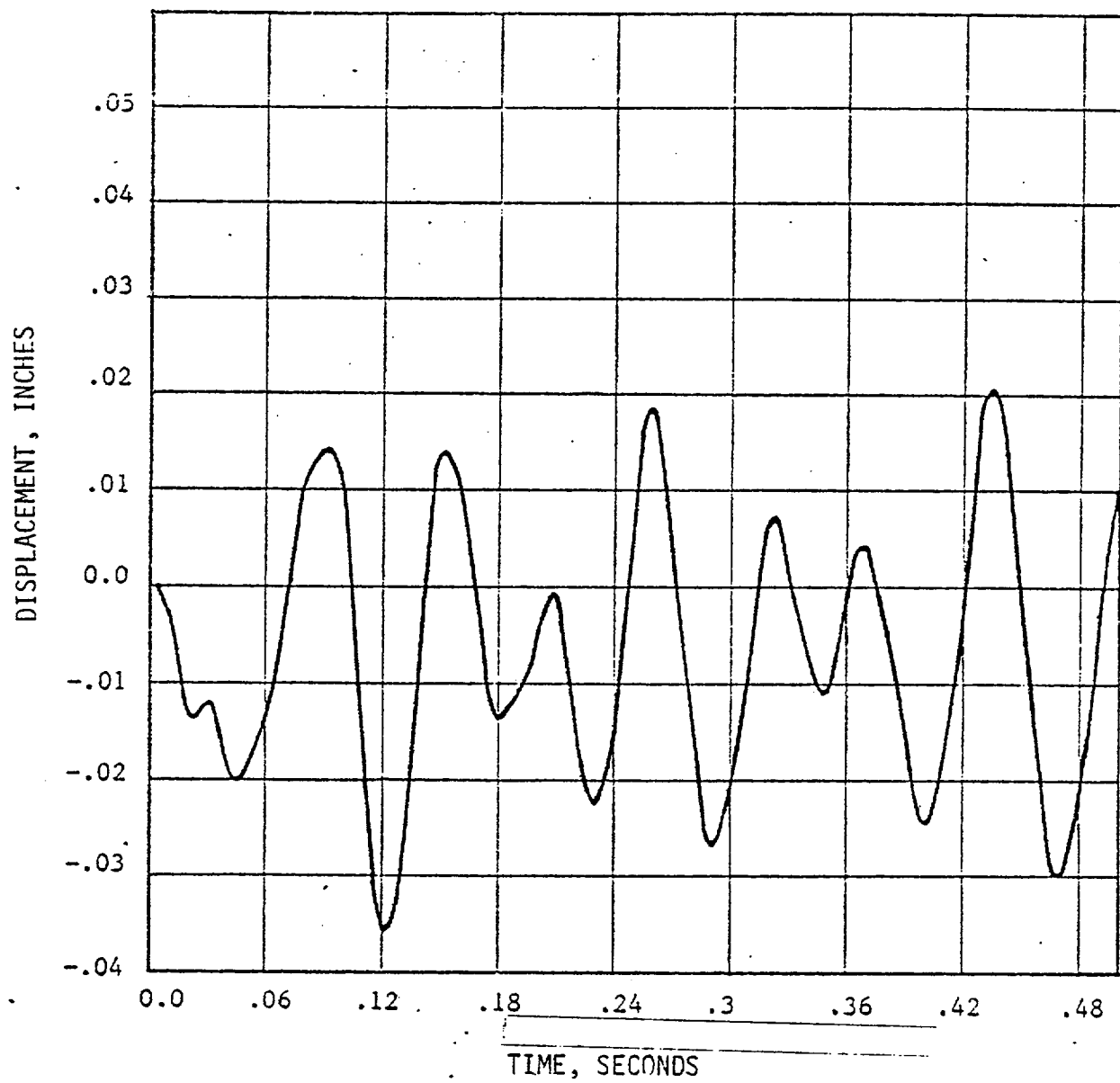


FIGURE 2.2-4

LOCA Displacement History
Imposed on Tube Model, X Direction

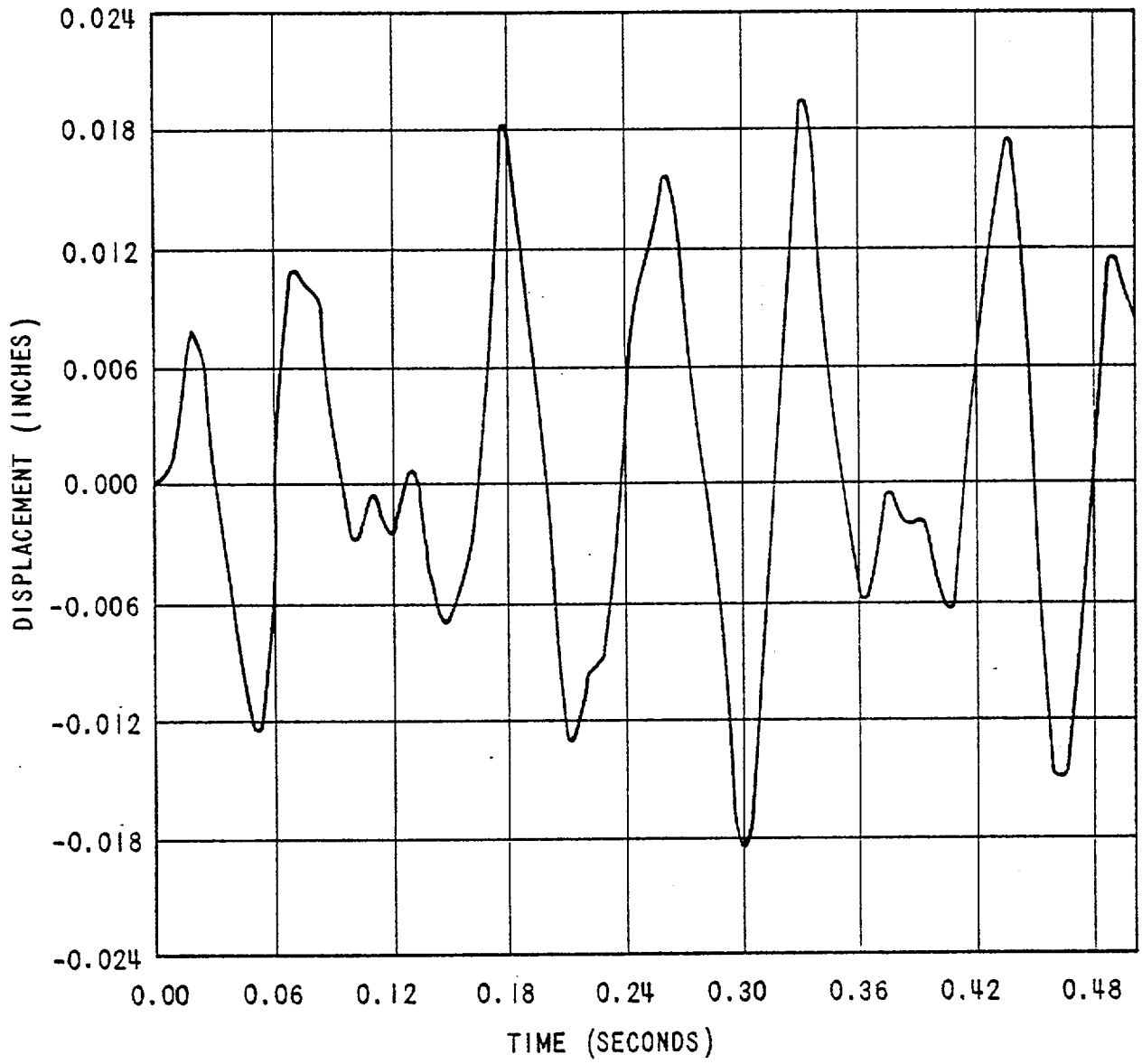


FIGURE 2.2-5 LOCA Displacement History Imposed on Tube Model, Y Direction

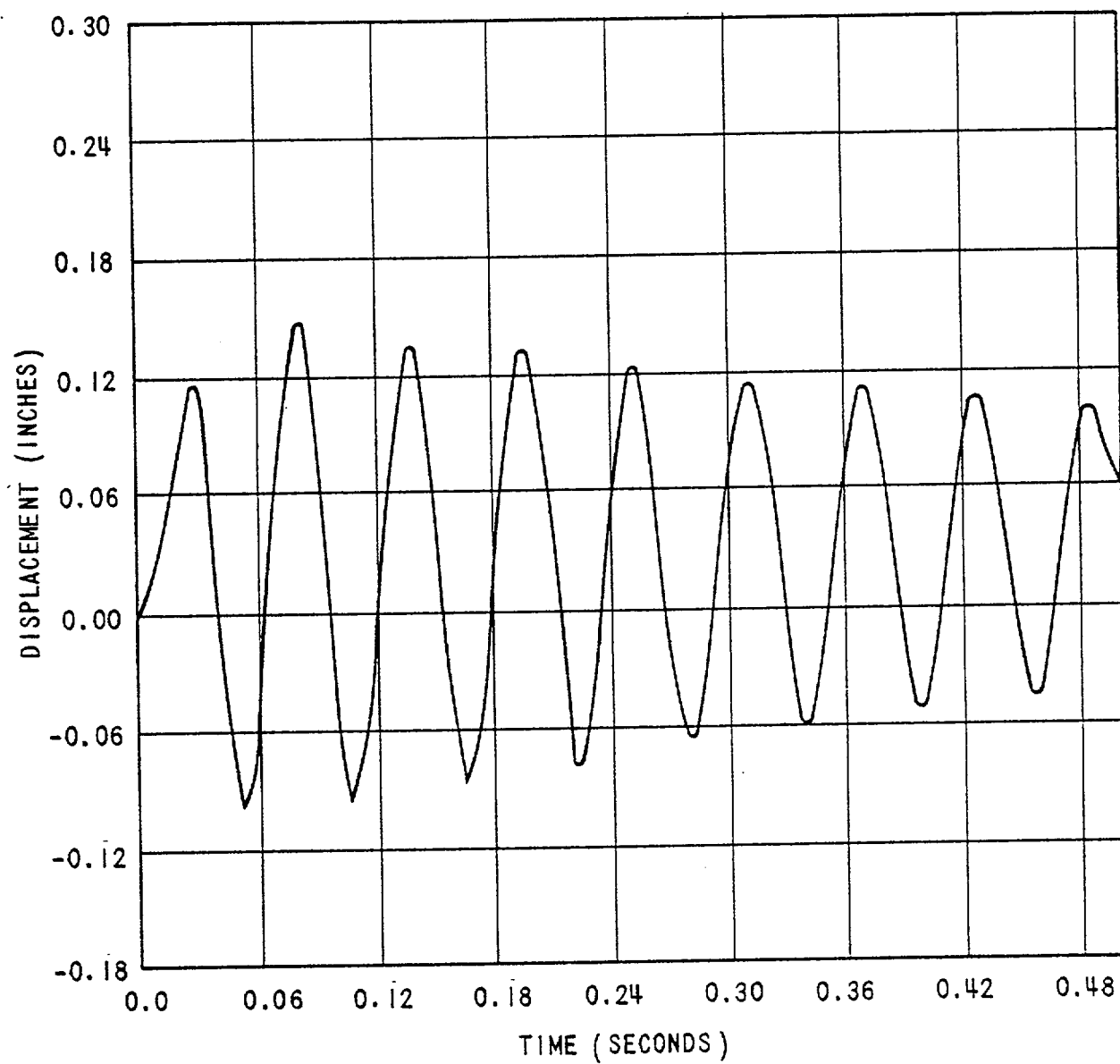


FIGURE 2.2-6 LOCA Displacement History Imposed on Tube Model, Z Direction

2.3 SEISMIC LOADS

2.3.1 METHOD OF DYNAMIC SEISMIC ANALYSIS

During an earthquake, the steam generator receives excitation from the motion of the reactor containment building. The dynamic response of the steam generator is evaluated by the response spectrum method of analysis. The response spectrum curve employed in the seismic analysis is an envelope of the floor response spectra at elevations in the reactor containment building corresponding to the upper and lower supports on the steam generator. The vessel is supported on four pads, which are an integral part of the channel head casting. High strength bolts secure the support pads to the steam generator field support system. Upper support brackets, located near the junction of the lower shell and transition cone, provide additional lateral stability for the vessel. A 51 Series model was selected which was considered as having support characteristics also appropriate for use with a Model D. The response spectrum employed in this analysis is illustrated in Figure 2.3-1. The damping ratio is 1%.

The structure is modeled by beam elements and massless elastic support elements. The elastic support elements, illustrated schematically by linear springs, are 6x6 matrices representing the stiffness of the upper and lower support systems. The stiffness of the attached piping is included in the support system. The beam element is a straight bar of uniform cross-section with six degrees of freedom per nodal point (three translations and three rotations). The element is capable of resisting axial forces, shear forces, bending moments and twisting moments. The influence of shear deformation on the lateral displacements is included so that the element can represent relatively deep structural shapes.

The mathematical model is comprised of a shell beam (elements 1 through 18), a tube bundle beam (elements 19 through 33), and a separator assembly beam (elements 34 through 40), as shown in Figure 2.3-2. A hinge has been introduced at node 38 of the separator assembly beam to model the connection between the swirl vane cylinders and the downcomer barrels. The longitudinal axes of the shell, tube bundle and separator assembly beams all coincide with

the longitudinal axis of the steam generator. The horizontal linkages, indicated by the double lines, represent coupling between the steam generator shell and the internals. The dry weight of the steam generator shell and internals, as well as the weight of the primary and secondary water, is lumped at the nodal points of the assemblage.

Stiffness and inertia properties of the steam generator and internals are formulated using the direct stiffness procedure.

The first step in the response spectrum analysis procedure is to determine the natural frequencies and corresponding mode shapes of the idealized structure. Using the mode shapes, the equations of motion are uncoupled. By means of the response spectrum curve, the maximum stresses and deflections in each mode are computed. The total modal response is obtained by taking the square root of the sum of the squares of the maximum response in each mode.

Both horizontal and vertical earthquake motions are assumed to be acting simultaneously. The stresses resulting from each of the three components of earthquake loading are computed independently, and the final stresses are then calculated by absolute summation.

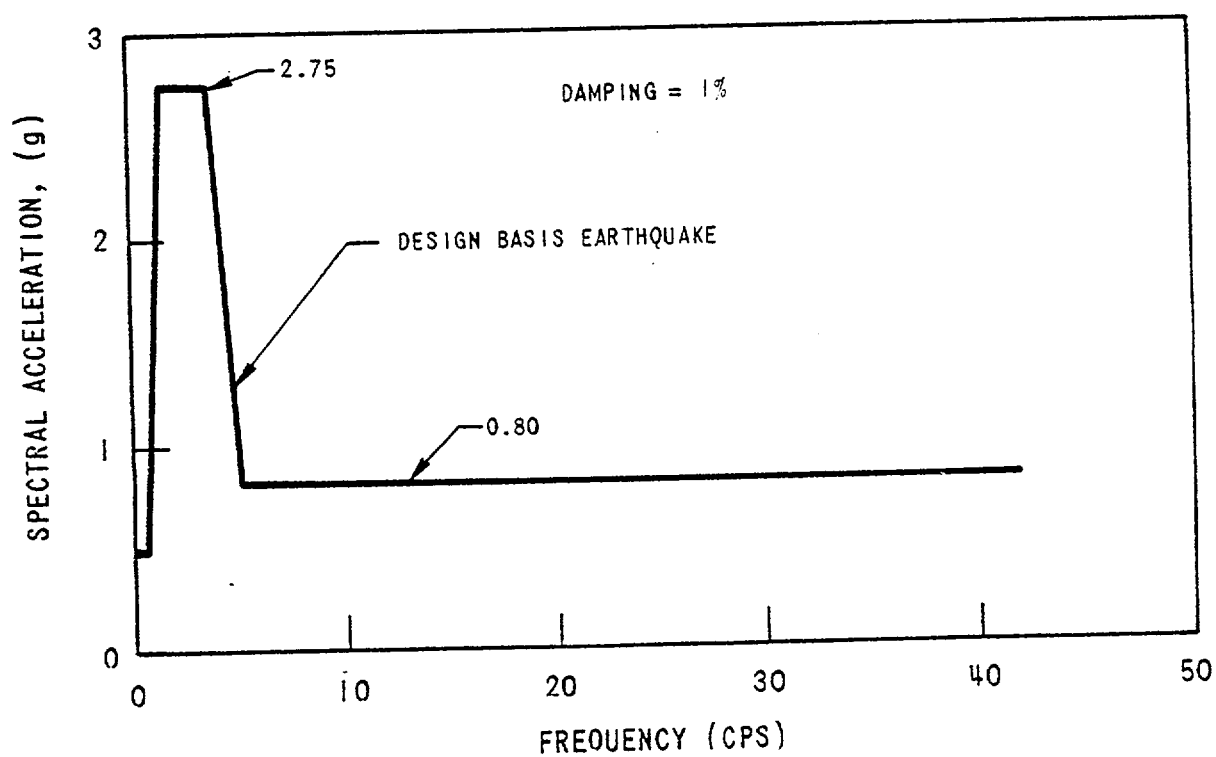


FIGURE 2.3-1 Horizontal Response Spectrum Curve

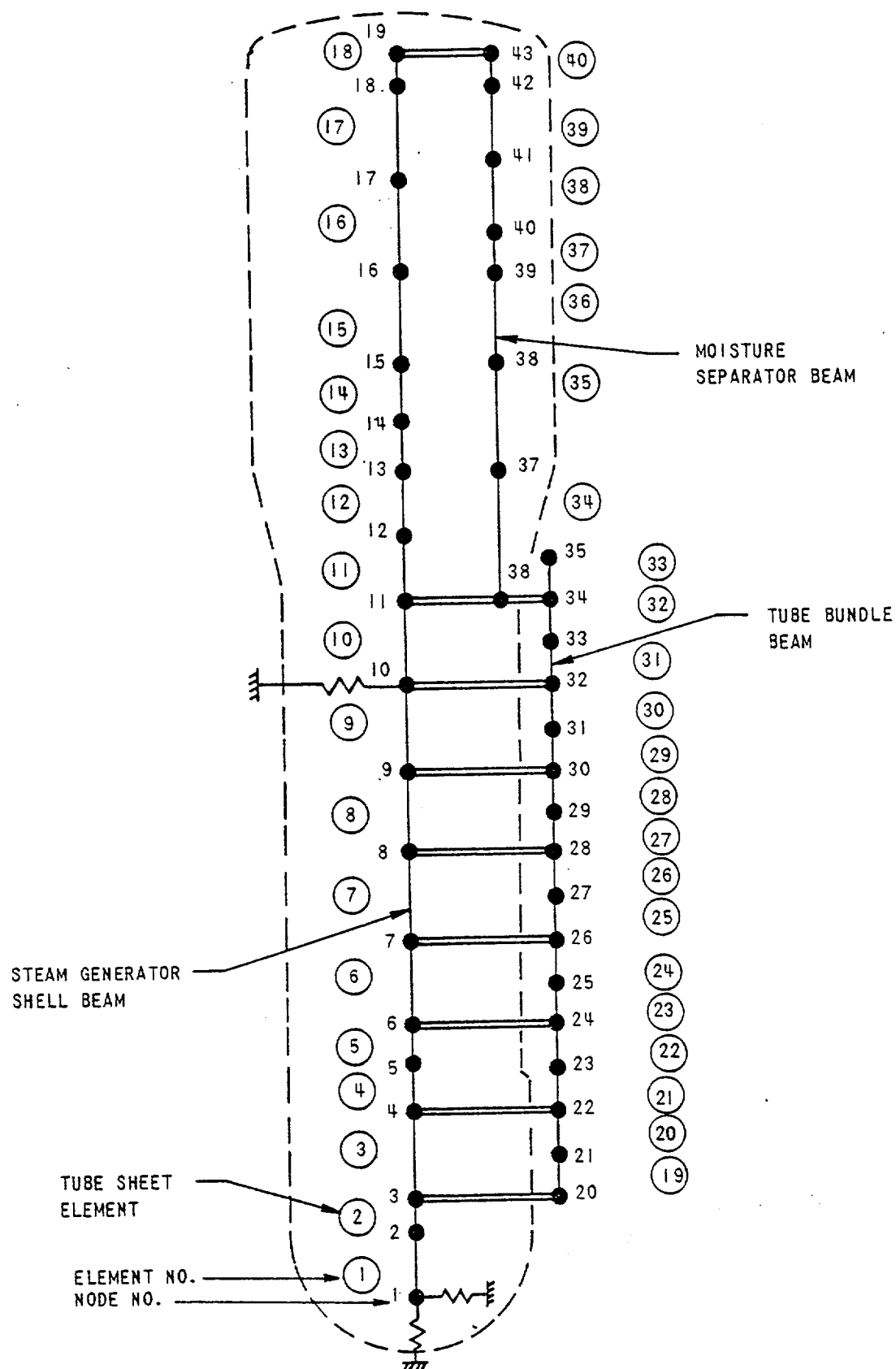


FIGURE 2.3-2 Seismic Model of Steam Generator

2.4 DESCRIPTION OF COMPUTER CODES

2.4.1 DESCRIPTION OF BLODWN-2 CODE

BLODWN-2 is a digital computer program for calculation of local fluid pressure, flow and density transients that occur in reactor coolant systems during a loss of coolant accident. This program applies to the subcooled, transition and saturated two-phase blowdown regimes. The Code can evaluate the pressure and velocity transients for a maximum of 2400 locations (120 equivalent pipes subdivided 20 times each).

BLODWN-2 is based on the method of characteristics wherein the resulting set of ordinary differential equations, obtained from the laws of conservation of mass, momentum and energy are solved numerically utilizing a fixed mesh in both space and time.

Although spatially one-dimensional conservation laws are employed, the code can be applied to describe three-dimensional system geometries through the use of the equivalent piping networks. Such piping networks may contain any number of pipes or channels of various diameters, dead ends, branches (with up to six pipes connected to each branch) contractions, expansions, orifices, pumps and free surfaces (such as in a pressurizer). All types of system losses (such as friction, contraction, expansion, etc.) are considered.

The adequacy of the BLODWN-2 code to predict acoustic wave behavior following a pipe rupture has been demonstrated by comparing BLODWN-2 calculation with various experimental results.^[3]

2.4.2 DESCRIPTION OF SATAN-V CODE

SATAN-V is a comprehensive digital computer program developed to simulate the entire range of the hydraulic transients caused by a loss-of-coolant accident in a Pressurized Water Reactor System. The code is capable

of describing the transient from the initial subcooled to transition, two-phase, and saturated steam blowdown.

The code uses the one-dimensional lumped parameter approach in which the entire primary loop system is divided into a maximum of 96 elements or equivalent flow branches. The fluid properties are considered uniform and thermodynamic equilibrium is assumed, in each element.

Pump characteristics, pump coast down and cavitation, core and steam generator heat transfer including the W-3 DNB correlation are incorporated in the simulation. A bubble rise-steam separation model and nuclear kinetics considerations are also included in the code.

The adequacy of the SATAN code to predict the hydraulic behavior during blowdown of the Reactor Coolant System, has been verified by comparing SATAN calculations with various experimental results.

2.4.3 DESCRIPTION OF STHRUST CODE

The STHRUST code computes blowdown hydraulic loads on the primary loop components from the blowdown information calculated by the SATAN-V code. The entire primary system is represented by the same two-loop model employed in the SATAN-V blowdown calculation.

The force nodes are selected along the two-loop geometric model of a reactor plant where the vector forces and their components in a global coordinate system are calculated. Each force node is associated with a control volume which may contain one of the two blowdown (SATAN) control volumes depending on the location of the force node in the system. Each force control volume in turn, has one or two associated apertures (flow areas). The force is calculated at each aperture.

The major input information required for the code are:

1. Blowdown hydraulic information which is read directly from the SATAN-V result tape.

2. The orientation of the force node in the system which is input as three projection coefficients along the three coordinate axes of the global coordinate system.

2.4.4 DESCRIPTION OF FIXFM CODE

FIXFM is a digital computer program which determines the time-history response of a three-dimensional structure excited by an internal forcing function. FIXFM accepts normalized mode shapes, natural frequencies, forcing functions and an initial deflection vector. Inputs are determined by the WESTDYN-7 program. The program sets up the model differential equations of motion, which are then solved numerically by a predictor-corrector technique of numerical integration. The modal contributions are summed at various nodal or mass points throughout the structure to derive the actual time-history response.

2.4.5 DESCRIPTION OF WESTDYN-7 PROGRAM

WESTDYN, a Westinghouse adaption of the A. D. Little Co. program^[5], is a special purpose program for the static and dynamic analysis of redundant piping systems with arbitrary loads and boundary conditions. It computes, at any point in the piping system, the forces, deflections, and stresses that result from the imposed anchor or junction loads, thermal gradients in the system, and gravity loads, in any combination of the three orthogonal axes. The piping system may contain a number of sections, a section being defined as a sequence of straight and/or curved members lying between two network points. A network point is 1) a junction of two or more pipes, 2) an anchor or any point at which motion is prescribed, or 3) any arbitrary point.

Any location in the system may sustain prescribed loads or may be subject to elastic constraint in any of its six degrees of freedom. For example, hangers may be arbitrarily spaced along a section and may be of the rigid, flexible, or constant force type.

The response to seismic excitation is analyzed by normal mode, response spectral superposition technique with a lumped mass system. The eigenvalue routines used are the Jacobi rotation and the Givens-Householder schemes^[6]. The maximum spectral acceleration is applied for each mode at its corresponding frequency from response spectra to obtain the amplitude of the modal coordinate for each mode. A basic assumption is that the maximum modal excitation of each mode occur simultaneously. The forces, deflections, support reactions, and stresses are calculated for each significant mode. The total response is computed by combining the contributions of the significant modes by several methods, one of which is the square root of the sum of the squares method.

The applicability and validity of the WESTDYN program has been demonstrated by running test problems and comparing the results from this program with the results of hand calculations, other programs, etc. A summary of these test problems is described in Reference [7].

2.4.6 DESCRIPTION OF SEISMIC ANALYSIS PROGRAM

The response spectrum method is used for the seismic analysis of the steam generator. The structure is idealized by beam elements with up to six degrees of freedom per joint. In addition, pin-jointed bar elements and elastic support elements can be used in the structural idealization.

Two computer programs, SHAKE2 and RESPAN, were written to perform the numerical computations. A description of the input data to the programs is presented, and example problems are given in Reference [8]. Output from program SHAKE2 includes the natural frequencies and mode shapes for the structure. RESPAN gives estimates of the maximum displacements, accelerations, forces, moments and stresses developed in the structure during the earthquake.

3.0 RESULTS OF ANALYSIS

3.1 TUBE ANALYSIS

3.1.1 DISCUSSION OF LOADING

Loading on the steam generator U-tubes under the faulted condition of the combined LOCA plus SSE is the summation of several effects. It consists of the pressure history resulting from a severance of the primary piping which for the purposes of this report is considered at the steam generator coolant outlet nozzle, the resultant shaking of the unit at its supports, and the loads imposed on the unit as a result of a SSE. Each contribution is studied independently, and the results superimposed.

As a result of LOCA, there are several loading phenomena which must be considered on the U-bend region due to the rapid decay of pressure within the tube. The first is the pressure history which manifests itself primarily as a rarefaction wave. The rarefaction wave data was generated in a primary coolant loop analysis which modeled the largest radius U-bend tube.

Following the rarefaction wave, a quasi-steady blowdown flow is established in the U-tube. This flow creates two other loading phenomena on the tube; centrifugal fluid forces in the bend region and frictional forces throughout the tube length.

The loading contribution due to shaking of the steam generator, induced by the pipe break, is obtained from a study of a 51 Series steam generator which has support characteristics considered to be also representative of a typical Model D unit. In this assumption, consideration was given to the comparison of support stiffnesses and steam generator weight distributions. The components of displacement caused by LOCA are input to the steam generator tube model at the upper support points.

In the case of loads imposed on the U-tubes due to the SSE, the seismic loads were derived from analysis of a 51 Series Unit.

3.1.2 LOADS ON TUBES

3.1.2.1 Assumptions

The analysis of the tube bundle shown in Figure 3.1-1, when subjected to LOCA and deadweight loading is accomplished through the use of the time-history capability of the STASYS computer code.^[9] The STASYS model consists of three-dimensional elastic pipe elements, both straight and curved.

The transition from the tube bundle to model employed several assumptions. These were:

1. Only the largest radius tube in the bundle was modeled. It was determined that this tube is the most severely loaded in addition to being the most flexible.
2. A conservative approach to the problem was taken by neglecting the U-tube anti-vibration bars. It has been previously determined that they do not significantly affect in-plane response of the tube bundle. Therefore, the mass of the tube bundle is not coupled to the modeled tube.

The largest bend radius, minimum wall tube is modeled with the wall thickness it is expected to have after forty (40) years of service (erosion causing a slight thinning). These tube dimensions are, for the Model D;

$$t = 0.036 \text{ ins.}$$

$$\text{O.D.} = 0.754 \text{ ins.}$$

$$R_B = 53.25 \text{ ins.}$$

Where t = wall thickness, ins.

O.D. = outside diameter, ins.

R_B = tube bend radius, ins.

Figure 3.1-2 shows the finite element model with its nodal points specified. The model extends to the second tube support plate, located at nodes 1 and 19. The uppermost support plate is located by nodes 4 and 16. Each of the support plate nodes are simply supported in the X and Y directions and pinned in the Z direction.

The node locations on the U-tube in the loop analysis pressure history correspond to those nodes specified in the finite element model used for the U-tube response study. Graphical representation of the pressure history at several nodes is shown in Figures 2.1-8 through 2.1-12.

The displacements, due to the shaking of the steam generator induced by the pipe break, are imposed on the nodes representing the two uppermost support plates, namely nodes 1 and 19, and 4 and 16. Figures 2.2-4, 2.2-5 and 2.2-6 depict these X, Y, and Z components, respectively.

The tube material properties are from ASME Section III Code^[10] and are those of the Nickel-Chrome-Iron alloy designated as SB-163 (Inconel). The elastic properties at 600°F are:

$$\begin{aligned} E &= 29.2 \times 10^6 \text{ psi} \\ \nu &= 0.3 \end{aligned}$$

where:

$$\begin{aligned} E &= \text{the Modulus of Elasticity} \\ \nu &= \text{Poisson's Ratio} \end{aligned}$$

The tube elements are attributed a density, ρ , composed of the sum of

$$\rho = \rho_T + \rho_F + \rho_S$$

where:

- ρ_T = the density of the tube material
- ρ_S = the density of the fluid within the tube
- ρ_F = the density of the secondary fluid displaced by the tube.

The value ρ_F is taken at its minimum value during the pressure history, which is 0.01736 lbs/in^3 . The tube material density is 0.304 lb/in^3 , and ρ_S is calculated at the normal operating conditions and found to be 0.002382 lb/in^3 . Therefore, the material density is input as:

$$\rho = 0.00083871 \frac{\text{lb-sec}^2}{\text{in}^4}$$

Also incorporated in the STASYS model is a mass damping coefficient for the structure. From Reference (9), this quantity is input as α , where:

$$\alpha = 4\pi\xi f$$

with ξ = fraction of critical damping, %

f = expected frequency, hz

Previous studies on similar steam generator tube bundles indicate that the natural frequency of the large 51 Series U-tube is approximately 6 hz. Assuming a Model D tube will have approximately the same natural frequency and assuming a generally accepted value of 1% damping, the resulting mass damping coefficient is:

$$\alpha = 0.7539$$

3.1.2.2 Secondary Blowdown Effects

The centrifugal and frictional forces, caused by the quasi-steady blowdown phase, are calculated below;

1. The centrifugal force per unit length is

$$W_c = M_\ell \frac{V^2}{R}$$

where:

$$\begin{aligned}M_l & \text{ fluid mass per unit length} \\ & = \rho A/g \\ V & = \text{fluid velocity} \\ R & = \text{tube bend radius}\end{aligned}$$

This force is directed radially outward and has a peak value of 6.1 lb/ft for a 5 ft. radius bend and a 14.1 lb/in for a 2-3/16 in. radius bend. These numbers are calculated by taking the worst combination of mass velocity and density from the large tube output.

2. The friction force per unit length is given by

$$W_f = \frac{f}{D} \frac{L}{2} \frac{\rho}{g} AV^2$$

where:

$$\begin{aligned}f & = 0.015 \\ D & = \text{the tube diameter (0.718 in)} \\ \rho & = \text{density} \\ V & = \text{velocity} \\ g & = \text{gravity} \\ L & = \text{characteristic length}\end{aligned}$$

Applying the largest mass velocity and lowest density encountered in the pressure history study (Mass velocity = 3300 lbs/sec-ft² and $\rho = 31 \text{ lb/ft}^3$) results in

$$W_f = 3.86 \frac{\text{lbs}}{\text{ft.}}$$

The centrifugal and friction forces calculated above contribute insignificant stresses in comparison to the rarefaction wave loading as may be seen in the following sections.

3.1.3 STRESS LIMITS

The stress limits imposed on the U-tubes under Faulted condition limits are provided in the Appendix F criteria.^[11] For an elastic system analysis and an elastic component analysis the stress limits for nuclear components are:

$$P_m < \text{the smaller of } 2.4S_m \text{ or } 0.70 S_u$$
$$P_m + P_B < \text{the smaller of } 3.6S_m \text{ or } 1.05 S_u$$

where:

- P_m = Primary Membrane Stress, psi
- P_B = Primary Bending Stress, psi
- S_m = Allowable Stress Intensity at temperature^[10], psi
- S_u = ultimate stress from engineering stress-strain curve at temperature, psi

For the tube material, SB-163, with a specified minimum yield of 35 KSI^[12] at temperature,

$$S_m = 26,000 \text{ psi}$$

and

$$S_u = 75,000 \text{ psi}$$

applying these values results in the stress limits of:

$$P_m = 52,500 \text{ psi} = 0.7S_u$$
$$P_m + P_B = 78,750 \text{ psi} = 1.05 S_u$$

3.1.4 RESULTS FOR A HEALTHY TUBE

3.1.4.1 Combined Stresses for All Loads

The results presented here are stress intensities generated in a tube with D series proportions, thinned after forty years service, and lacking any flaws, when loaded by a combination of LOCA and SSE effects.

The Primary Membrane Stress Intensity is a maximum at $t=0$ seconds, when the tube is under the influence of its highest internal pressure differential. At this point in time:

$$P_m = 16,790 \text{ psi}$$

This stress is calculated from torus geometry equations, as applicable to the U-bend region, using the smallest tube bend radius.

The maximum response of the U-tube to the combined LOCA effects (rarefaction wave plus external shaking) is shown on Figures 3.1-3 through 3.1-12, for selected node points. Primary Membrane plus Primary Bending Stress Intensity ($P_m + P_B$) is found to be a maximum at the location associated with node 16, shown in Figure 3.1-11, at $T=0.06$ seconds after the primary coolant outlet line severance. This value, combined with the maximum seismic bending stress of 5,000 psi (see section 3.1.5.2 part 3) is:

$$P_m + P_B = 55,000 \text{ psi.}$$

Each of the values presented are within the specified limits of:

$$P_m < 52,500 \text{ psi}$$

$$P_m + P_B < 78,750 \text{ psi.}$$

In obtaining the results for the combination of the loading phenomena due to LOCA, several conservative assumptions are made. The STASYS computer code output gives values of maximum stress at a specific plane on the tube length, but it does not indicate circumferentially on the plane, where the stress occurs. In the multi-degree of freedom system studied here, these stress locations may be located anywhere around the circumference, regardless of this fact, it was convenient to superimpose all values absolutely at a given output location. The final stress output, also reflects the combination of twice the maximum shear stress for each of the rarefaction and shaking effects. Finally, the seismic stresses are superimposed absolutely on the stress effects due to LOCA. The maximum seismic stress intensity found on the tube's worst location is assumed to occur at every location on the model.

3.1.4.2 Stresses Due to Individual Loads

1. Pressure History

The effects of the rarefaction wave in the large tube are graphically represented in terms of stresses, in Figures 3.1-8 through 3.1-17, and displacements in Figures 3.1-18 through 3.1-22.

Several locations of the U-tube are selected to give a representative picture of the output for times between 0.0 seconds and 0.5 seconds which represented the period of maximum load application. The locations chosen correspond to nodal points 4, 8, 10, 12 and 16 for the stresses, and nodal points 5, 7, 10, 13 and 15 for the deflections. The location of these points can be found in Figure 3.1-2.

The stress output depicts: the axial component of stress due to pressure, the maximum bending stress at the outer wall, the maximum stress on the outer wall, and the minimum stress on the outer wall. These figures show that the bending stress, due to the rarefaction wave, is the major contributor to the stress level in the tubes.

The bending stress is a maximum at the upper tube support plates. At node location 16, the maximum stress reaches a value of 48,000 psi, at $t=0.06$ seconds. (See Figure 3.1-17).

The frictional force due to the quasi-steady blowdown flow in the tube is calculated to be a maximum of 3.86 lb/ft. This force corresponds to a shear stress of less than 2 psi and is therefore negligible.

The load from the fluid centrifugal force in the U-tube region causes less than 400 psi axial stress in the tube. This was considered negligible. A study was made on the bending which occurs in the U-tube region due to the variation of fluid mass and velocity with position. It was found that there is less than a one pound change in centrifugal force around the tube and therefore the bending stress arising are also neglected.

2. Effects on tube bundle of support movement due to LOCA

The effect of the shaking of the steam generator due to the forces associated with the severance of the primary coolant outlet pipe, is represented graphically in Figures 3.1-23 through 3.1-27, for the induced stresses; and in Figures 3.1-28 through 3.1-41 for in-plane and out-of-plane displacements.

The maximum stress value which is also very nearly the maximum bending stress, reaches a peak of 12,500 psi. This value occurs at node 10 at $t=0.2$ seconds, as shown in Figure 3.1-25.

Comparison of these values with the rarefaction wave effect indicates this to be a secondary effect on the tube stresses.

3. Tube Bundle Response due to SSE

The seismic stresses developed in the steam generator tubes are summarized in Table 3.1-1. The maximum normal stresses (SIGI and SIGJ) at the ends of each element, together with the maximum shear stress (TAU), is printed for the SSE loading. Node I denotes the lower end of the element, while node J denotes the upper end. Element and nodal point numbers refer to the mathematical model illustrated in Figure 2.3-2. The values given represent the maximum stresses that are expected to occur as a result of the simultaneous application of the three components of the design basis earthquake. Since earthquakes are oscillatory in nature, the sign on these quantities can be either plus or minus, i.e. tensile or compressive.

The maximum normal stress in the tube bundle, 5.0 ksi, occurs at the elevation of the uppermost tube support plate (node 34, Figure 2.3-2) and is primarily due to bending.

3.1.5 PERMISSIBLE CRACK LENGTHS FOR A HEALTHY TUBE

Since tube flaws, when they occur, do so in the vicinity of the tubesheet region, this area of the tube has been investigated for maximum permissible flaw sizes under SSE plus LOCA loads. The loads on a given tube consist

of those due to rotation of the tube sheet caused by the rarefaction wave and the loads due to modal response of the tube under seismic and blowdown shaking.

Tube stresses due to LOCA have been conservatively estimated as due to the pressure differential across the tube, which is a maximum at normal operating conditions just prior to the pipe rupture; plus those due to the maximum encountered rotation, θ , of the tube sheet. The shortest tube length, L , investigated is that between the top of the tubesheet and the first baffle plate. Both ends are assumed to carry a moment, (See Figure 3.1-40).

The maximum rotation of the tube sheet is derived from the tubesheet analysis.

$$\theta_{\max} \text{ about the divider lane} = 0.64 \times 10^{-3} \text{ degrees}$$

$$\theta \text{ normal to the divider lane} = 0.34 \times 10^{-3} \text{ degrees}$$

$$\theta_{\max} = \sqrt{(0.64^2 + 0.34^2)} \times 10^{-3} = 0.72 \times 10^{-3} \text{ degrees}$$

The rotation in the plane of the tubesheet is 0.13×10^{-3} degrees and is considered negligible. From Roark^[13], for a beam with one end fixed and one end supported with an end couple:

$$M_{\max} = M_o = \frac{4EI\theta}{L}$$

$$\sigma_{\max} = \frac{MR}{I} = \frac{4ER\theta}{L}$$

$$E = 29.2 \times 10^6 \text{ psi}$$

$$\theta_{\max} = 0.72 \times 10^{-3} \text{ degrees} = 13 \times 10^{-6} \text{ radians}$$

$$R_{\max} = 0.377 \text{ in.}$$

$$L_{\min} = 7.0 \text{ in.}$$

$$\sigma_{\max} = \pm \frac{4 \times 29.2 \times 10^6 \times 0.377 \times 13 \times 10^{-6}}{7.0}$$

axial

$$= \pm 80 \text{ psi}$$

As can be seen, tubesheet rotation and the stresses induced by this effect are negligible.

Flaws in Westinghouse steam generator tubes have been predominantly oriented in the axial direction. Tests at Westinghouse with tubes loaded by combined internal pressure and axial bending moment and with axial slots simulating typical flaws, have shown that the axial loads do not significantly affect crack propagation until the axial stress is increased to levels close to the tube yield stress.

The stresses caused by the pressure differential across the tube are calculated by:

$$\sigma_{\text{hoop}} = \frac{PR}{t} ; \sigma_{\text{axial}} = \frac{PR}{2t}$$

For D series tube proportions,

$$\Delta P_{\max} = 1485 \text{ psi (maximum expected operating } \Delta P)$$

$$R_{\text{mean}} = 0.359 \text{ in}$$

$$t_{\min} = 0.036 \text{ in}$$

$$\sigma_{\text{hoop}} = 14,800 \text{ psi}$$

$$\sigma_{\text{axial}} = 7,400 \text{ psi}$$

Blowdown shaking also introduces additional stresses. Since the stress in the straight tube section near the U-bend region due to its dynamic response, is higher than that near the tube sheet, this stress is used. In the top, straight section, the maximum stress due to shaking is 8100 psi, (see Fig. 3.1-23). Additional axial bending stress due to seismic response in the tubesheet vicinity, from the seismic analysis, is:

$$\sigma_{\max} = \pm 1000 \text{ psi}$$

The combined axial stresses are:

	<u>D Series</u>
Pressure =	7400 psi
LOCA Shaking =	8100 psi
Seismic =	<u>1000 psi</u>
Total	16,500 psi

Tube material yield stress, at 600°F is [12]:

$$S_y = 35000 \text{ psi}$$

As can be seen, the combined axial stresses are approximately 50% of yield stress and will therefore not be considered as contributing to crack propagation.

The hoop stress due to internal pressure is the most significant stress tending to cause crack formation. Considering the D series tube:

$$\sigma_{\text{hoop}} = 14800 \text{ psi}$$

From Reference [14], Equation 2, the maximum permissible flaw size is derived from:

$$\sigma_f = \sigma_h \cdot M$$

where:

$$\sigma_f = \text{flow stress, psi} = \frac{S_y + S_u}{2.4} \text{ from Ref. [6]}$$

S_y = yield stress, psi

S_u = ultimate stress, psi

σ_h = nominal hoop stress, here equated to the stress intensity

$M = f(\lambda)$ = stress magnification factor from Fig. 3.1-41

$$\lambda^2 = \frac{C^2}{Rt} \sqrt{12(1-\nu^2)}$$

C = half crack length, ins

R = mean radius, ins

t = tube wall thickness, ins

ν = Poissons Ratio

For the minimum geometry tube and using nominal material properties;

$$S_y = 35000 \text{ psi, at } 600^\circ\text{F}^{[12]}$$

$$S_u = 75000 \text{ psi, at } 600^\circ\text{F}^{[12]}$$

$$\sigma_f = \frac{S_y + S_u}{2.4} = 45800 \text{ psi}$$

From the referenced equation

$$M = \frac{\sigma_f}{\sigma_h} = \frac{45,800}{14,800} = 3.1$$

From Fig. 3.1-41

$$\lambda = 5.0, \text{ for } M = 3.1$$

$$\text{from } \lambda^2 = \frac{C^2}{Rt} \sqrt{12(1-\nu^2)}$$

$$C^2 = \frac{\lambda^2 Rt}{\sqrt{12(1-\nu^2)}}, \text{ and with } R = 0.359 \text{ ins; } t = 0.036 \text{ ins. for the 'D' series tube geometry.}$$

$$= \frac{(5.0)^2 \times 0.359 \times 0.036}{\sqrt{10.92}}$$

$$C = 0.32 \text{ in.}$$

Therefore the total allowable crack length is 0.64 inch for the 'D' series

3.1.6 TUBE THINNING

An investigation was performed to determine the margin of tube wall thinning which could be tolerated without exceeding ASME Code, Section III Faulted Condition stress limits when subjected to combined LOCA and SSE loads. Section 3.1.3 outlines the Faulted Condition limits; these are:

Allowable Primary Membrane Stress, $P_m = 52,500$ psi

Allowable combined Primary Membrane and Bending Stress, $P_m + P_B = 78,750$ psi

A parametric study, varying the tube wall thickness showed that D Series tubes with a minimum wall thickness of:

$t = 0.026$ in. (0.75 in. nominal diameter tubing)

would have combined bending and membrane stresses of:

$P_m + P_B = 75,100$ psi (0.75 in. nominal diameter)

which is less than the allowable limit.

For the 51 Series Steam Generator tubing (0.875 in nominal diameter and 0.050 in. nominal wall thickness) a simplified calculation to determine minimum uniform wall thickness based on combined LOCA and SSE loading conditions and ASME Code, Section III, Faulted Condition stress limits results in a value of 0.021 in. This thickness results in combined bending and membrane stress of:

$P_m + P_b = 72,800$ psi (0.875 in. nominal diameter tube)

The analysis for the study (on the D Series tubing) was identical to that described earlier in Section 3.1.1, with the exception of the tube wall thickness being 26 mils. Figures 3.1-42 through 3.1-46 give the stresses at the various node locations, due to the LOCA rarefaction wave; Figures 3.1-47 through 3.1-51 give the stresses at the various node locations due to shaking caused by LOCA; Figure 3.1-52 shows the maximum stress intensity which occurs at Node 16.

The Primary Membrane Stress Intensity is a maximum at $t = 0$ seconds, when the tube is under the influence of its highest internal pressure. At this point in time:

$$P_m = 23,000 \text{ psi}$$

This stress is calculated from torus geometry equations, as applicable to the U-bend region using the smallest bend radius. The Primary Membrane plus Primary Bending Stress Intensity ($P_m + P_B$) is found to be a maximum at the location associated with node 16, shown in Figure 3.1-52 at $t = .06$ seconds after the primary coolant outlet line severance. This value, when combined with the maximum seismic bending stress of 5000 psi, is,

$$P_m + P_B = 75,100 \text{ psi}$$

Summary

The minimal wall thicknesses determined here are based on several degrees of conservatism. First, the maximum stress values which occur at different locations in the tube bundle have been treated as if they acted at the same point. Second, the maximum stress levels resulting from each

* The various axial and circumferential (clock) positions, and the stress orientations at a specific point have been treated as an absolute summation

contributing load do not necessarily occur simultaneously; but are assumed to be simultaneous. Third, the ASME Faulted Condition stress limits are conservative when based on Engineering Stress-Strain Curves for determination of ultimate stress. A comparison of developed stresses for any given plastic strain in Figure 3.3-4 against that of Figure 3.3-5 illustrates this point.

The minimum wall thicknesses given here were governed by the conservatively assumed stress state at a particular location in the tube bundle (Node 16, tangent to the curved, U-bend region). The minimum wall thickness required to sustain LOCA plus SSE loadings at other locations (e.g., straight section above the tube sheet: Node Location 1) would be substantially lower as can be seen in Figures 3.1-3 through 3.1-12 for various Nodal locations.

Summary

Table 3.1-2 summarizes tube wall thickness and the equivalent stresses generated by combined DBA plus SSE loads.

3.1.7 EXTERNAL PRESSURE EFFECTS

Subsequent to primary system blowdown, the differential pressure across the tubes will be secondary side pressure minus containment back pressure.

Westinghouse tests of the 51 series 7/8 in. diameter, 0.050 in. wall straight tube indicate that a collapse pressure of 6400 psi at room temperature was obtained, for annealed Inconel material of 51,000 psi yield strength, at 0% tube ovality. An analytical correlation based on plastic limit analysis was developed in order that extrapolation of test results to tubes of different yield strength and wall thickness would be possible. This correlation was applied to determine the predicted collapse pressure for straight Inconel tubing with minimum yield strength for the ASTM material at design temperature and minimum specified wall thickness. This results in a collapse pressure of approximately 3000 psi for 0% ovality and 1830 psi for the maximum allowable 5% ovality at 600°F. Tests on U-bend specimens

of different radii show that collapse pressure increases with reduced bend radius and is always higher than the straight tube due to toroidal surface curvature effects.

TABLE 3.1-1
SSE STRESSES IN STEAM GENERATOR TUBES

<u>ELEMENT</u>	<u>SIGI</u>	<u>SIGJ</u>	<u>TAU</u>
19	1.0	1.0	.0
20	1.0	.8	.0
21	.8	.9	.0
22	.9	.8	.0
23	.8	1.0	.0
24	1.0	.9	.0
25	.9	.8	.0
26	.8	.8	.0
27	.8	.8	.0
28	.8	.8	.0
29	.8	1.0	.0
30	1.0	1.8	.0
31	1.8	2.4	.1
32	2.4	5.0	.1
33	5.0	.1	.1

Notes:

- (1) Units . . . ksi
- (2) Node and element numbers refer to Figure 2.3-2
- (3) Maximum normal stress = 5.0 ksi
- (4) See page 3.1-9 for definitions of stresses

TABLE 3.1-2

STRESSES DUE TO TUBE THINNING

Wall Thick- ness, ins.	Nominal Tube Diameter, ins.	Tube Type	Combined Primary Membrane and Bending Stresses, $P_m + P_B$, psi
0.036 ⁽¹⁾	0.75	Model D	55,000 ⁽²⁾
0.026	0.75	Model D	75,100 ⁽²⁾
0.021	0.875	Series 51	72,800 ⁽²⁾

Notes:

(1) Minimum D Series tube (0.039 in.) less 0.003 in. (estimated 40 year erosion)

(2) Allowable Faulted Condition Combined $P_m + P_B = 78,750$ psi

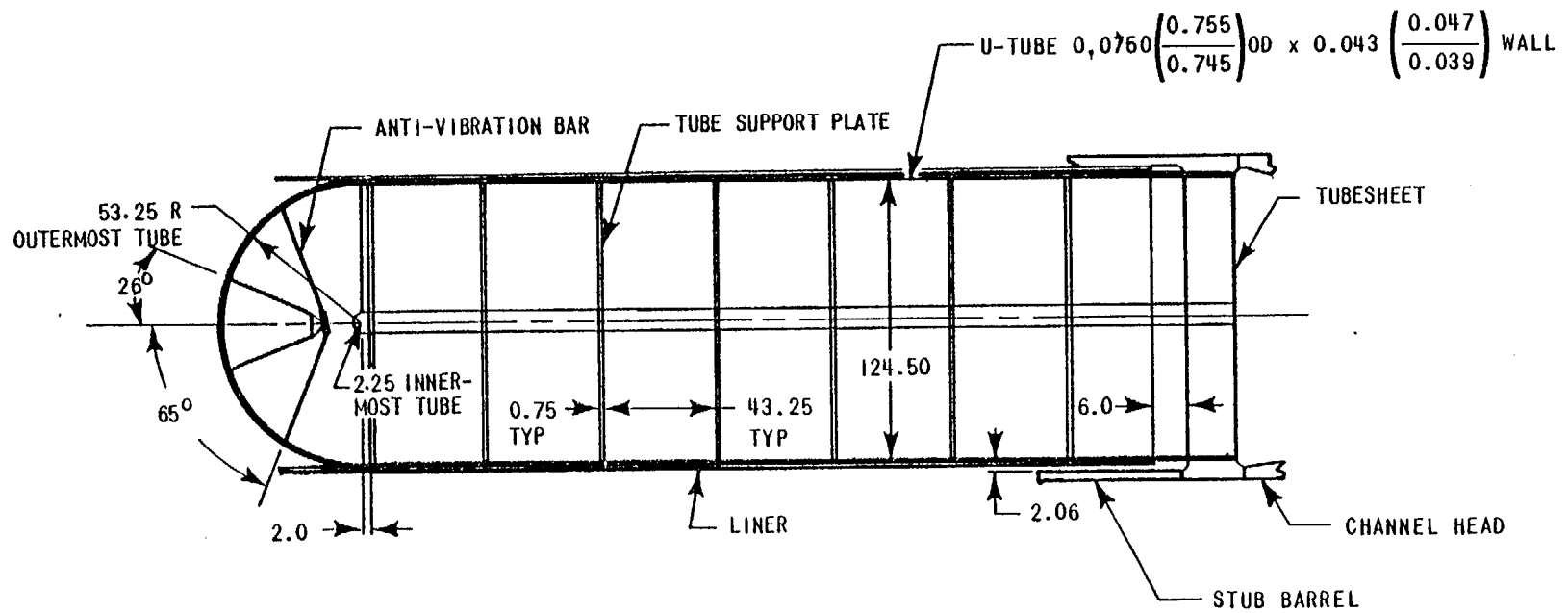


Figure 3.1-1. Model-D Steam Generator U-Tube Configuration

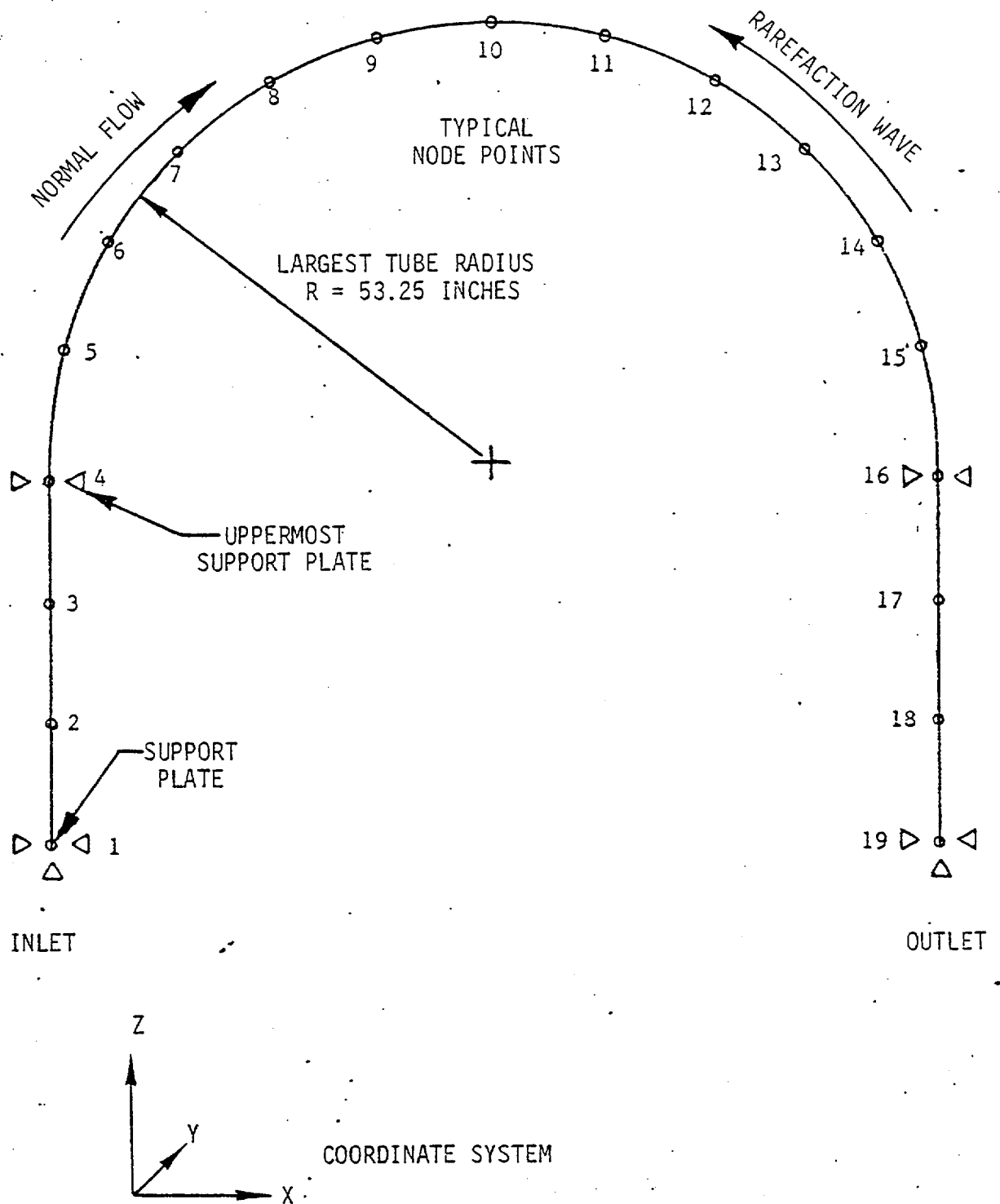


Figure 3.1-2

STASYS Tube Model - Elastic
Pipe Elements Model D Steam
Generator Largest Tube

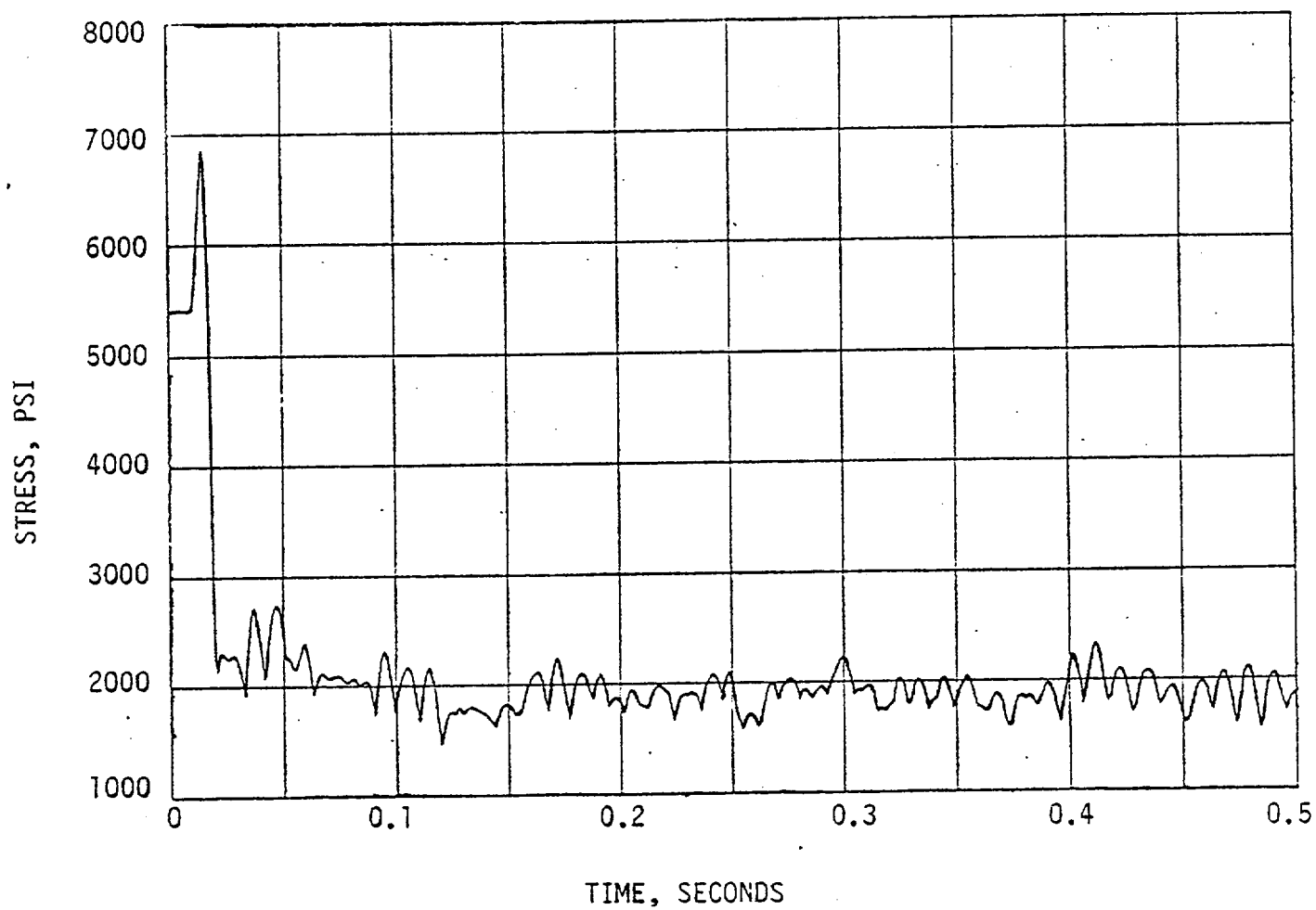


Figure 3.1-3 Maximum Stress Intensity on Tube Outer Wall
Node Location 1 - Total LOCA Effect

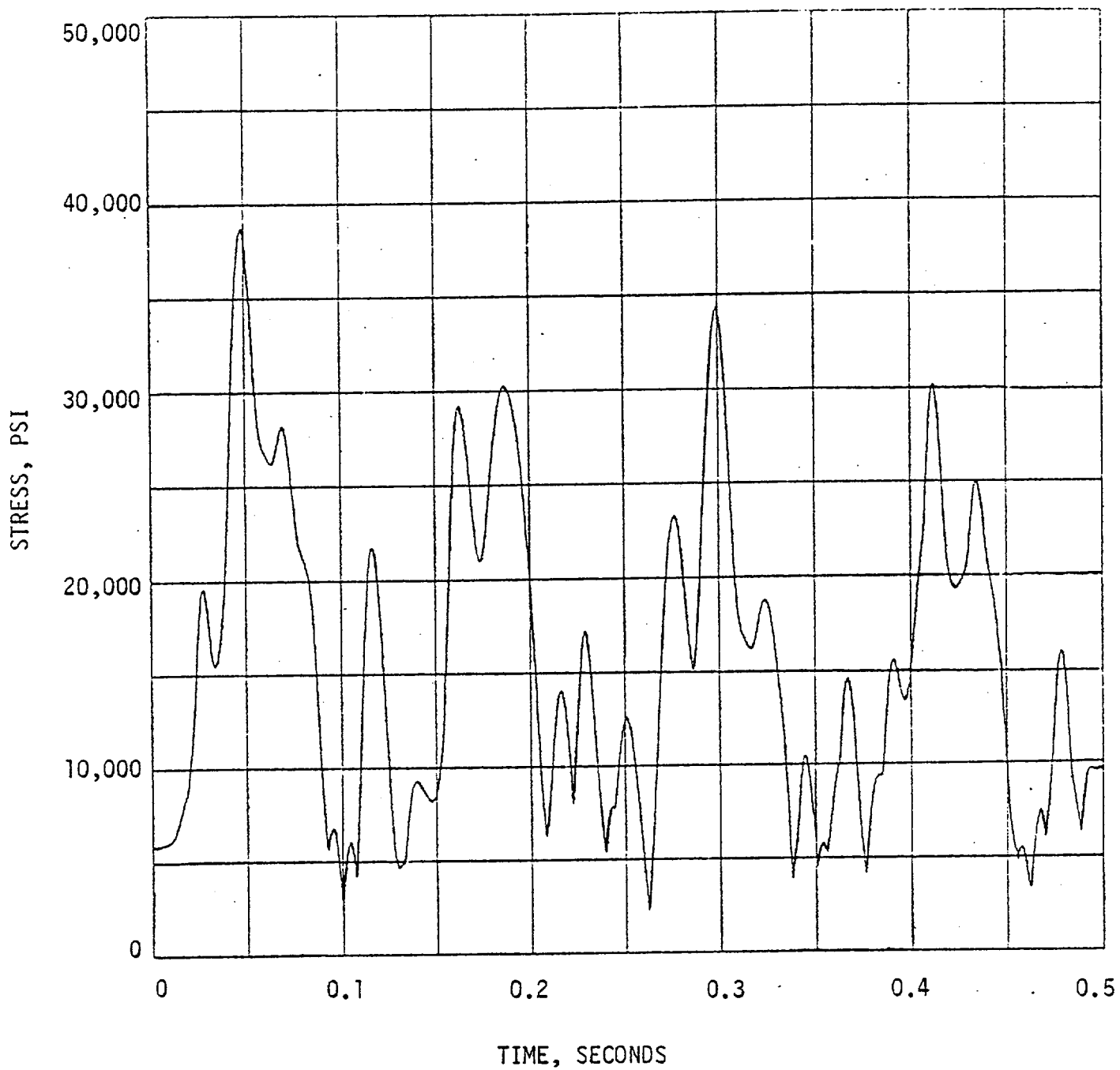


Figure 3.1-4 Maximum Stress Intensity on Tube Outer Wall
Node Location 3 - Total LOCA Effect

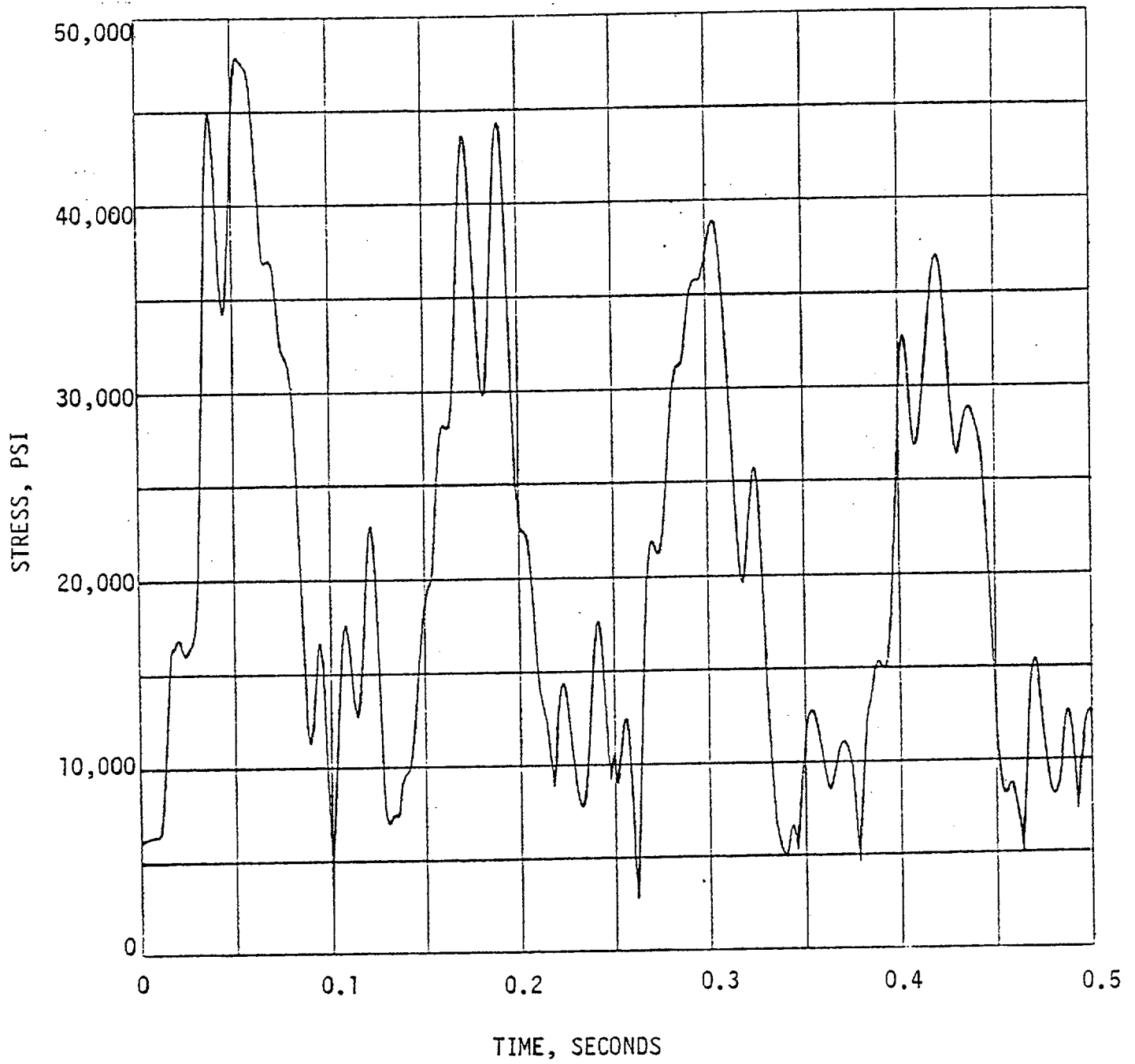


Figure 3.1-5 Maximum Stress Intensity on Tube Outer Wall
Node Location 4 - Total LOCA Effect

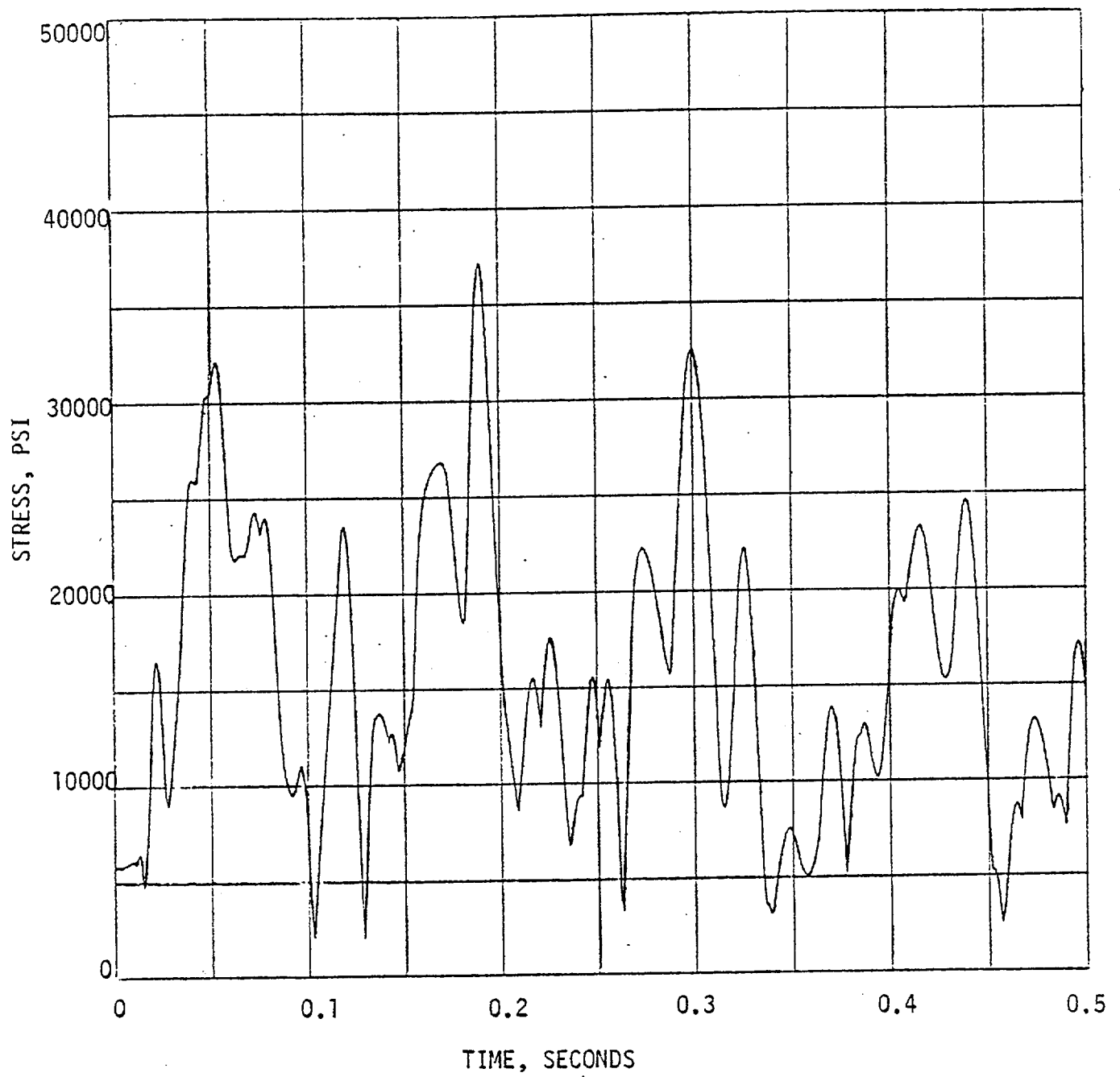


Figure 3.1-6 Maximum Stress Intensity on Tube Outer Wall
Node Location 6 - Total LOCA Effect

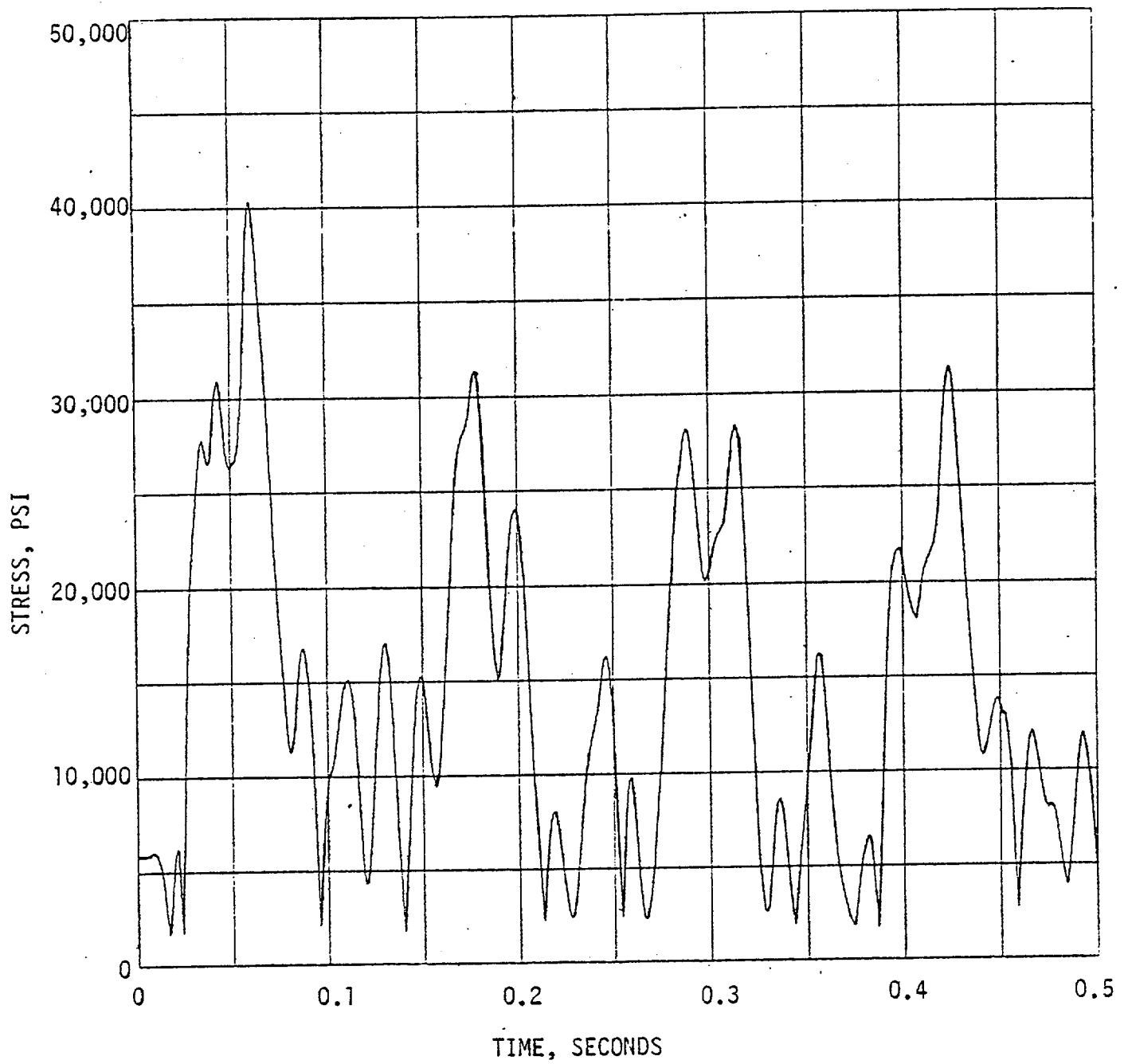


Figure 3.1-7 Maximum Stress Intensity on Tube Outer Wall
Node Location 8 - Total LOCA Effect

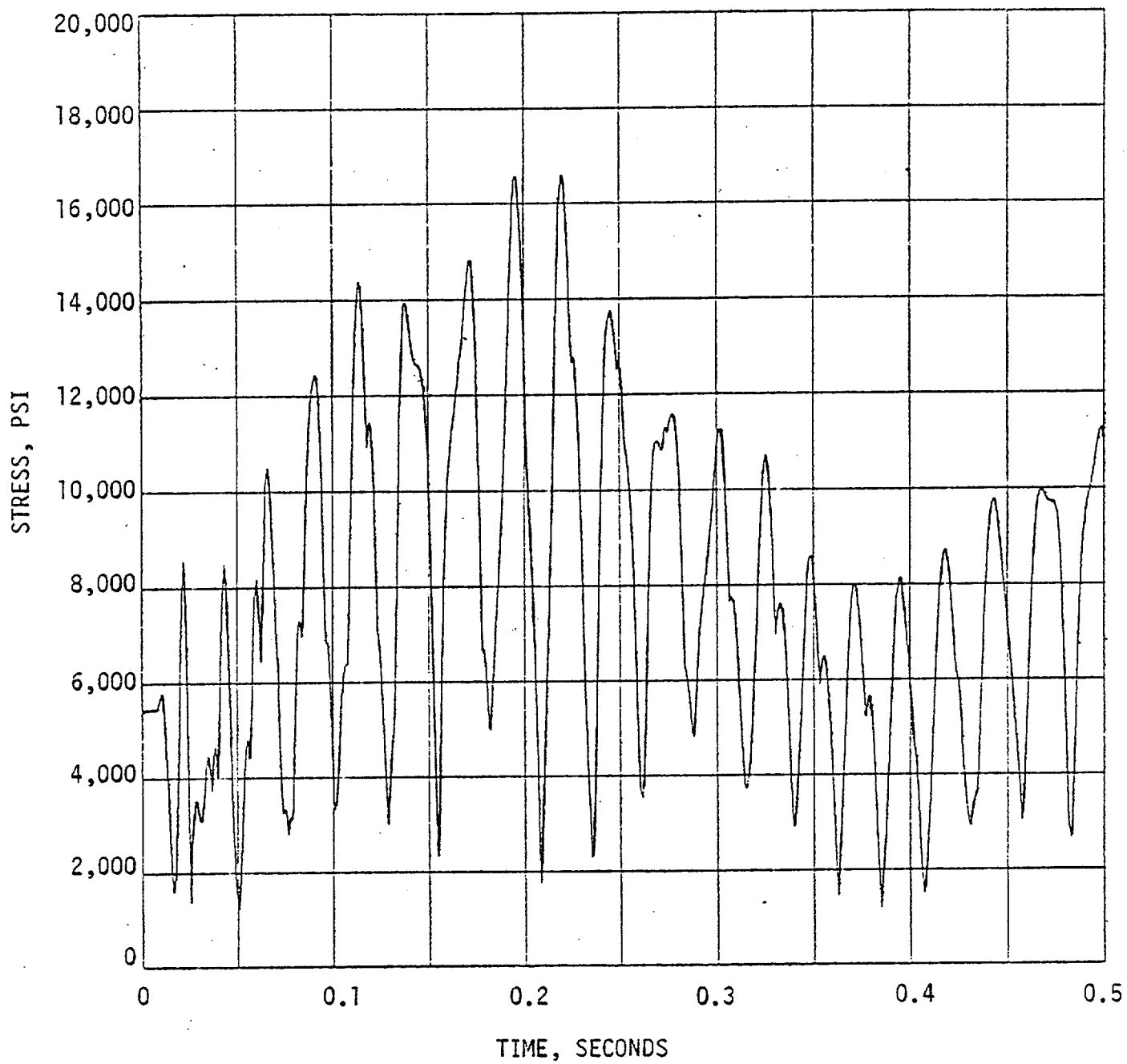


Figure 3.1-8 Maximum Stress Intensity on Tube Outer Wall
Node Location 10 - Total LOCA Effect

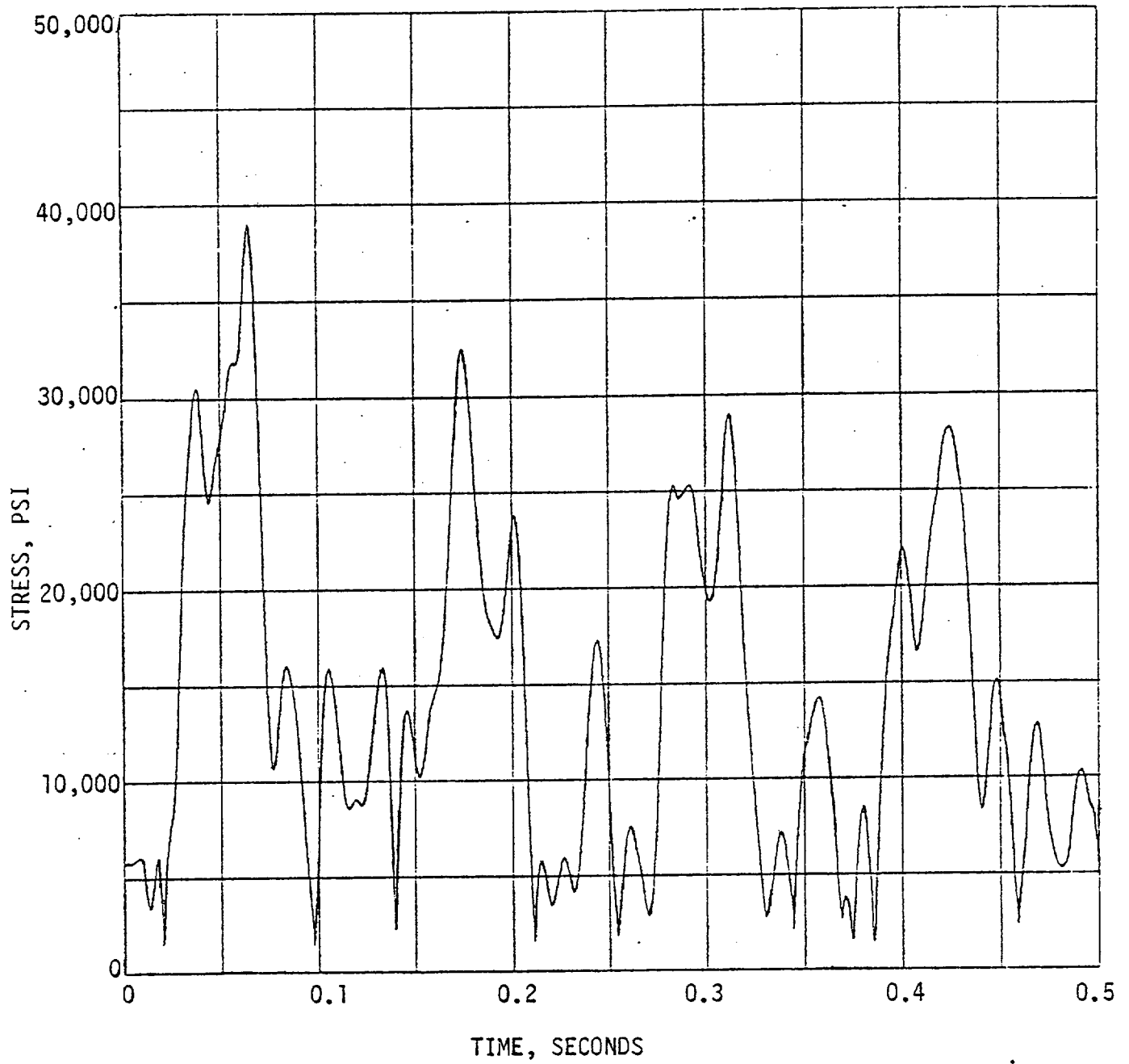


Figure 3.1-9 Maximum Stress Intensity on Tube Outer Wall
Node Location 12 - Total LOCA Effect

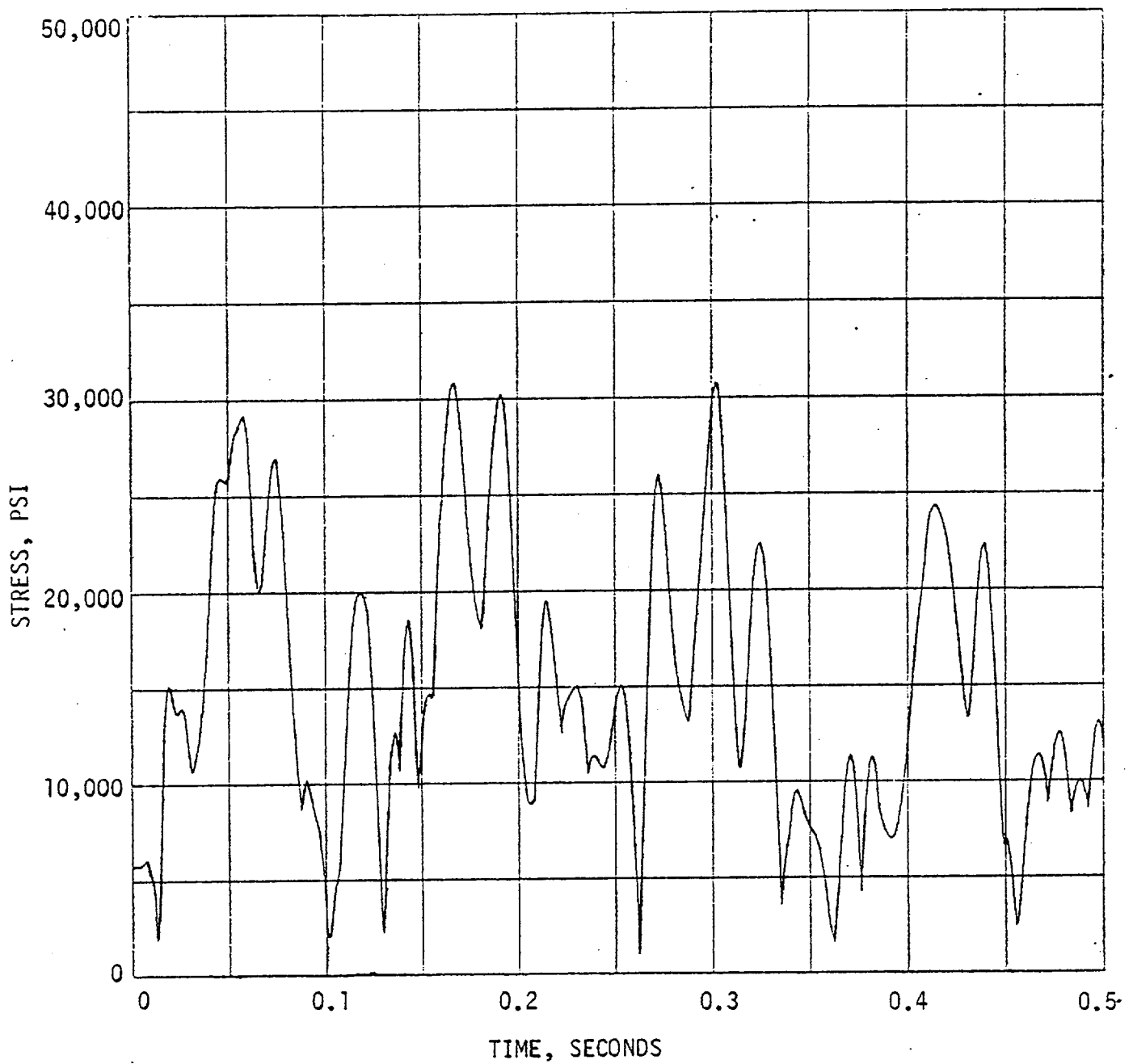


Figure 3.1-10 Maximum Stress Intensity on Tube Outer Wall
Node Location 14 - Total LOCA Effect

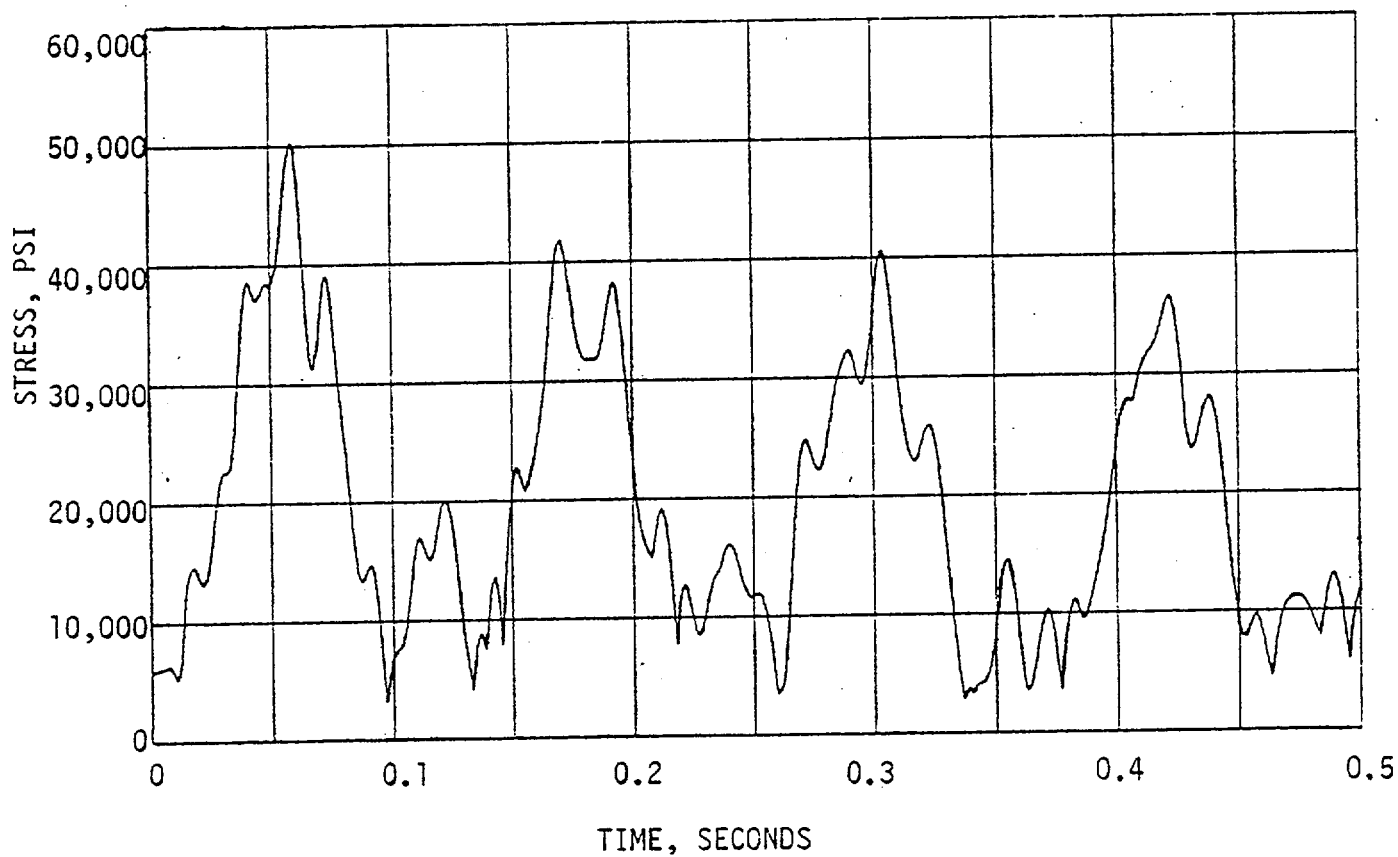


Figure 3.1-11 Maximum Stress Intensity on Tube Outer Wall
Node Location 16 - Total LOCA Effect

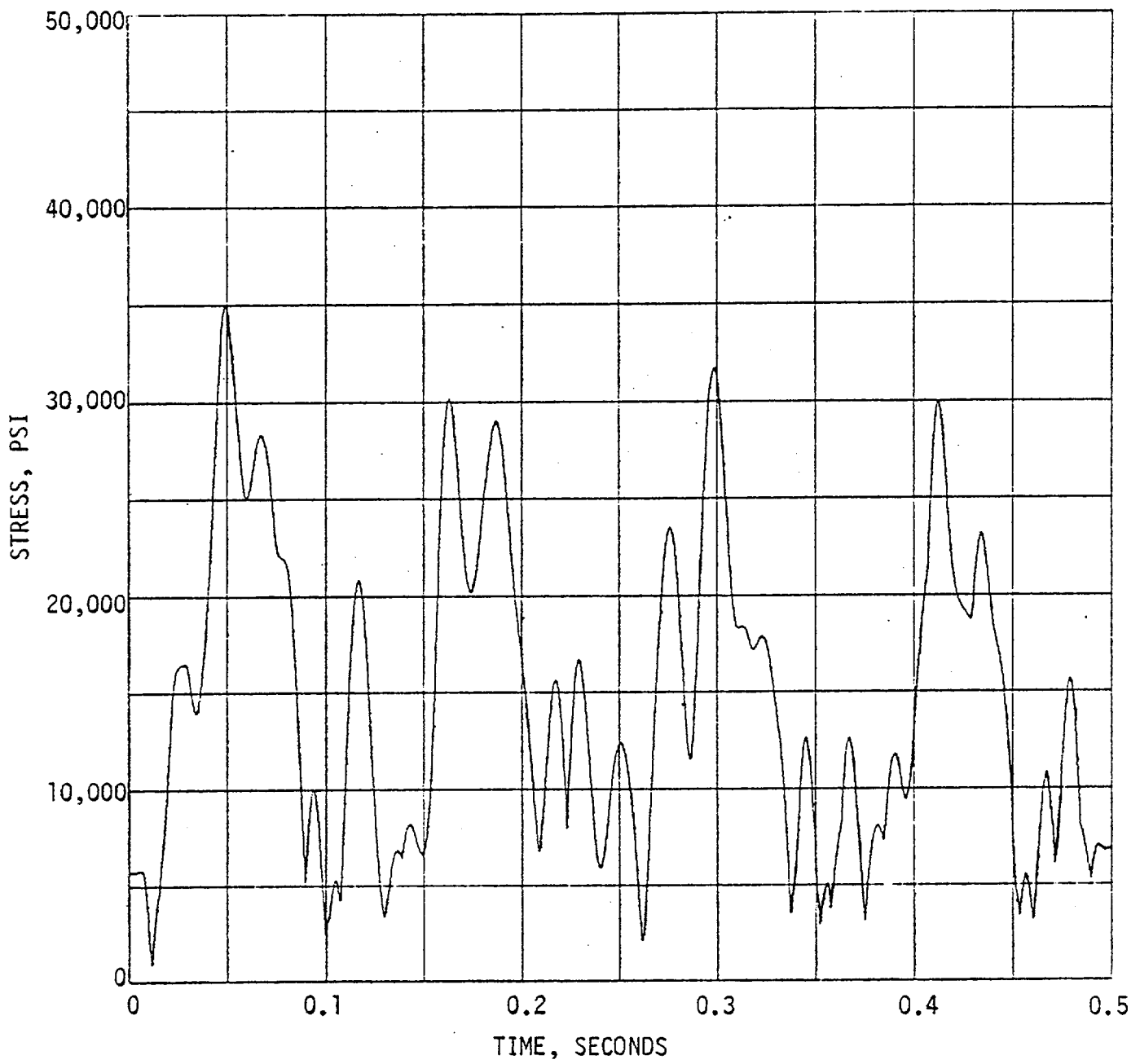


Figure 3.1-12 Maximum Stress Intensity on Tube Outer Wall
Node Location 17 - Total LOCA Effect

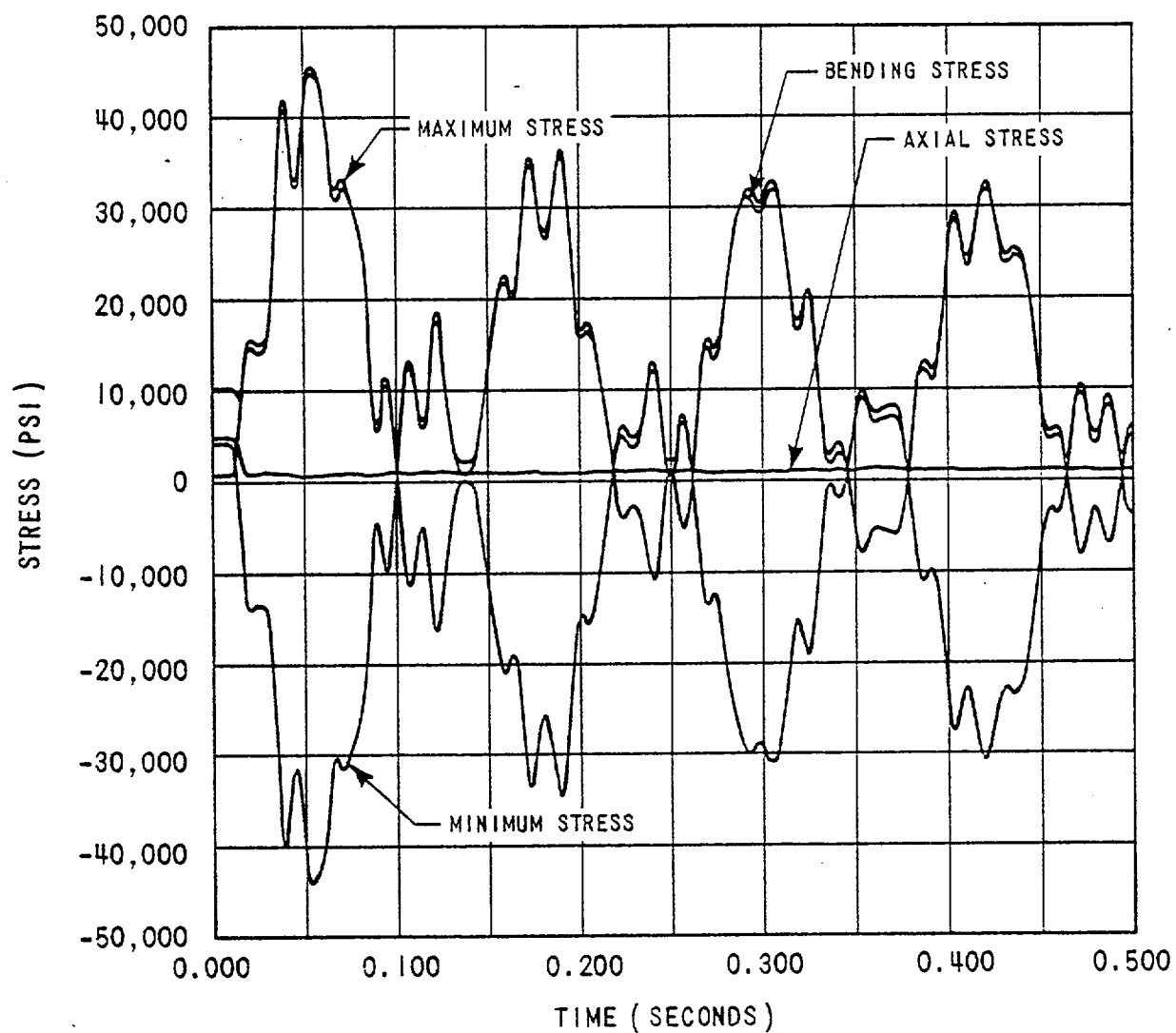


Figure 3.1-13 Stresses at Node Location 4 Due to LOCA Pressure History

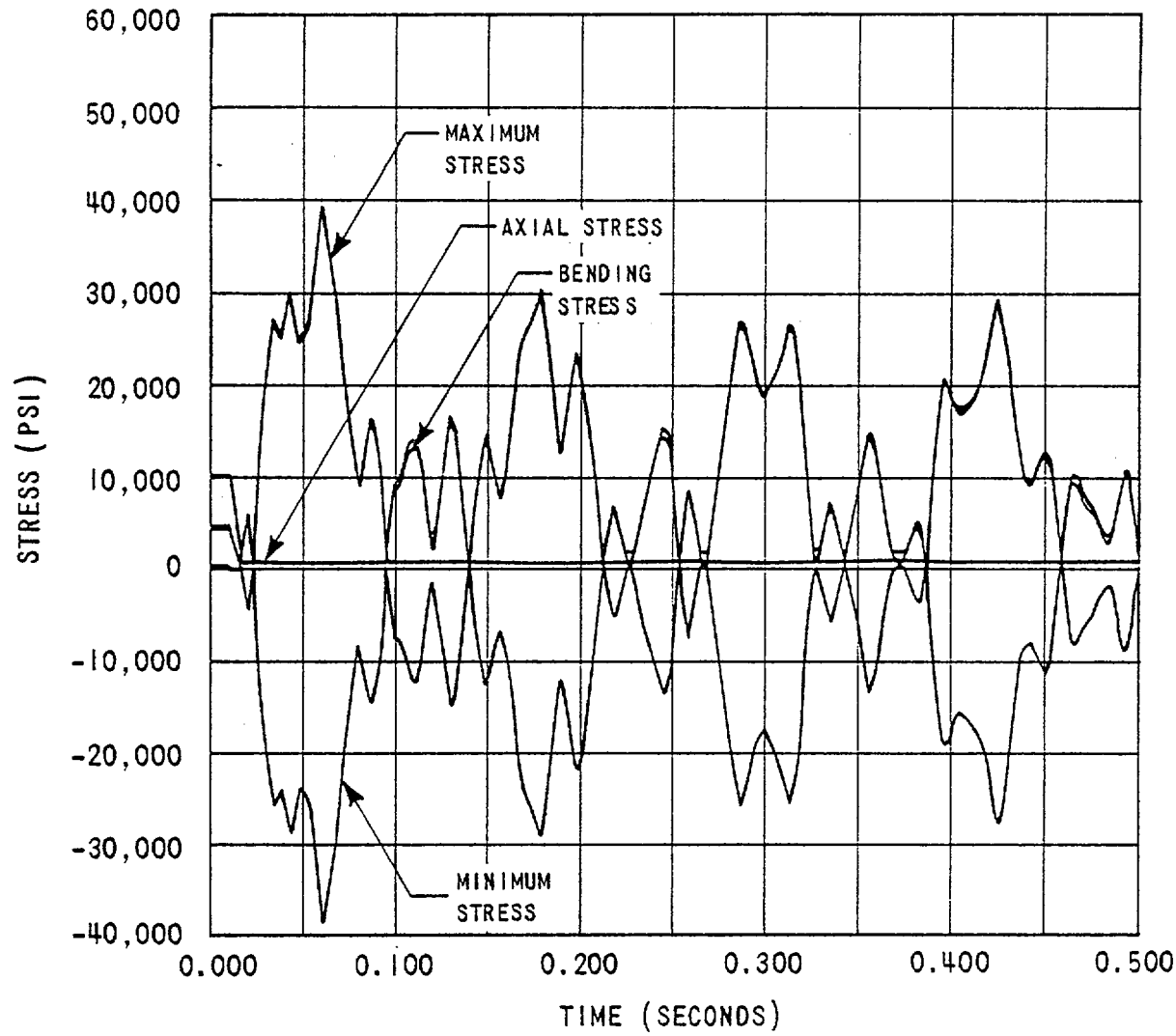


Figure 3.1-14 Stresses at Node Location 8 Due to LOCA Pressure History

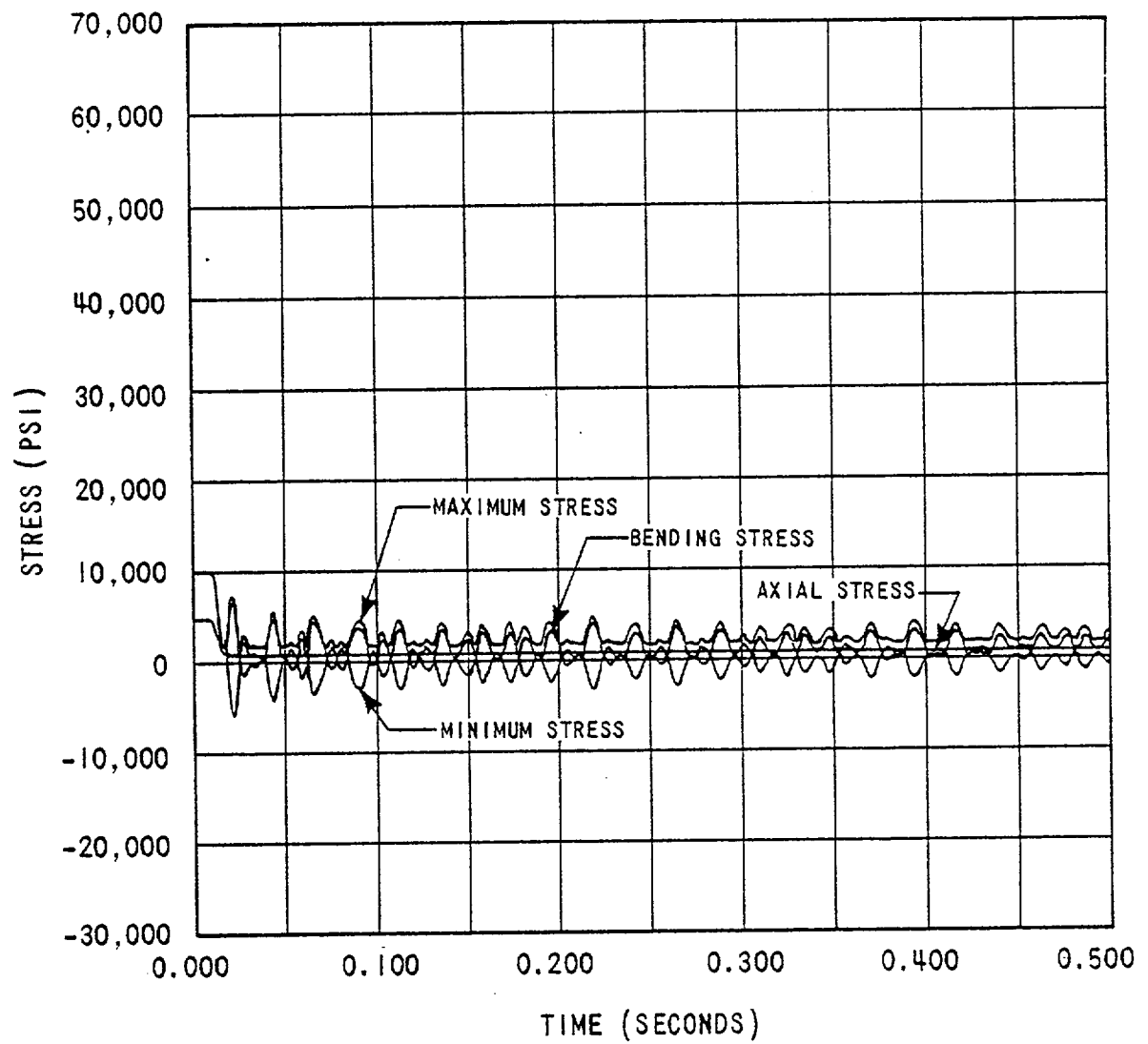


Figure 3.1-15 Stresses at Node Location 10 Due to LOCA Pressure History

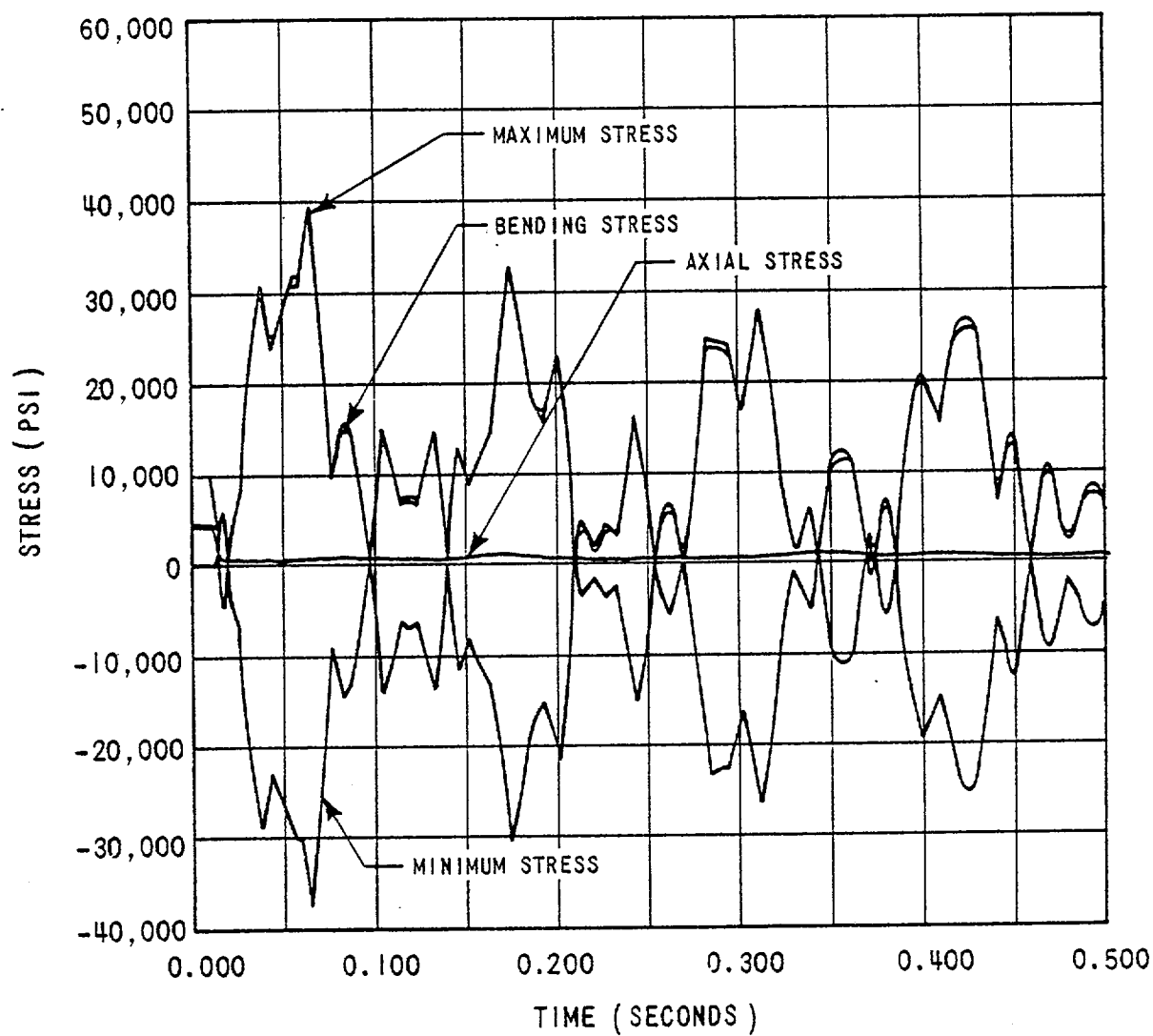


Figure 3.1-16 Stresses at Node Location 12 Due to LOCA Pressure History

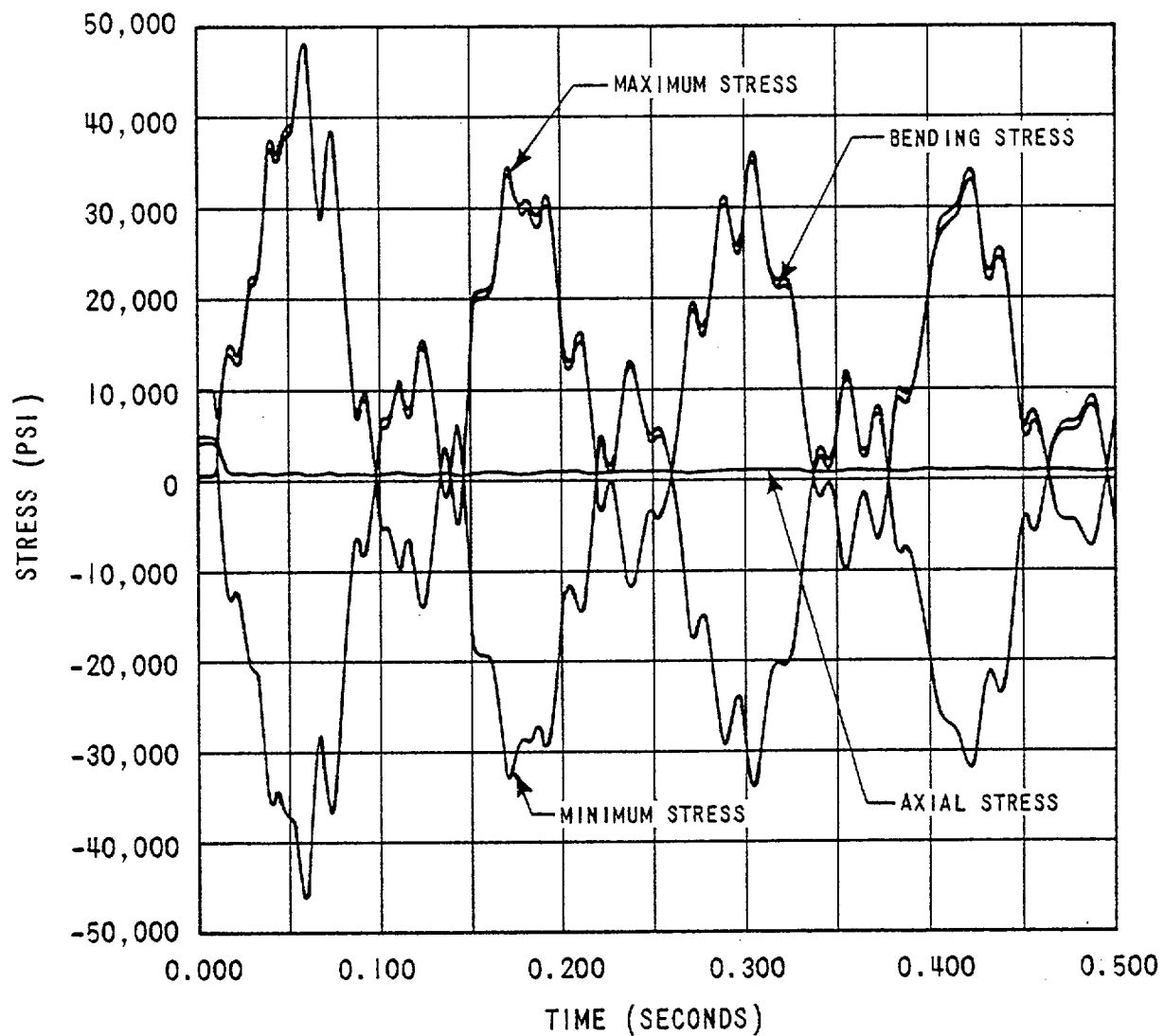


Figure 3.1-17 Stresses at Node Location 16 Due to LOCA Pressure History

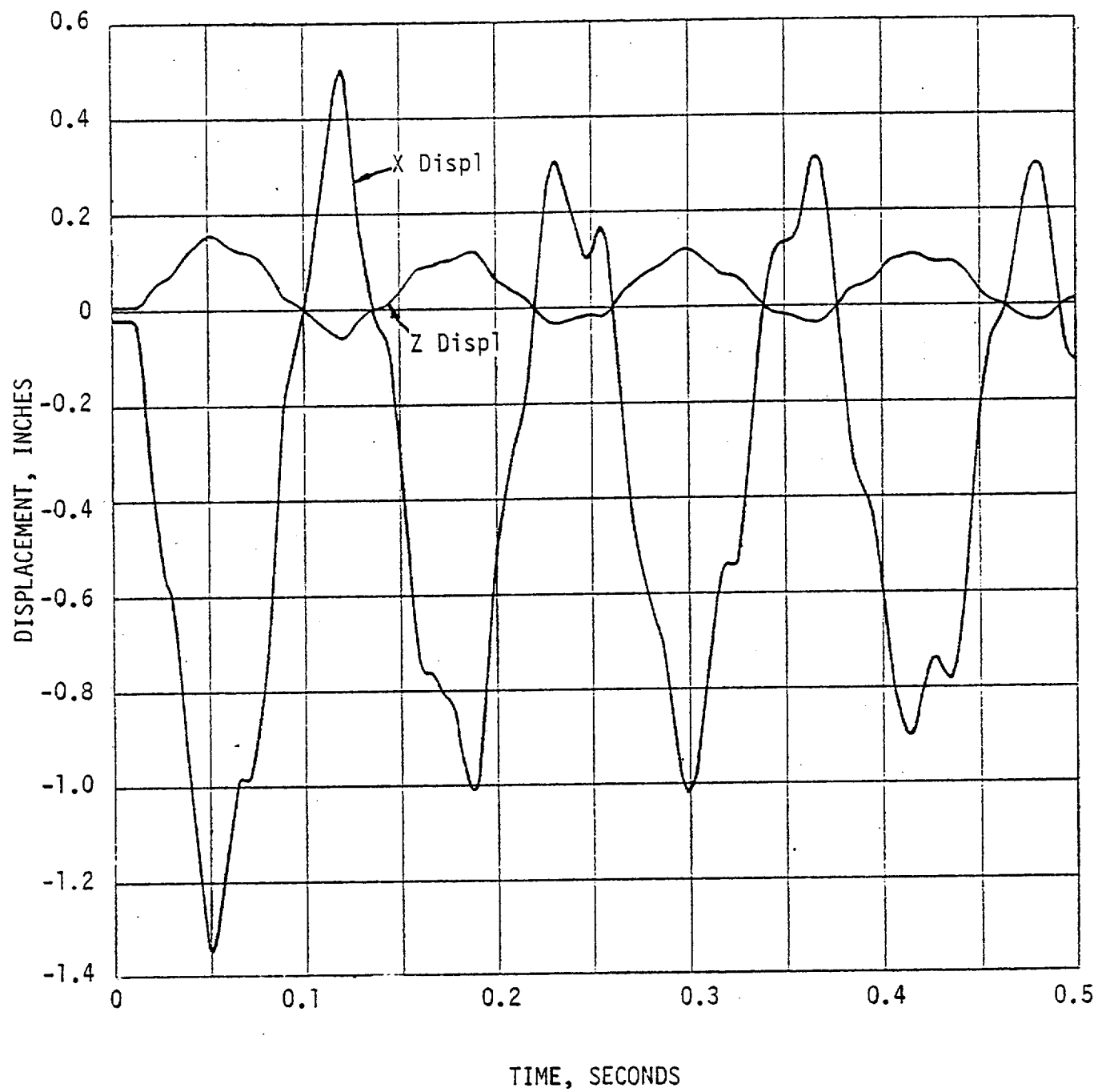


Figure 3.1-18 In-Plane Displacements of Node Location 5
Due to LOCA Pressure History

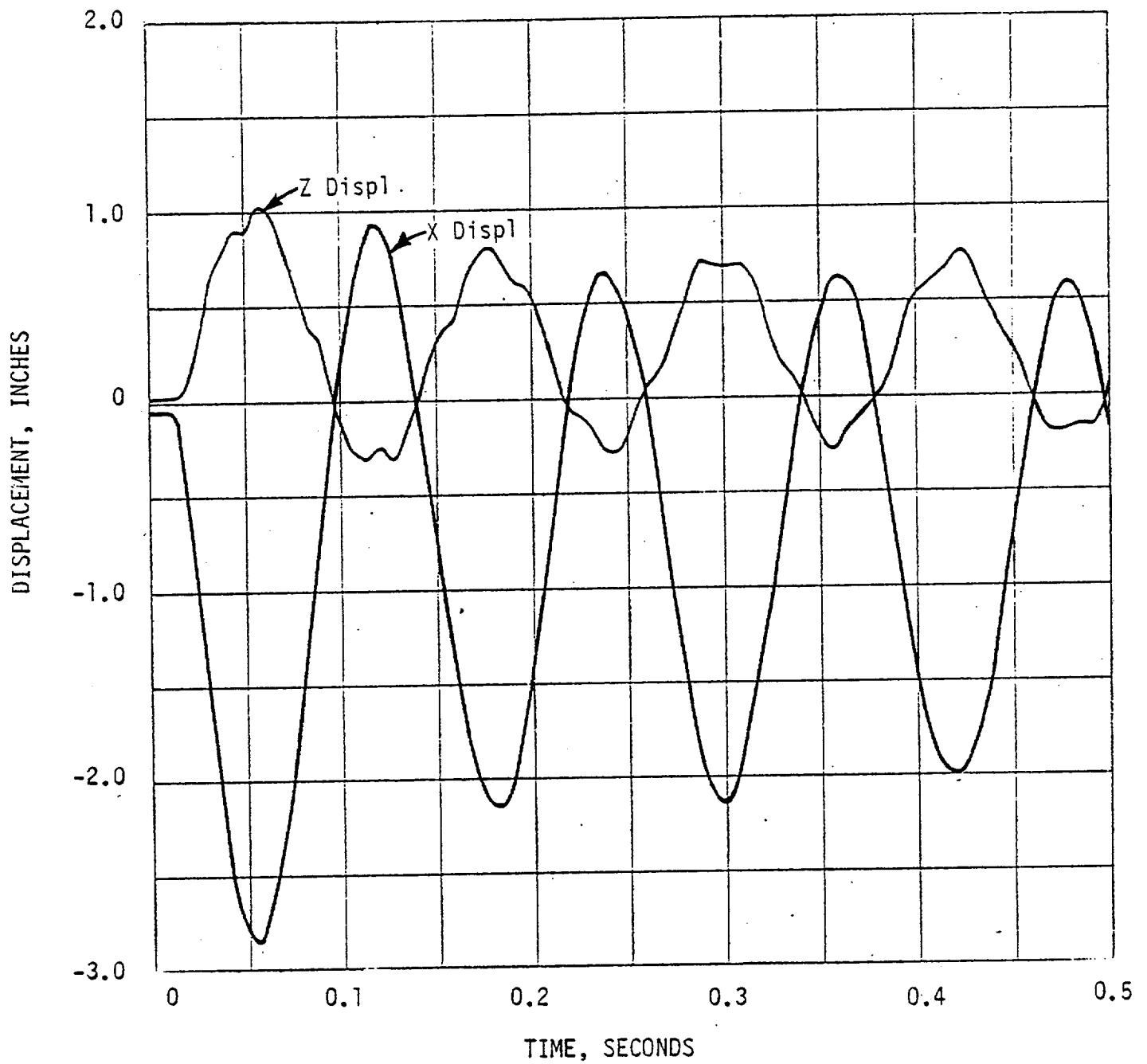


Figure 3.1-19 In-Plane Displacement of Node Location 7
Due to LOCA Pressure History

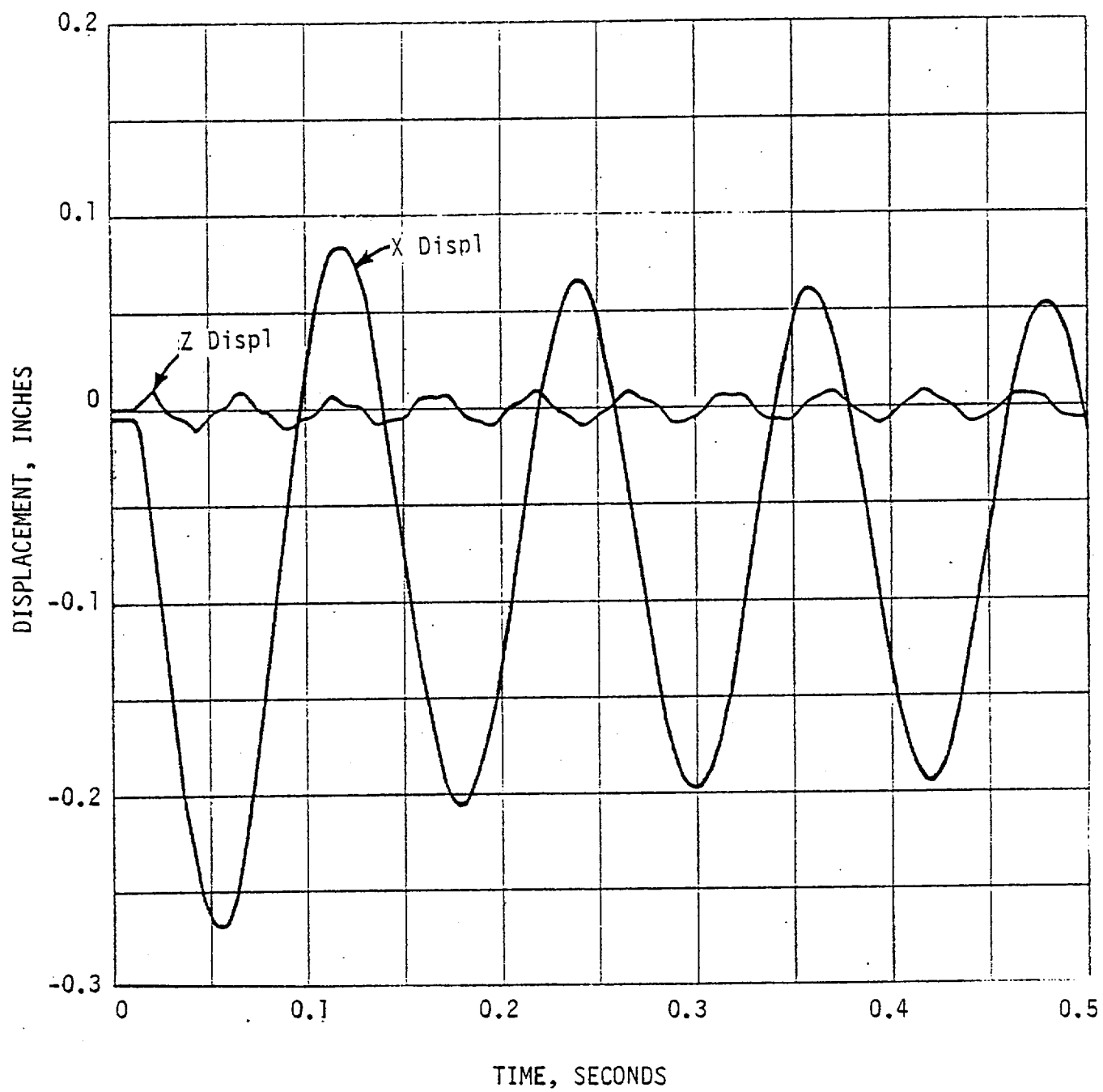


Figure 3.1-20 In-Plane Displacements of Node Location 10
Due to LOCA Pressure History

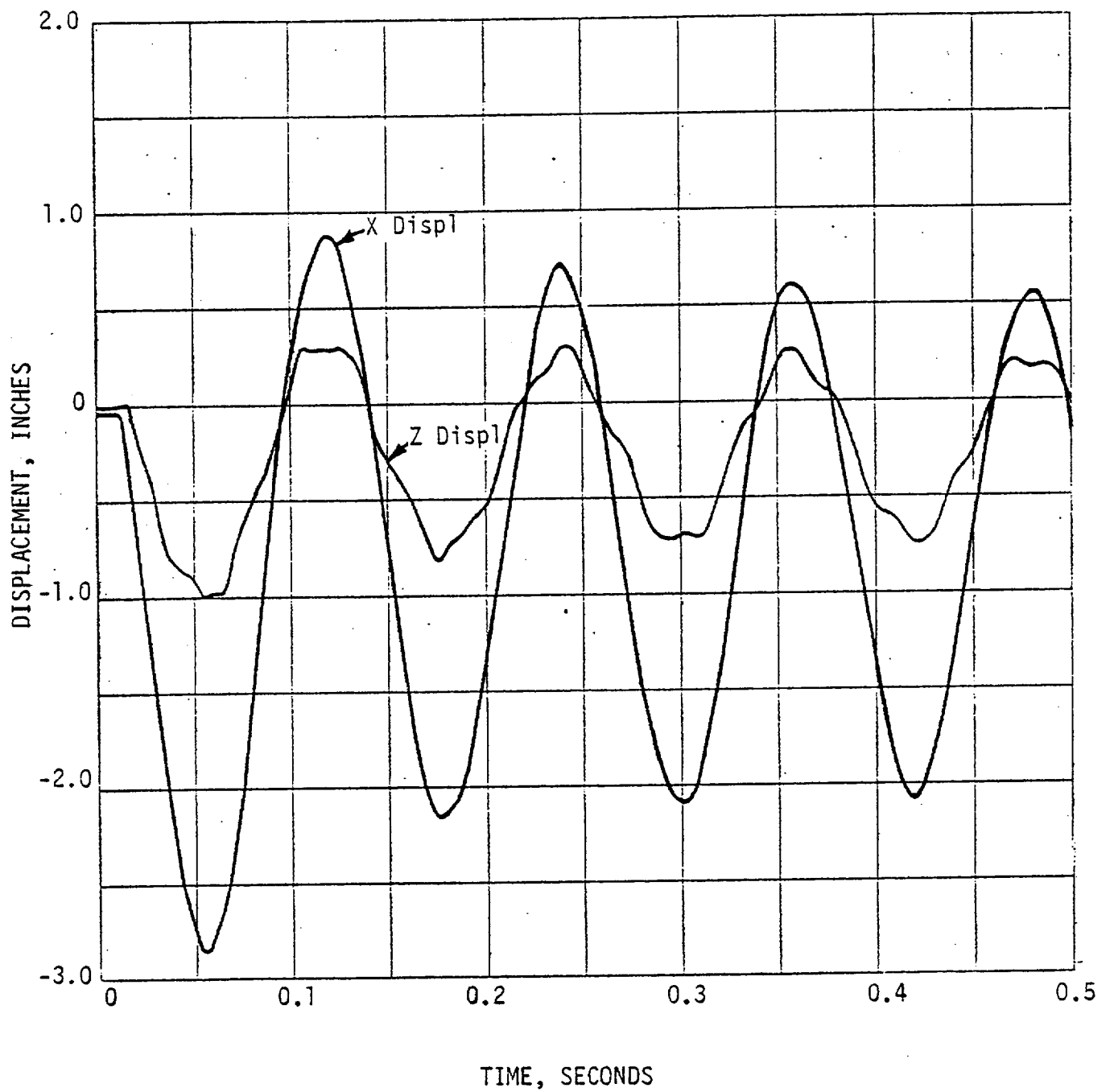


Figure 3.1-21 In-Plane Displacements of Node Location 13
Due to LOCA Pressure History

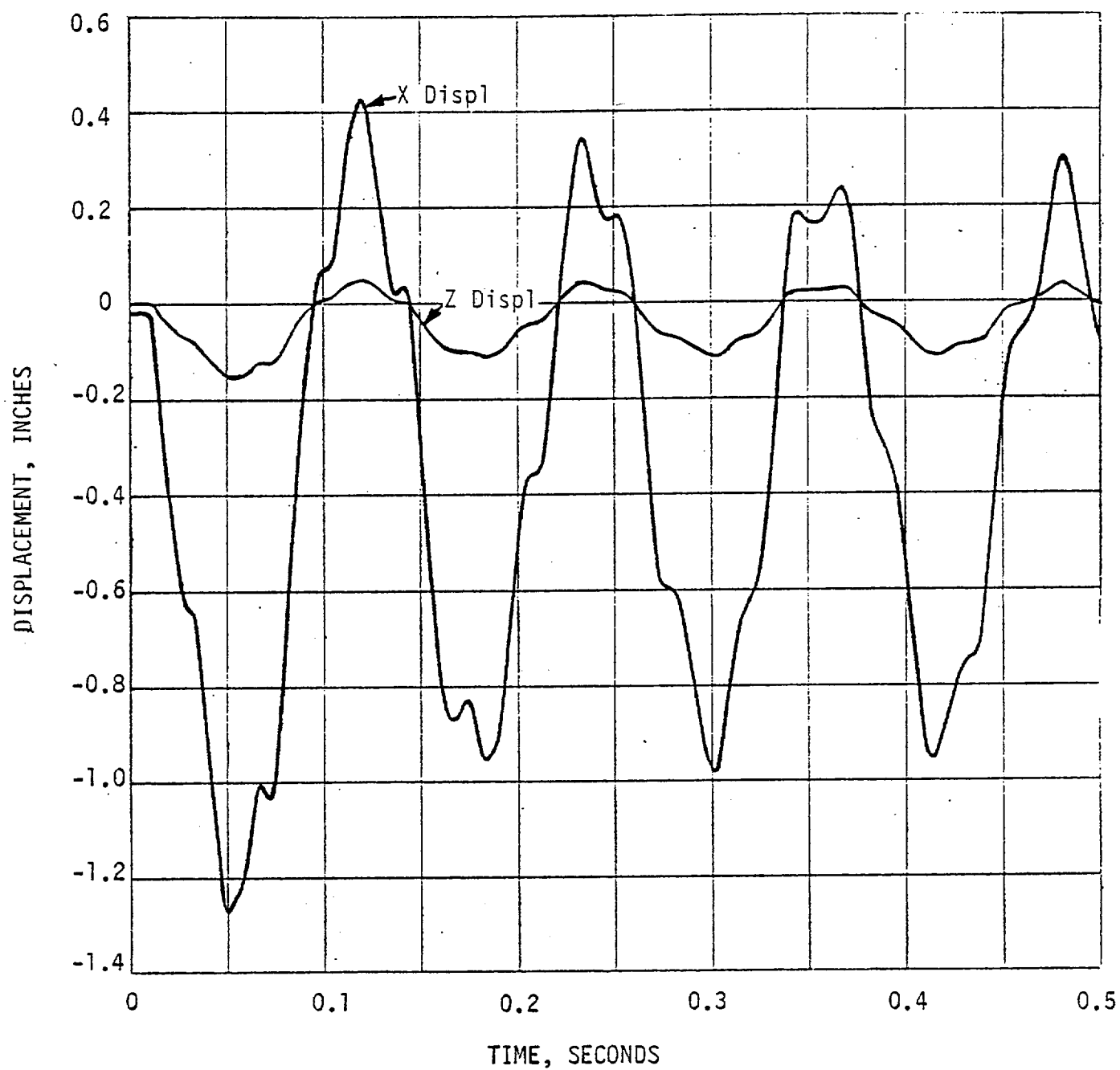


Figure 3.1-22 In-Plane Displacements of Node Location 15
Due to LOCA Pressure History

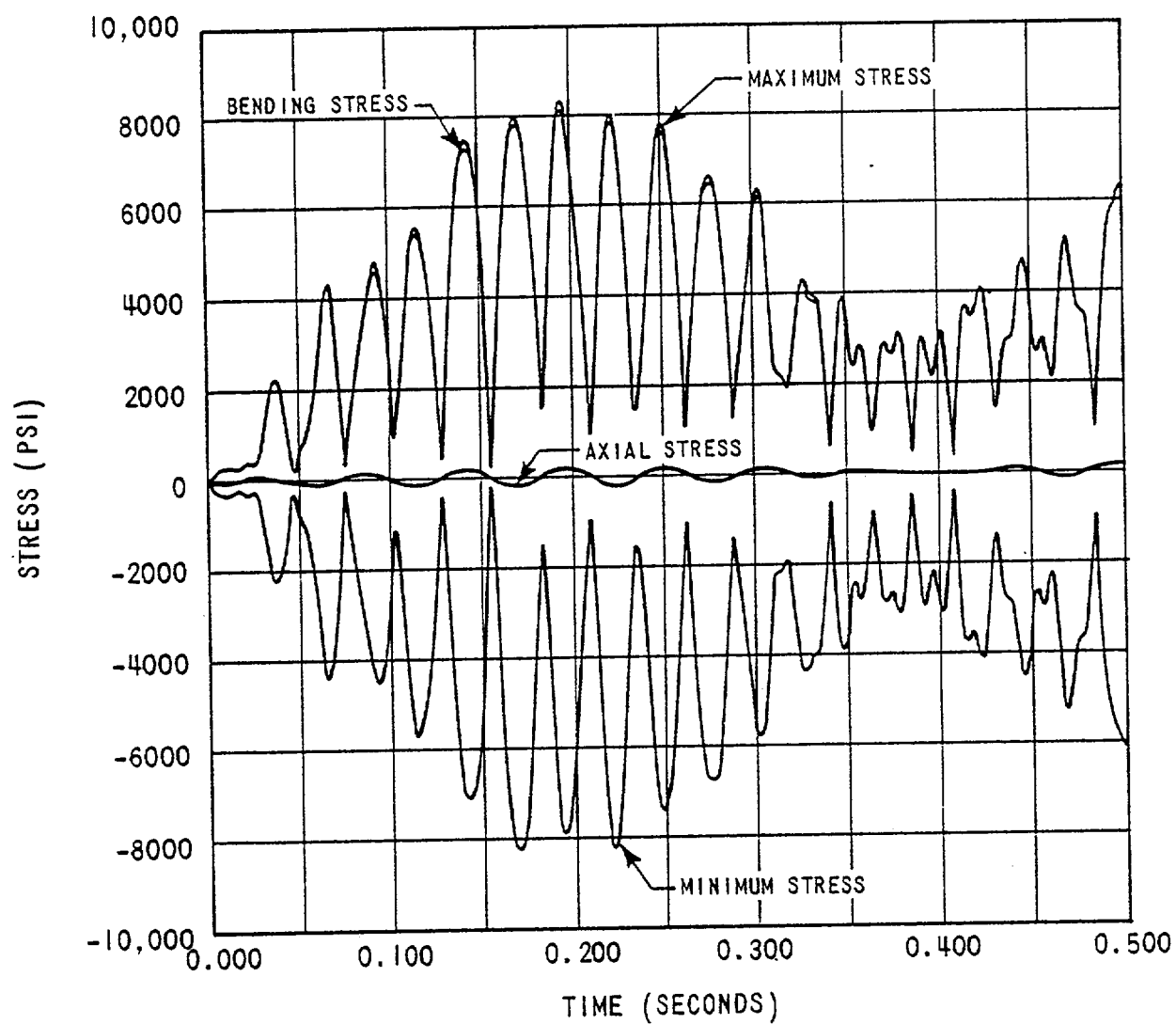


Figure 3.1-23 Stresses at Node Location 4 Due to LOCA Displacement History on Steam Generator

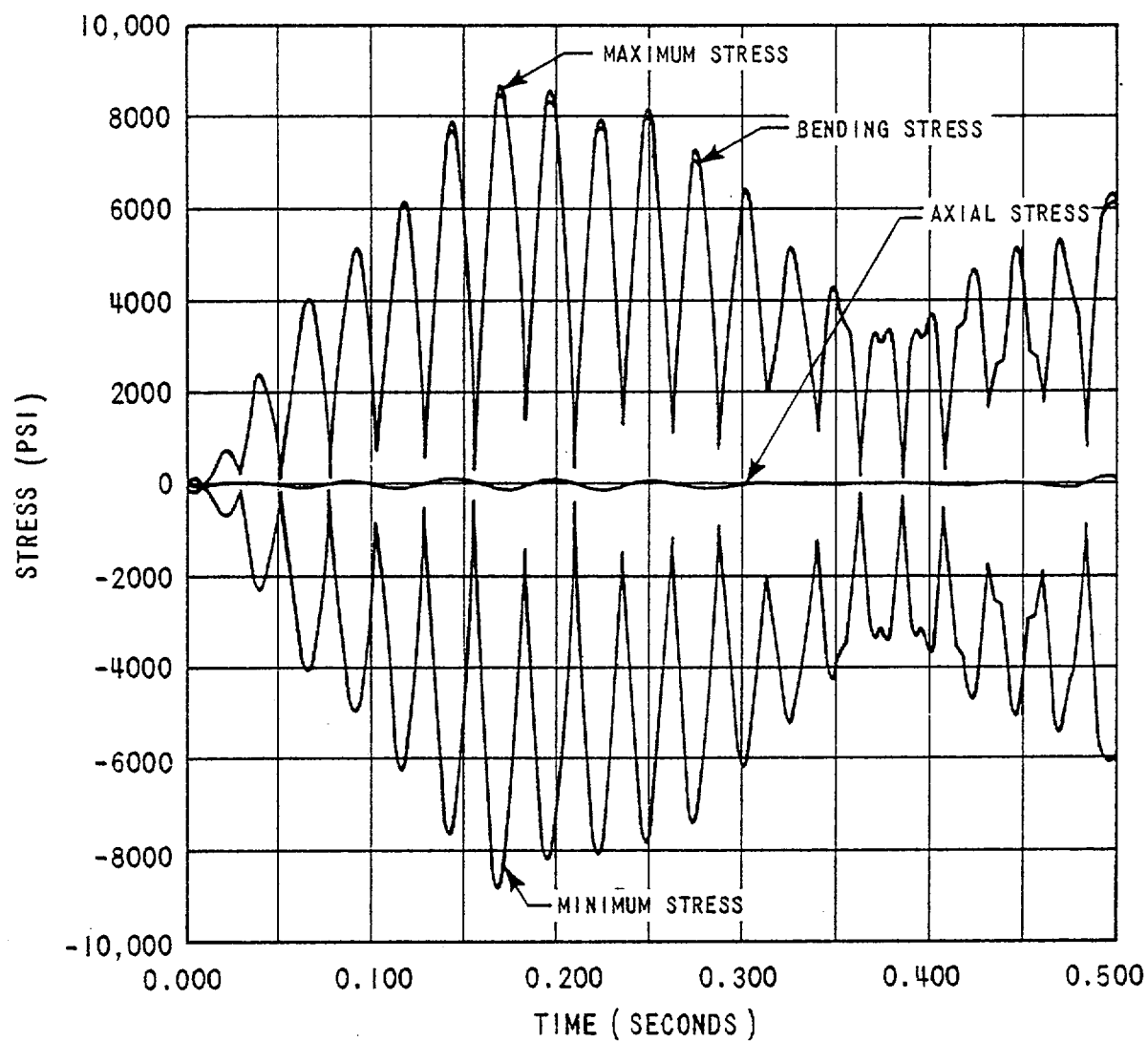


Figure 3.1-24 Stresses at Node Location 7 Due to LOCA Displacement History on Steam Generator

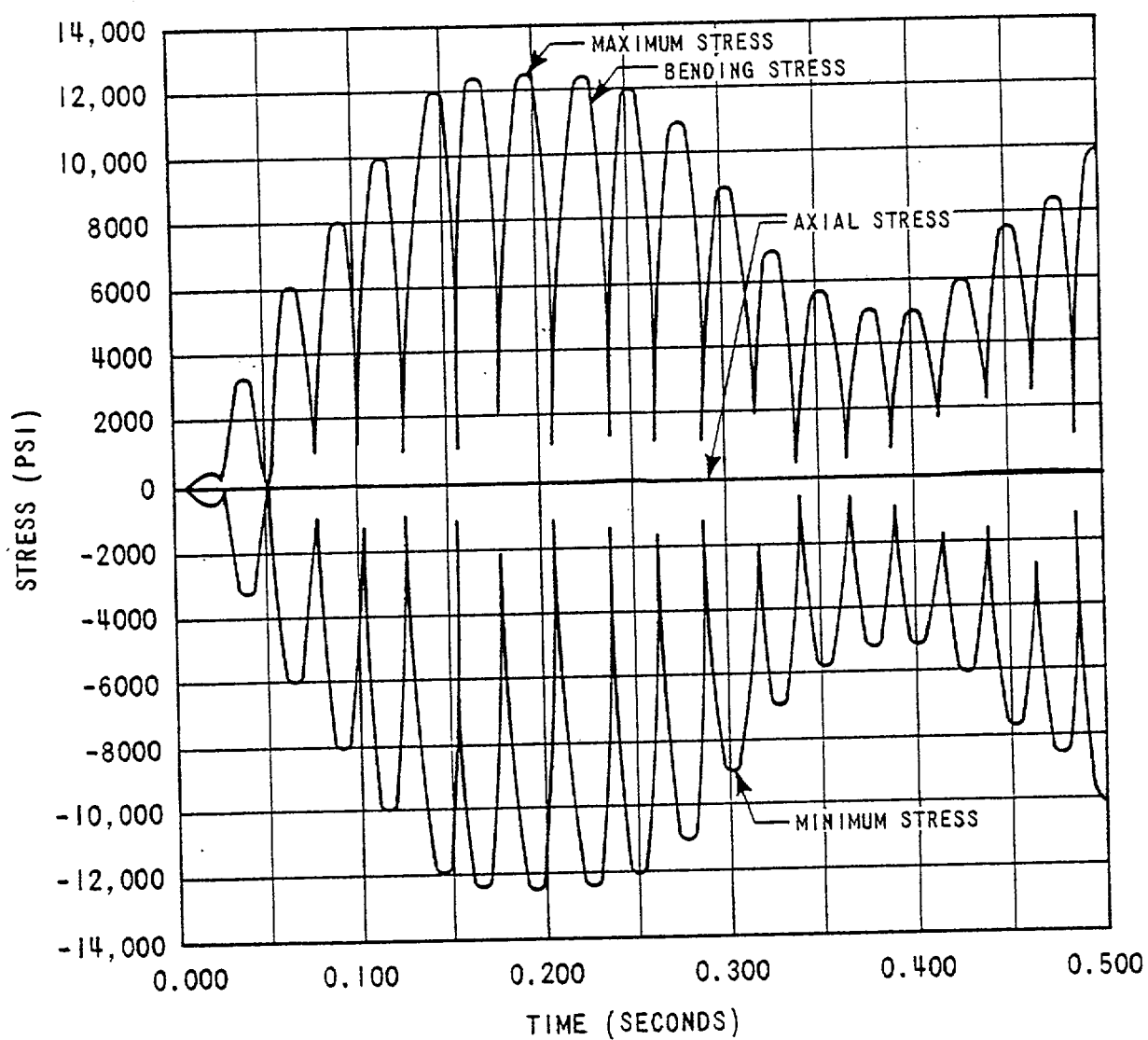


Figure 3.1-25 Stresses at Node Location 10 Due to LOCA Displacement History on Steam Generator

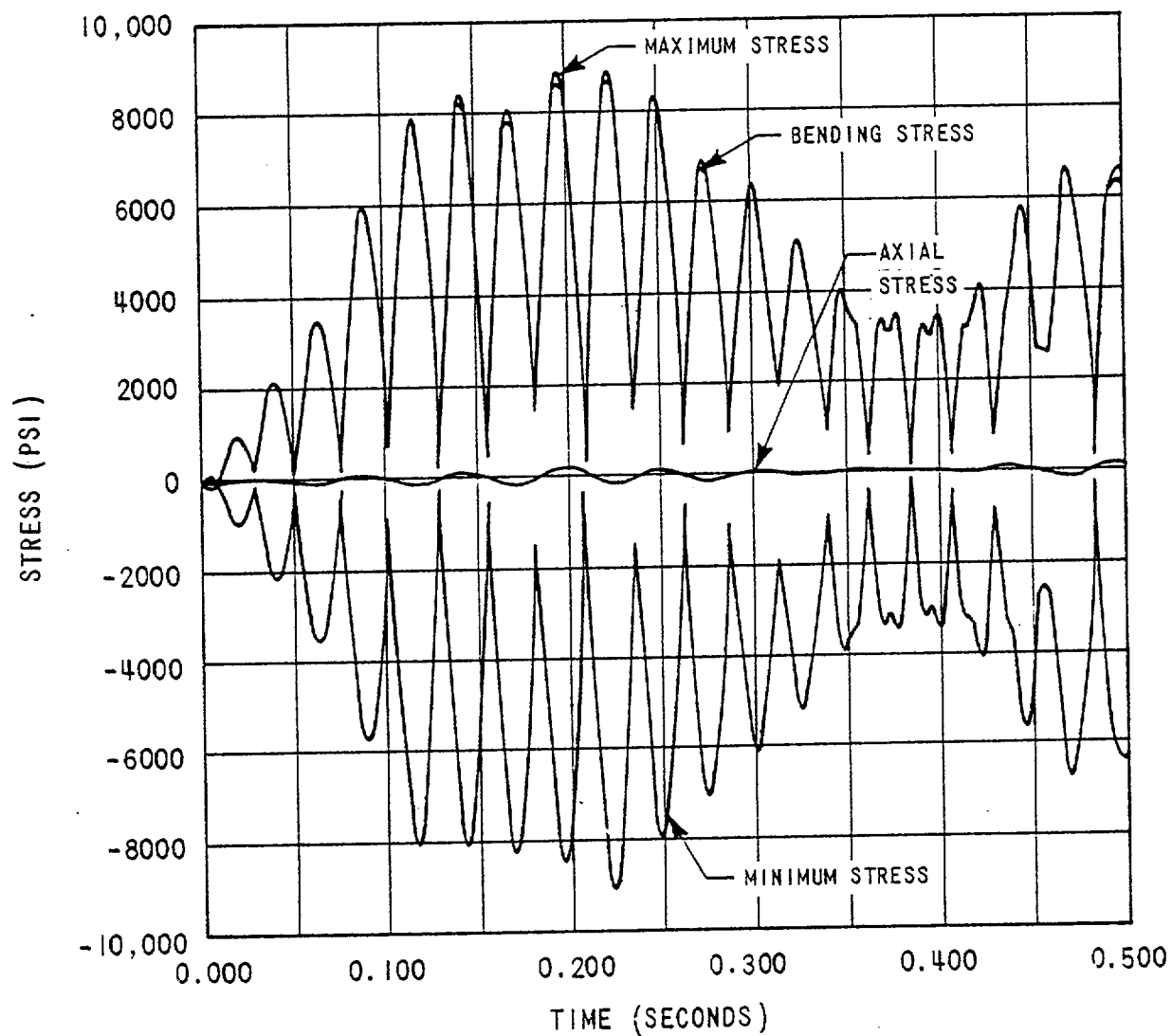


Figure 3.1-26 Stresses at Node Location 13 Due to LOCA Displacement History on Steam Generator

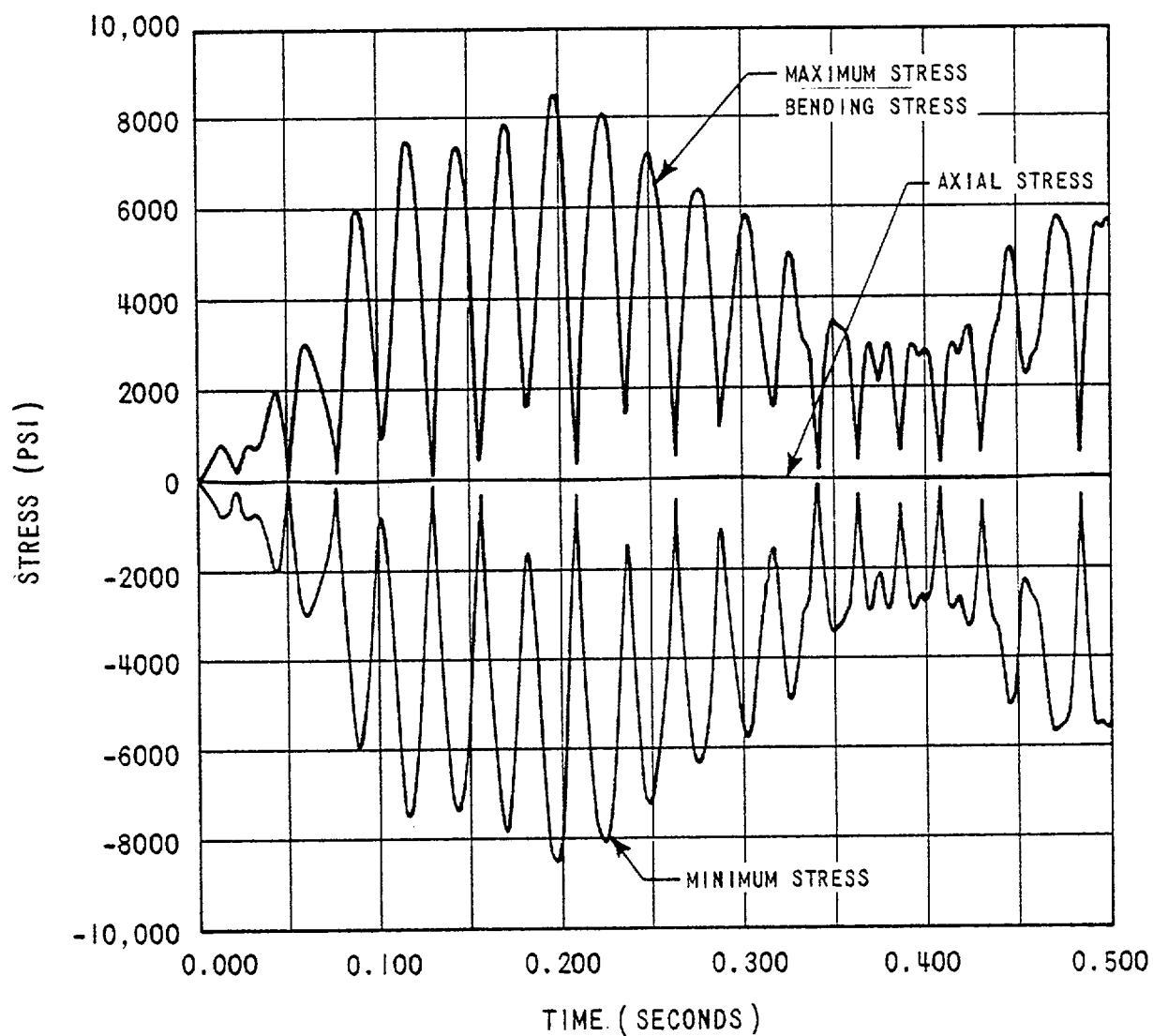


Figure 3.1-27 Stresses at Node Location 16 Due to LOCA Displacement History on Steam Generator

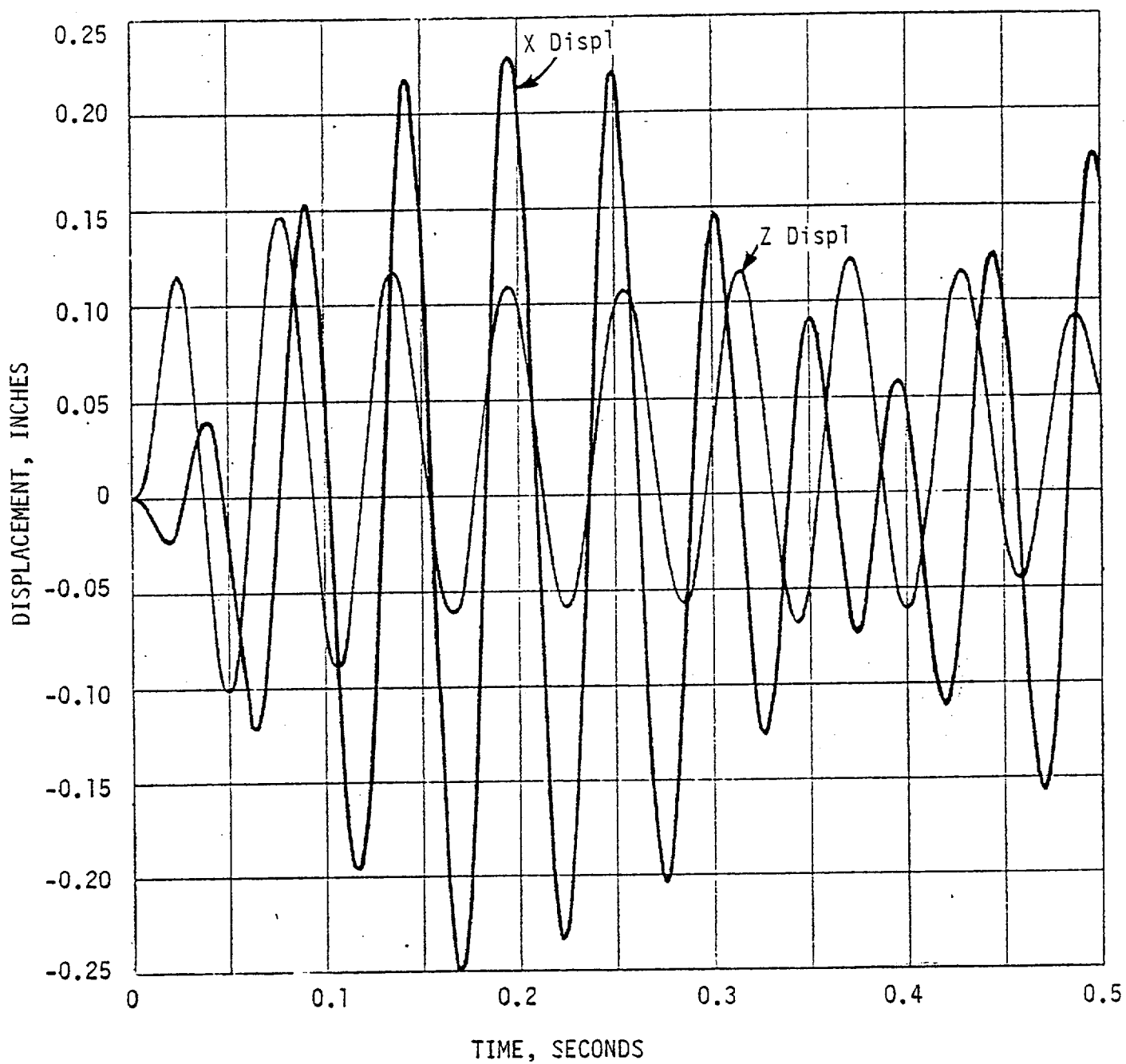


Figure 3.1-28 In-Plane Displacements of Node Location 5 Due to LOCA Displacement History on Steam Generator

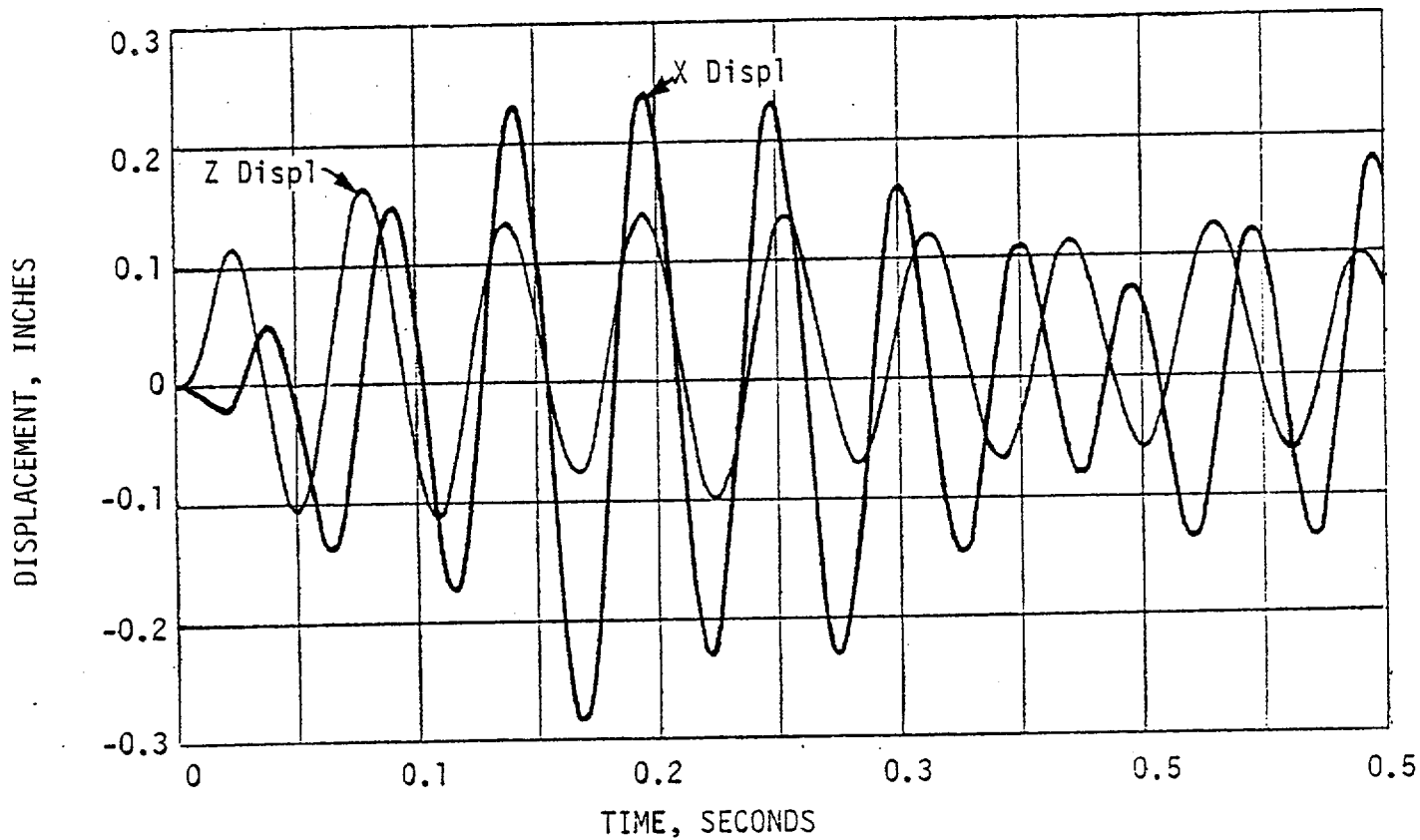


Figure 3.1-29 In-Plane Displacements of Node Location 7
Due to LOCA Displacement History on Steam Generator

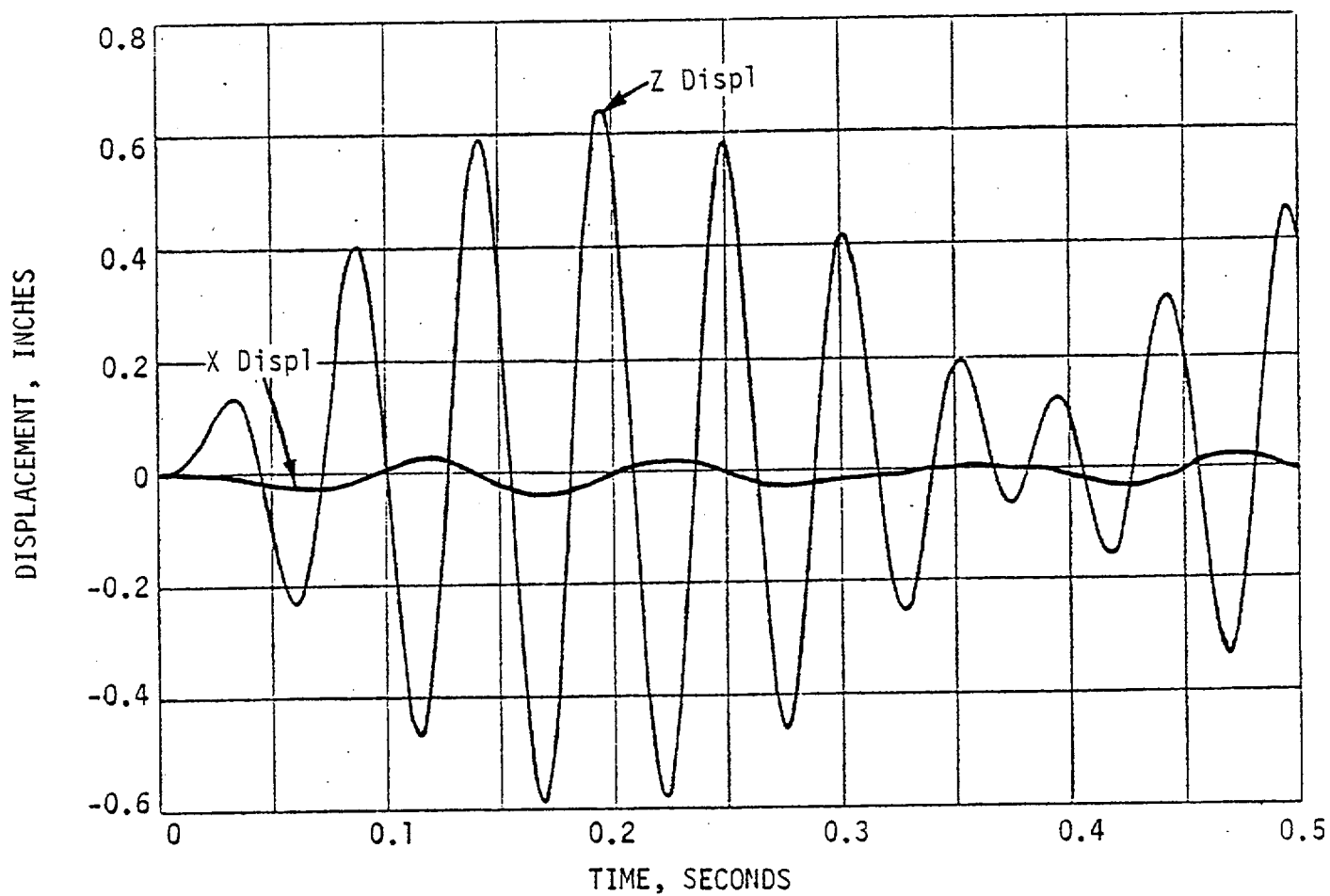


Figure 3.1-30 In-Plane Displacements of Node Location 10
Due to LOCA Displacement History on Steam Generator

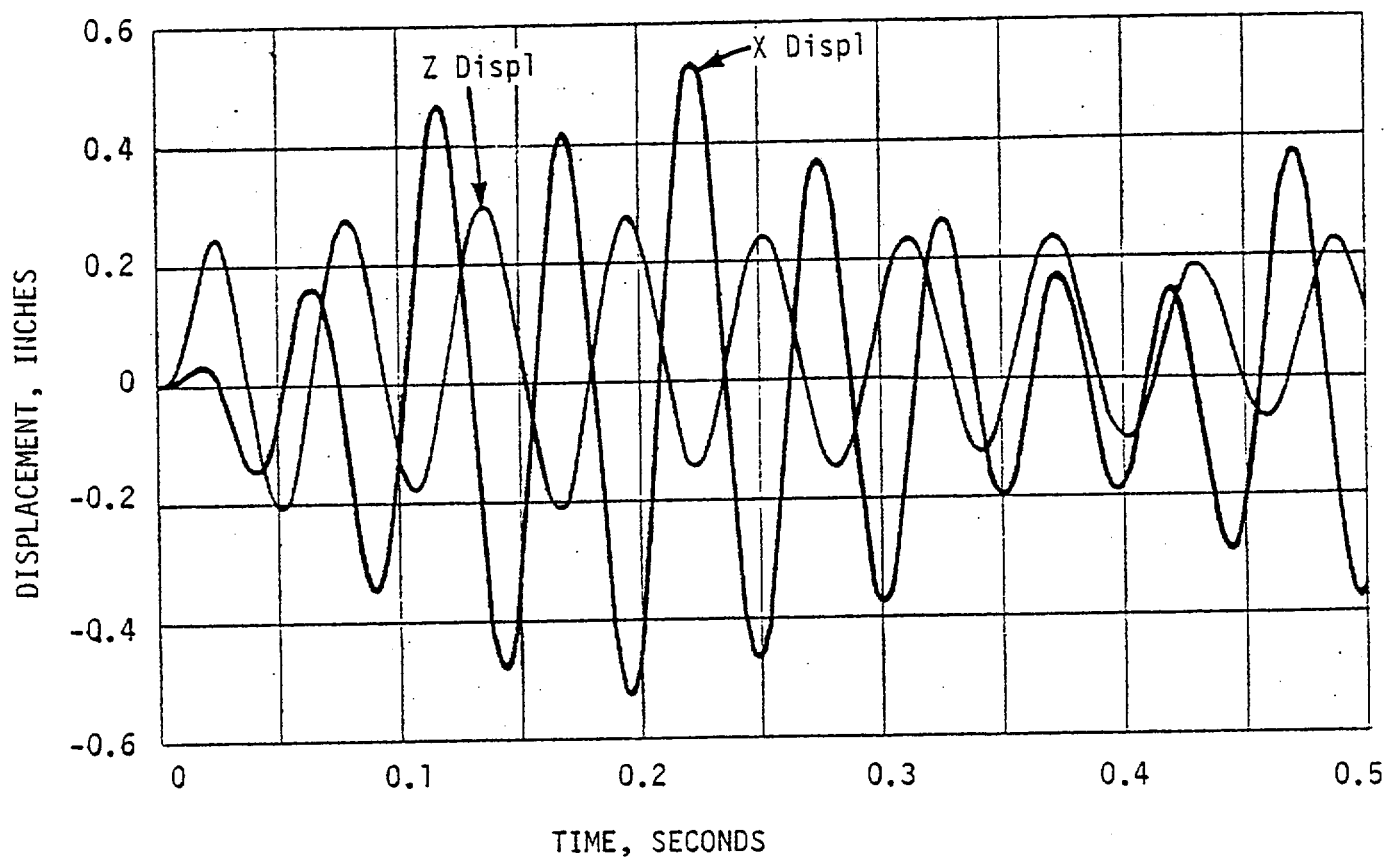


Figure 3.1-31 In-Plane Displacements of Node of Location 13
Due to LOCA Displacement History on Steam Generator

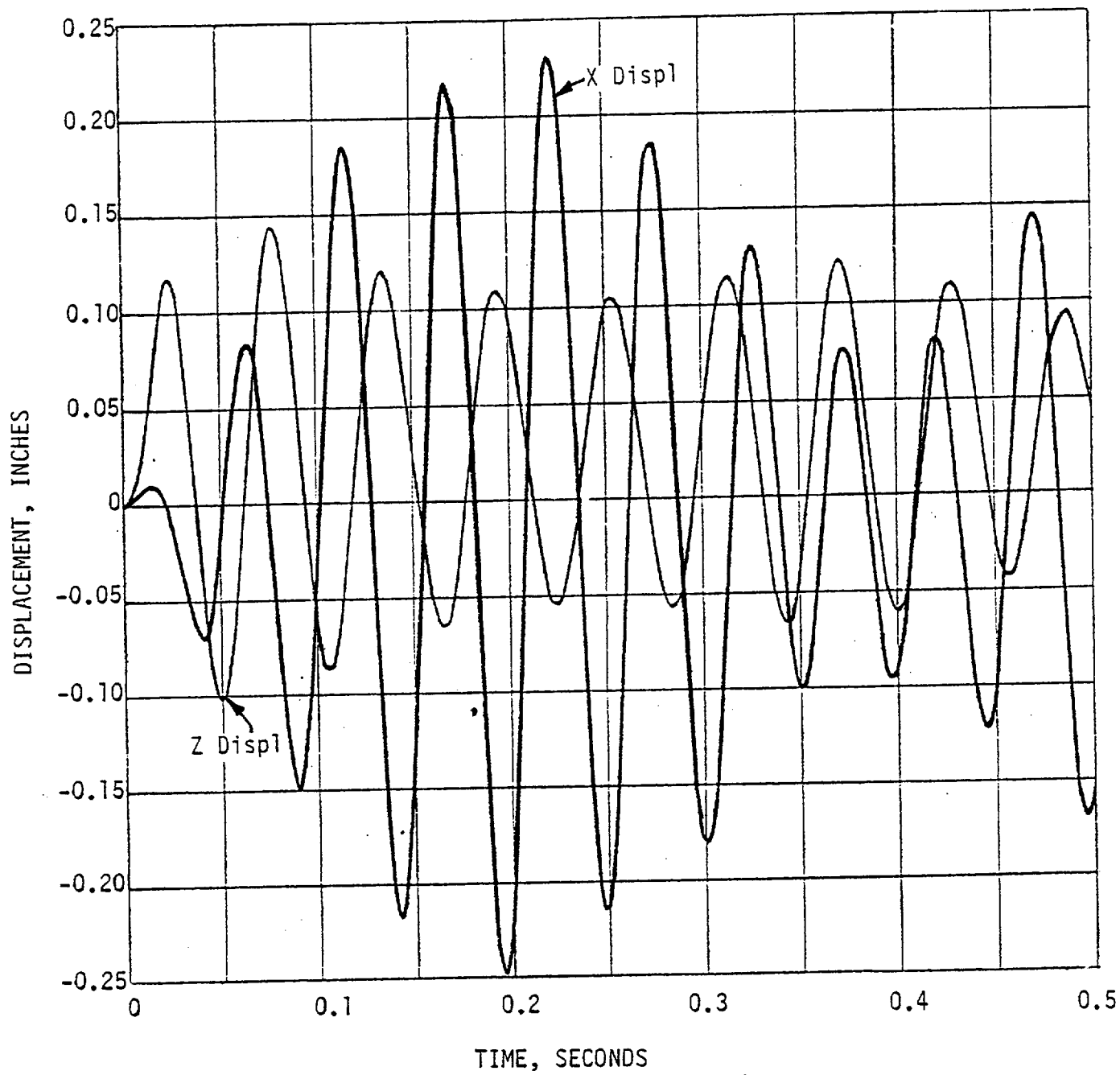


Figure 3.1-32 In-Plane Displacements of Node Location 15
Due to LOCA Displacement History on Steam Generator

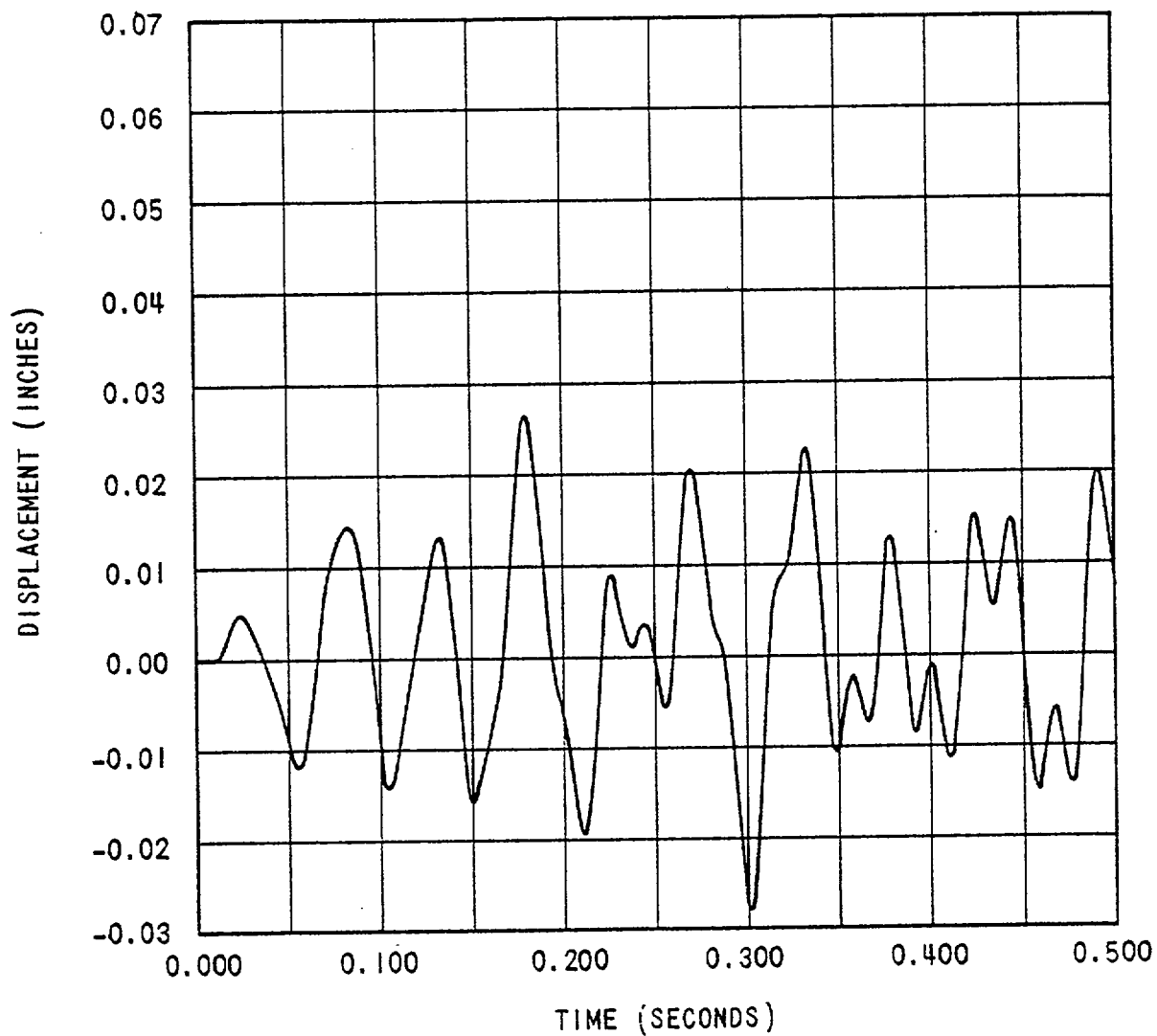


Figure 3.1-33 Out-of-Plane Displacements of Node Location 6 Due to LOCA Displacement History on Steam Generator

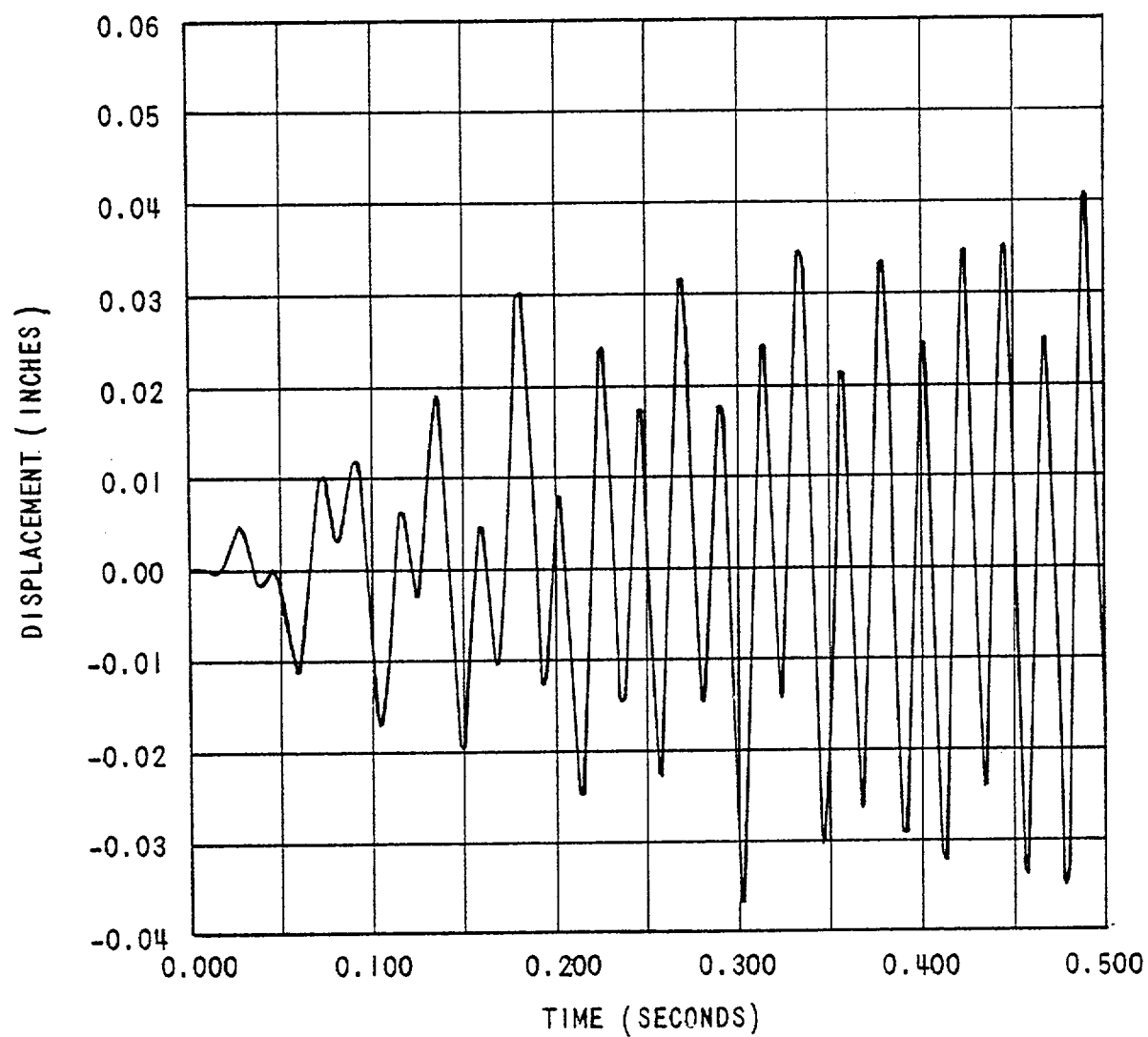


Figure 3.1-34 Out-of-Plane Displacements of Node Location 7 Due to LOCA Displacement History on Steam Generator

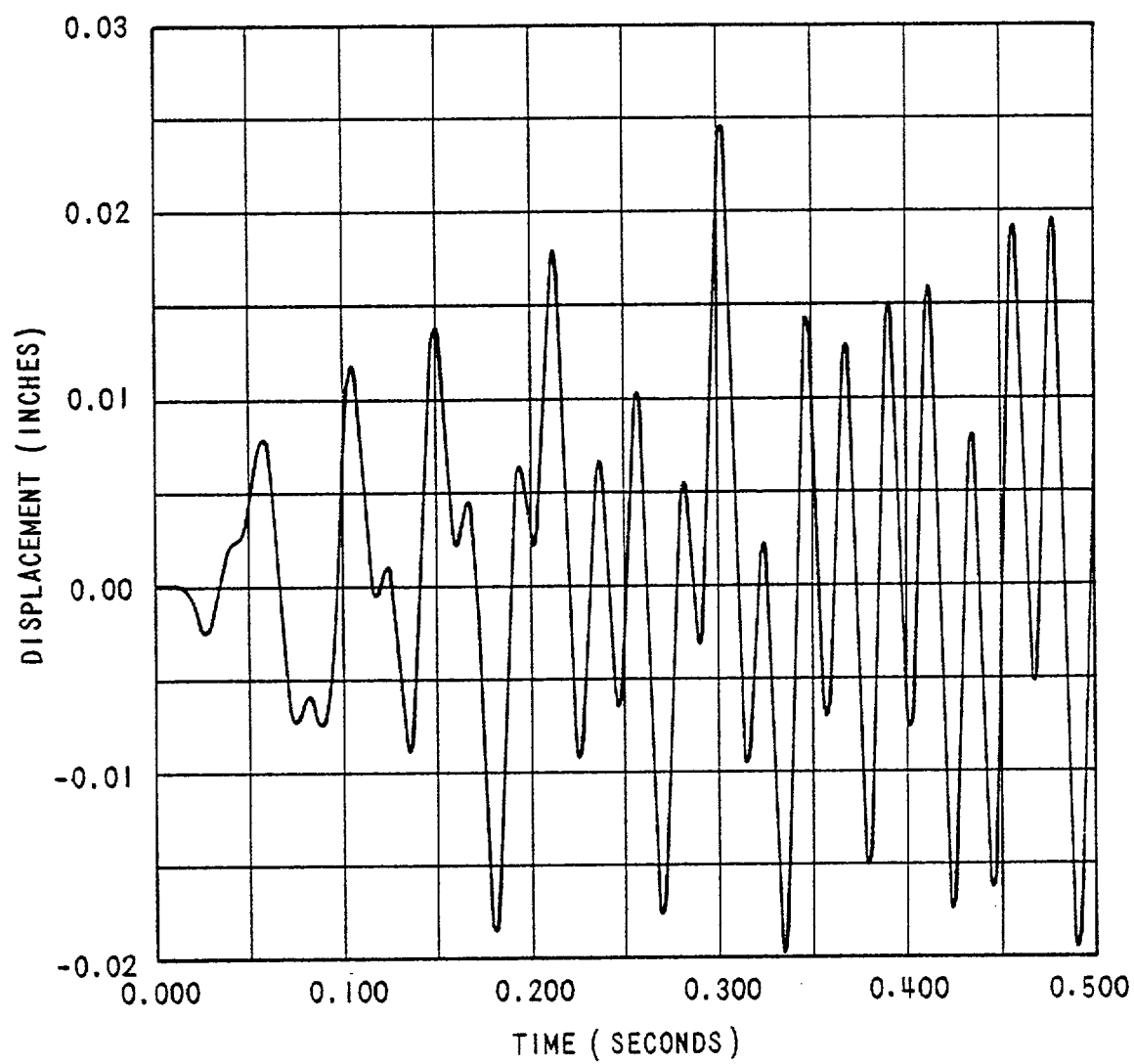


Figure 3.1-35 Out-of-Plane Displacements of Node Location 9 Due to LOCA Displacement History on Steam Generator

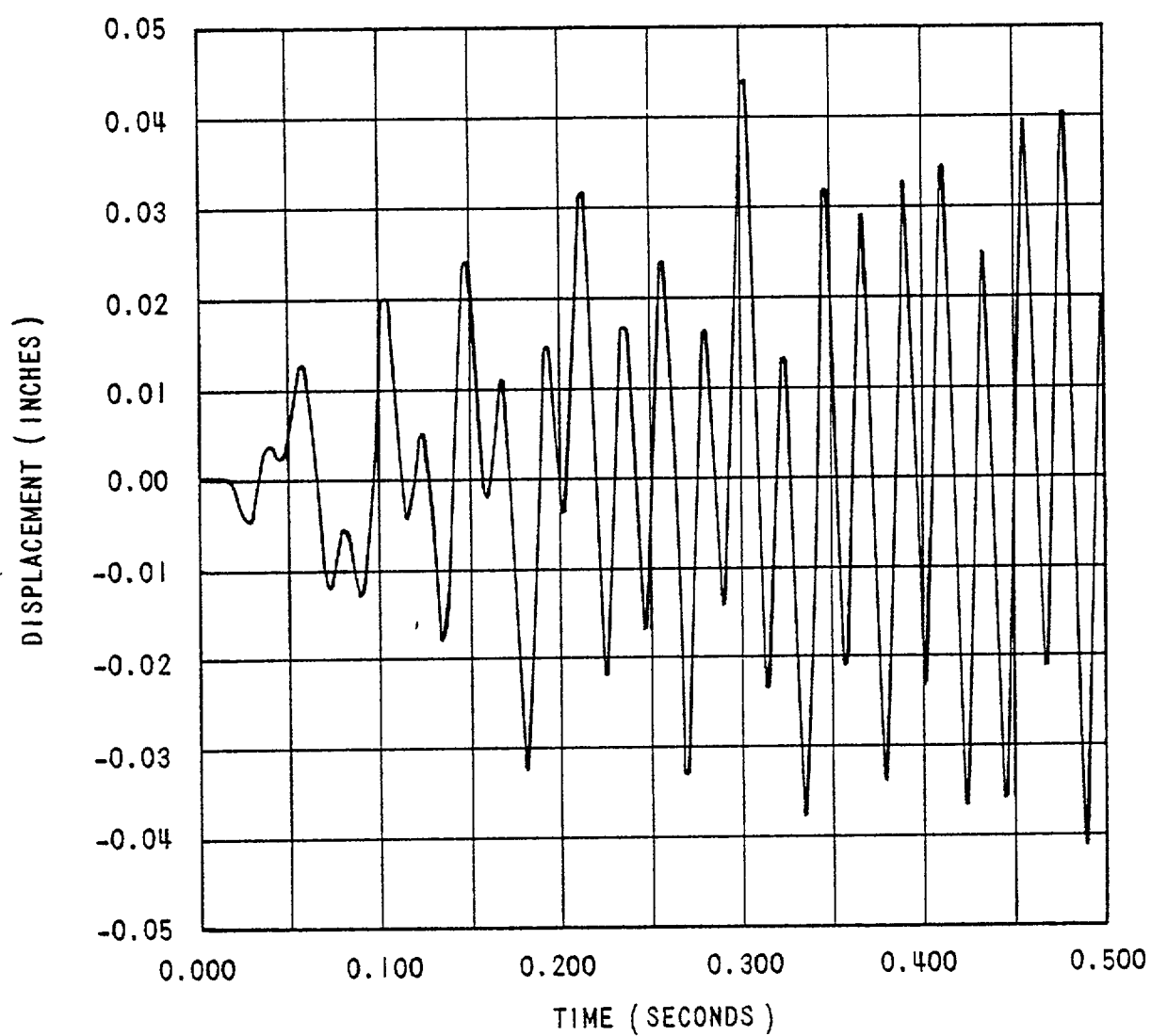


Figure 3.1-36 Out-of-Plane Displacements of Node Location 10 Due to LOCA Displacement History on Steam Generator

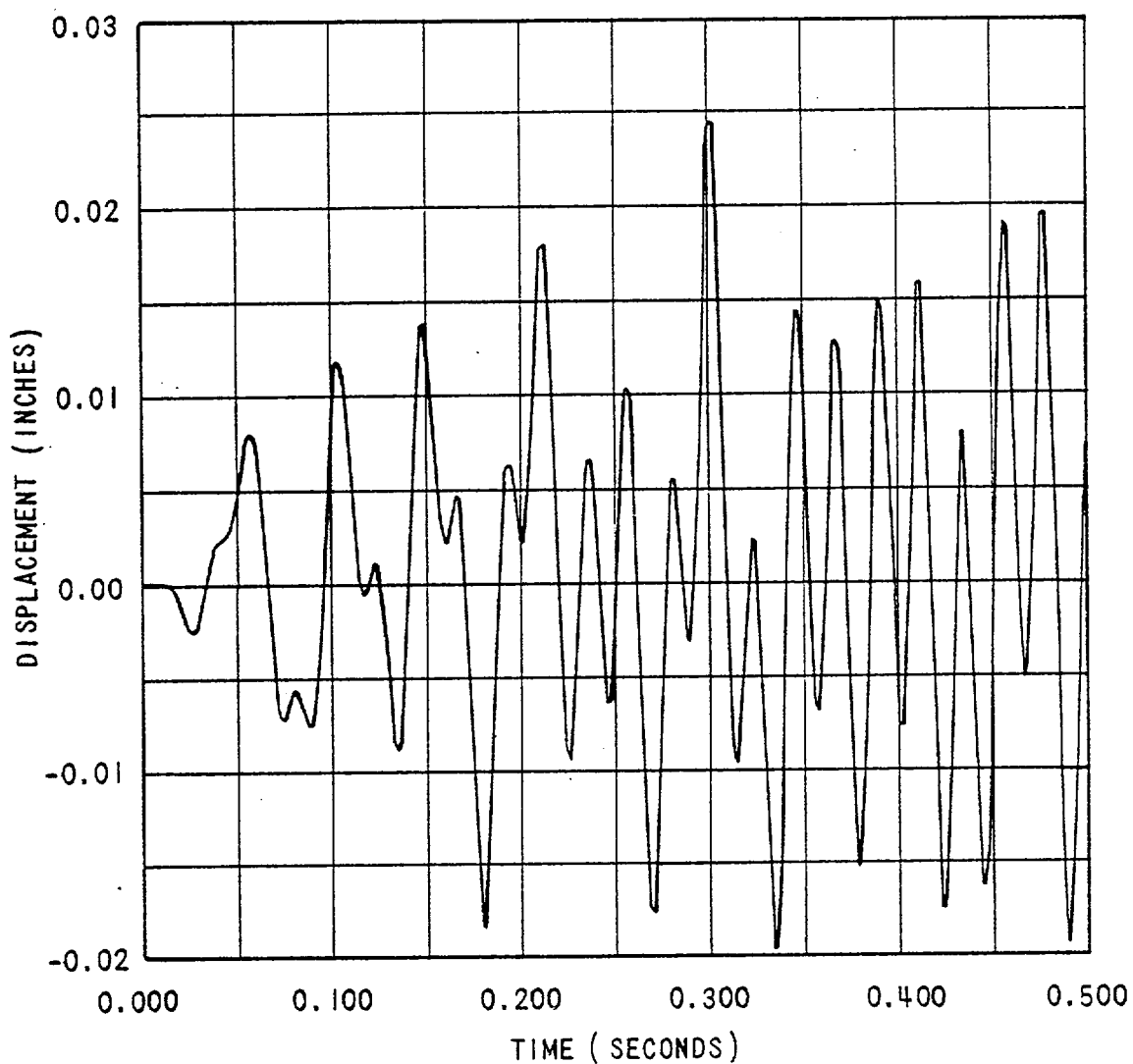


Figure 3.1-37 Out-of-Plane Displacements of Node Location 11 Due to LOCA Displacement History on Steam Generator

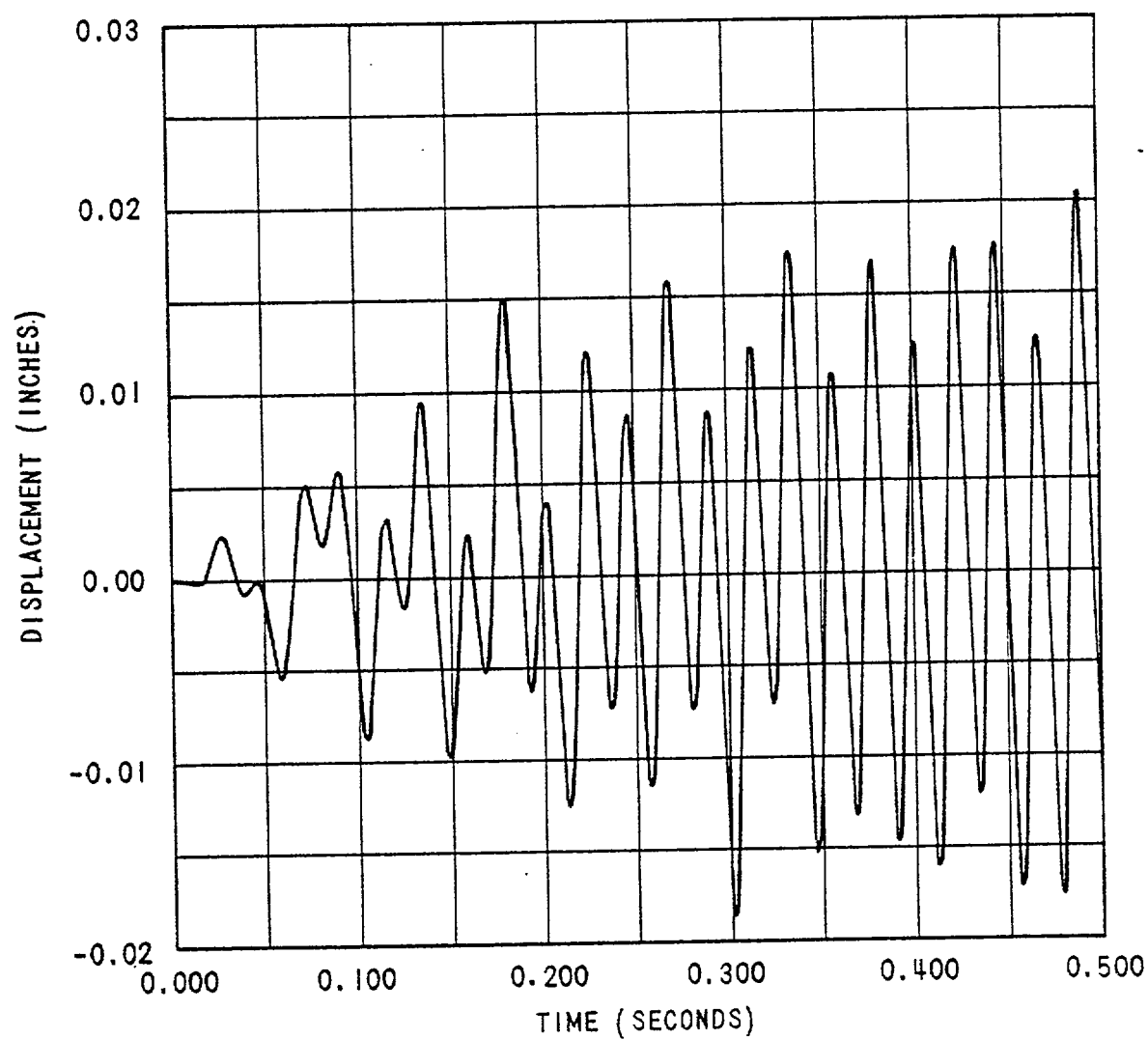


Figure 3.1-38 Out-of-Plane Displacements of Node Location 13 Due to LOCA Displacement History on Steam Generator

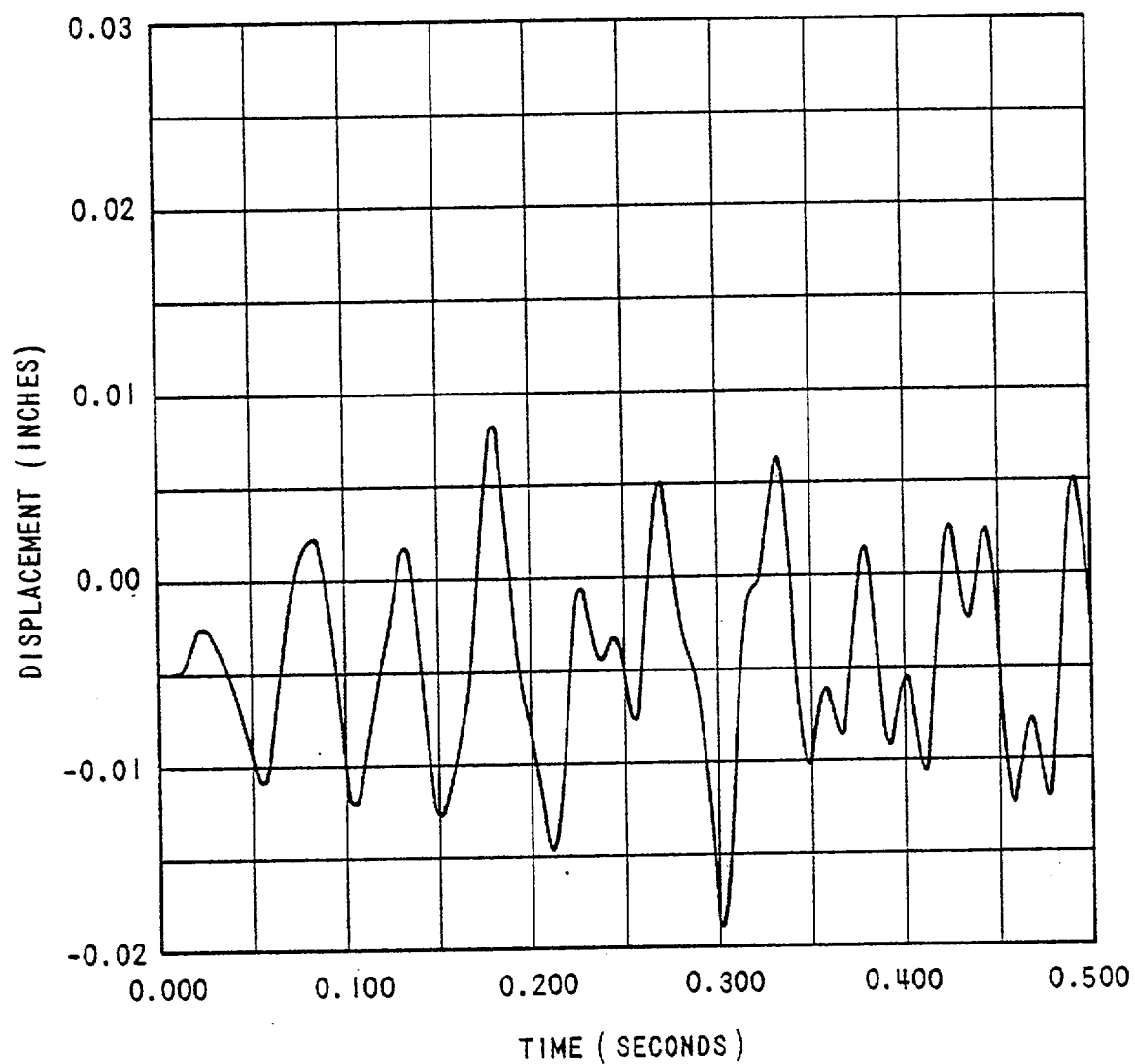


Figure 3.1-39 Out-of-Plane Displacements of Node Location 14 Due to LOCA Displacement History on Steam Generator

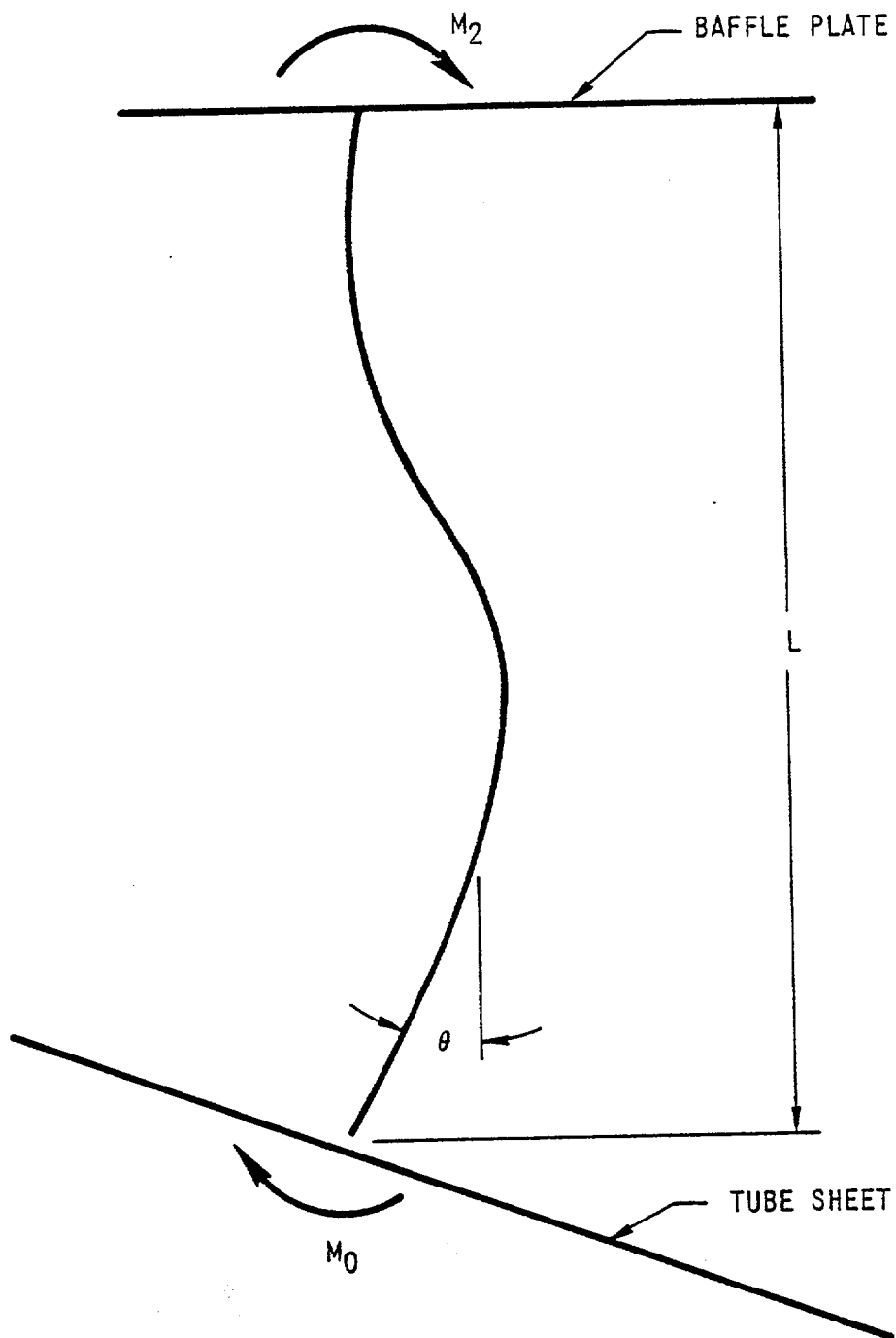


Figure 3.1-40 Tube Rotation in Vicinity of Tube Sheet

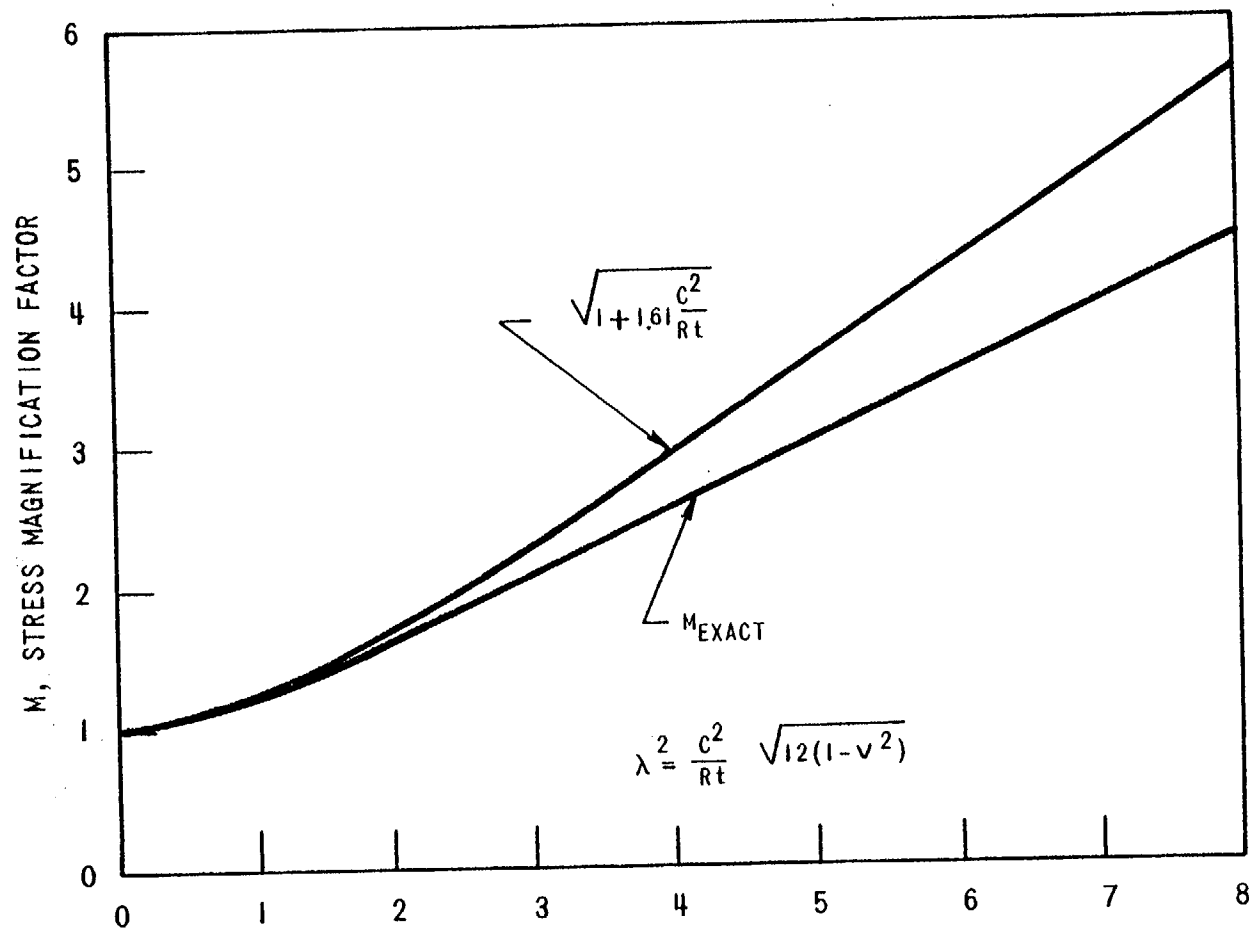


Figure 3.1-41 Relationship between λ and Stress Magnification Factor M

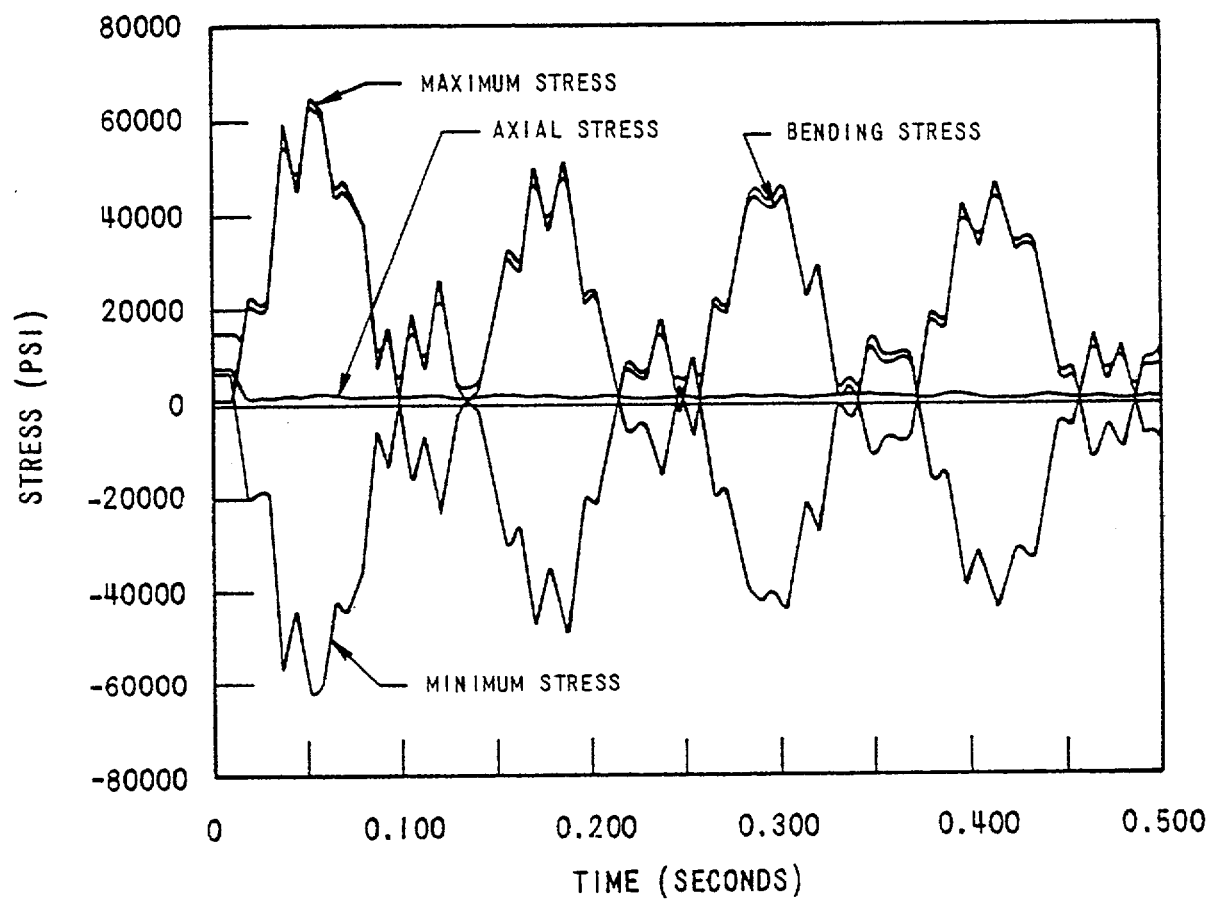


Figure 3.1-42 Stresses at Node Location 4 Due to LOCA Pressure History. Wall Thickness = .026"

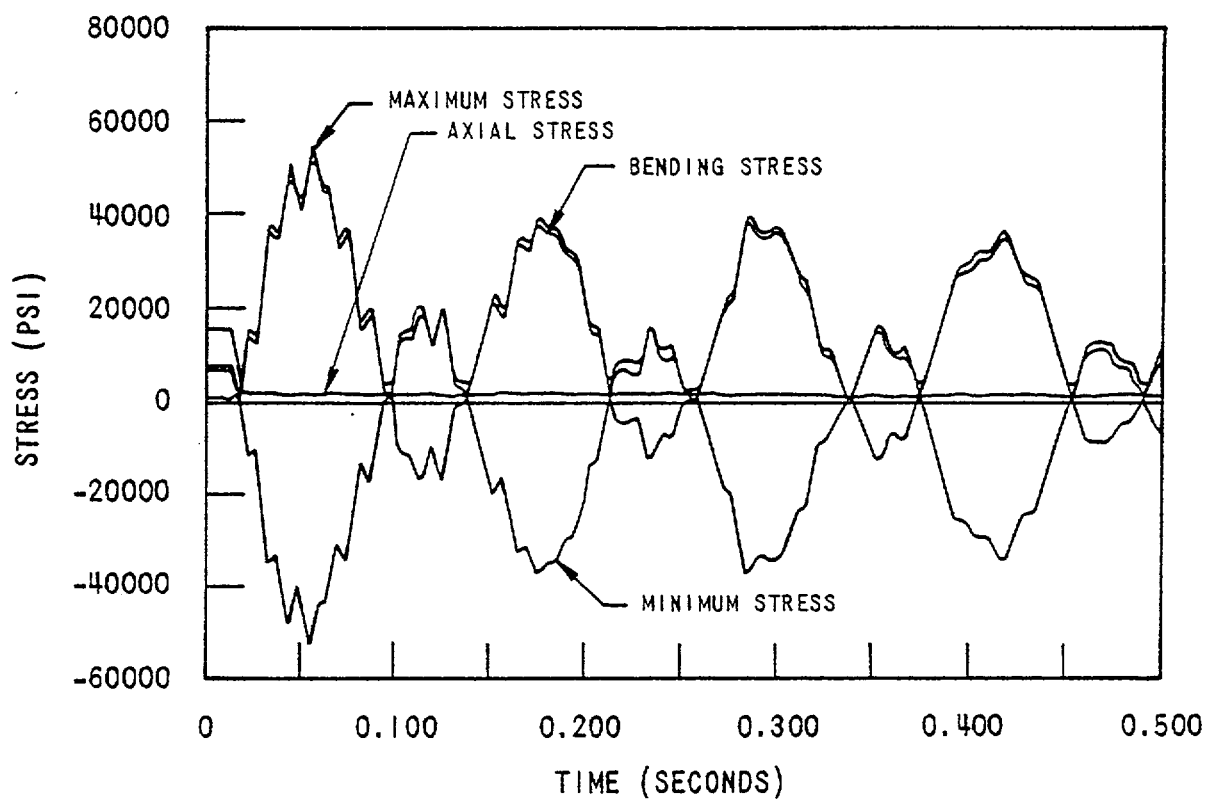


Figure 3.1-43 Stresses at Node Location 7 Due to LOCA Pressure History. Wall Thickness = .026"

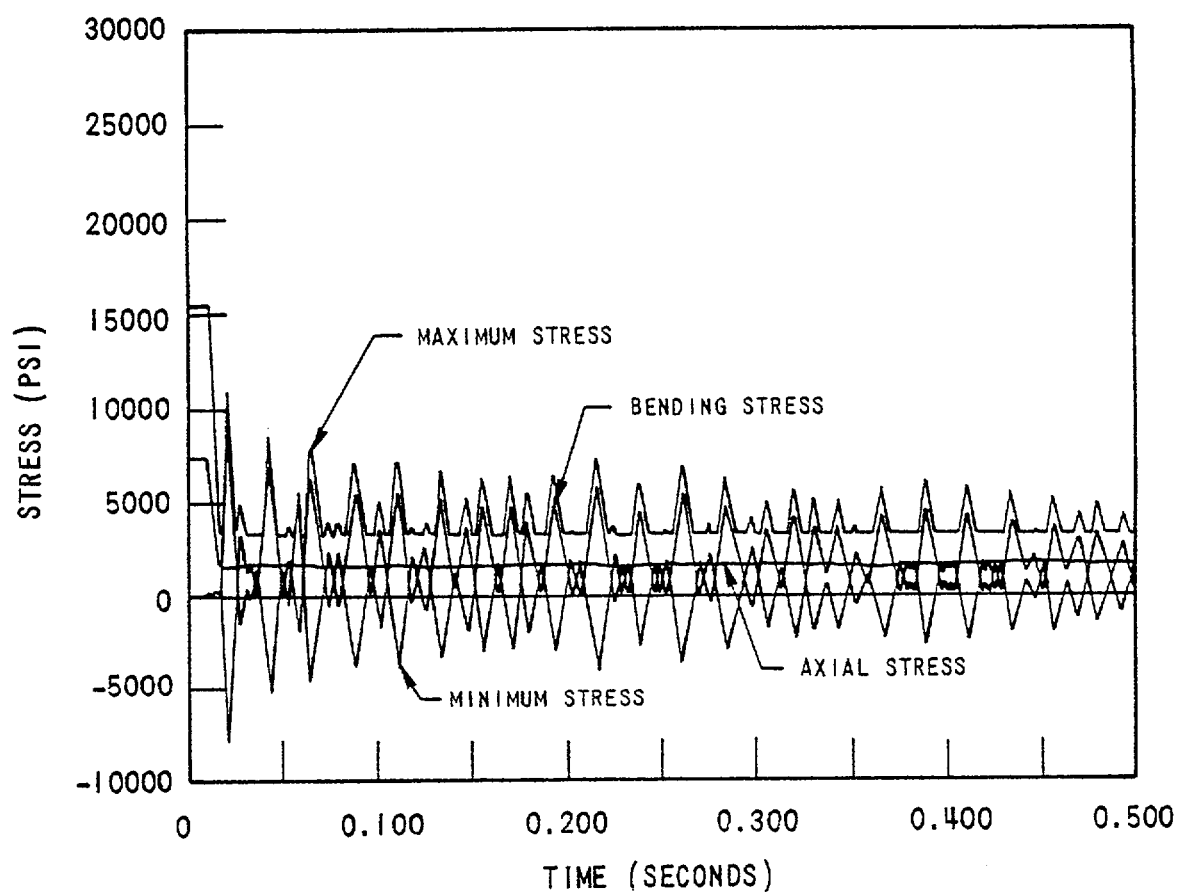


Figure 3.1-44 Stresses at Node Location 10 due to LOCA Pressure History. Wall Thickness = .026"

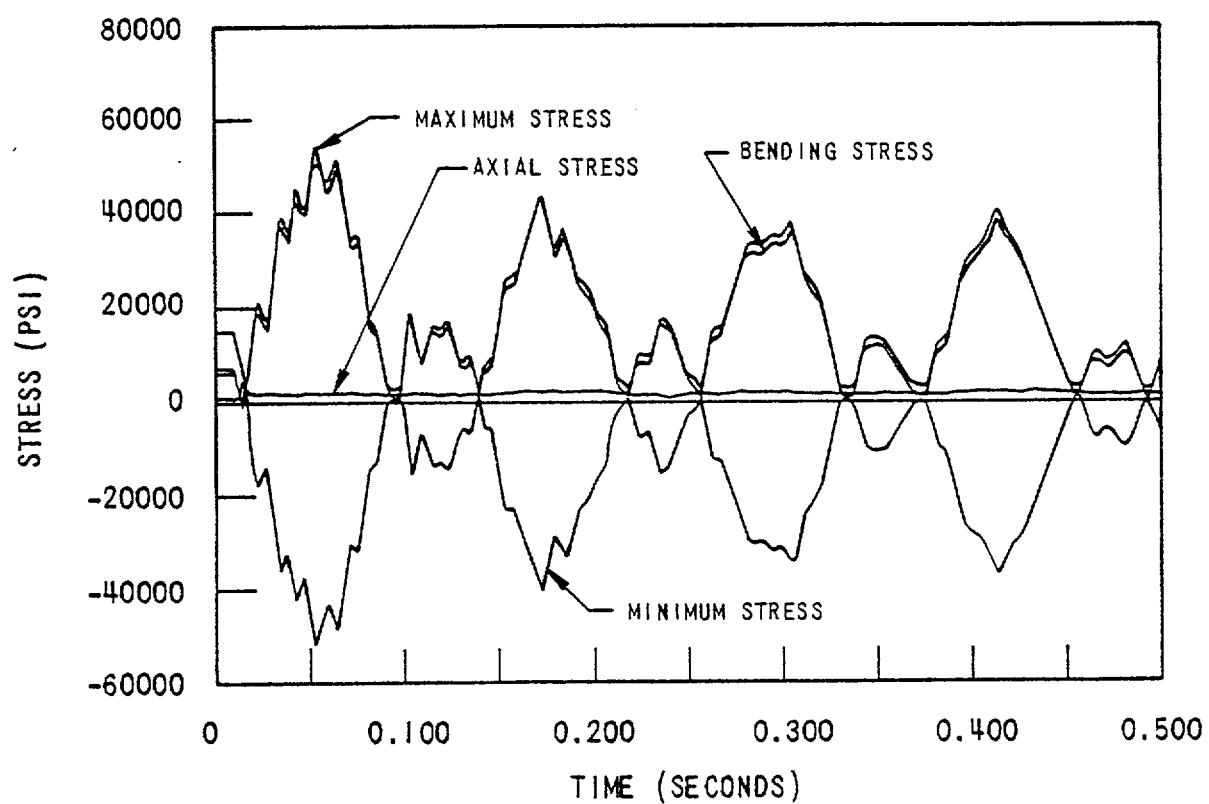


Figure 3.1-45 Stresses at Node Location 13 Due to LOCA Pressure History. Wall Thickness = .026"

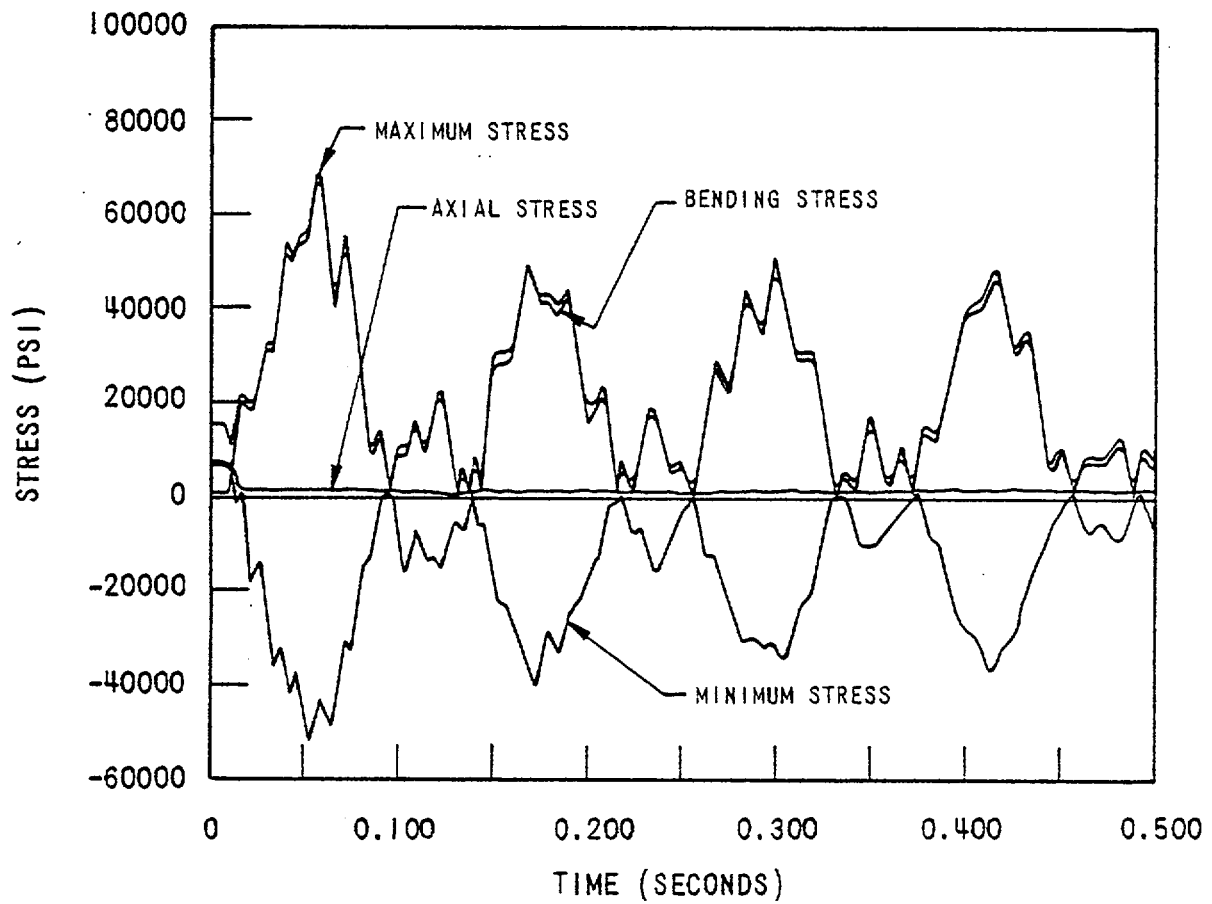


Figure 3.1-46 Stresses at Node Location 16 Due to LOCA Pressure History. Wall Thickness = .026"

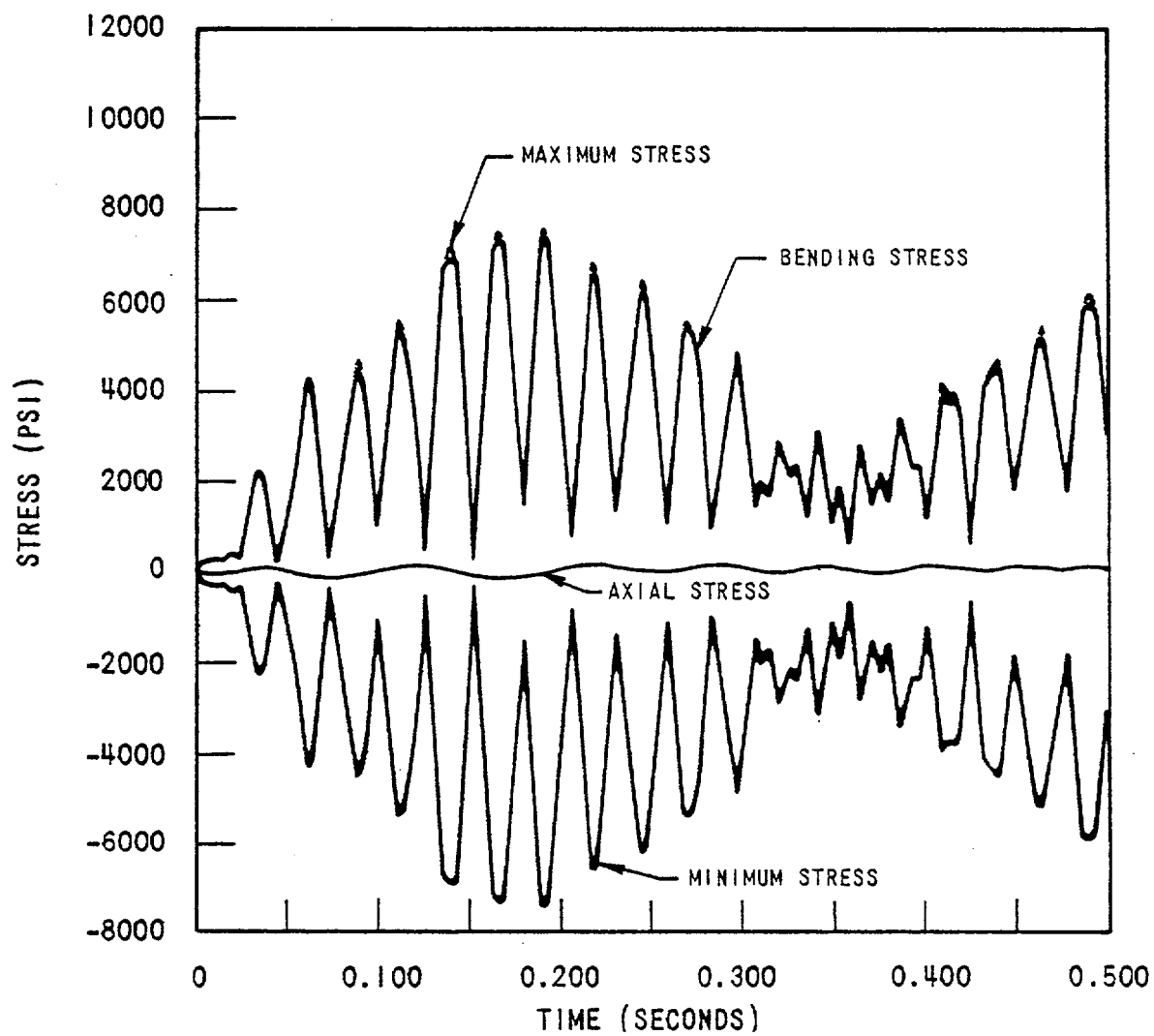


Figure 3.1-47 Stresses at Node Location 4 Due to LOCA Displacement History on Steam Generator. Wall Thickness = .026"

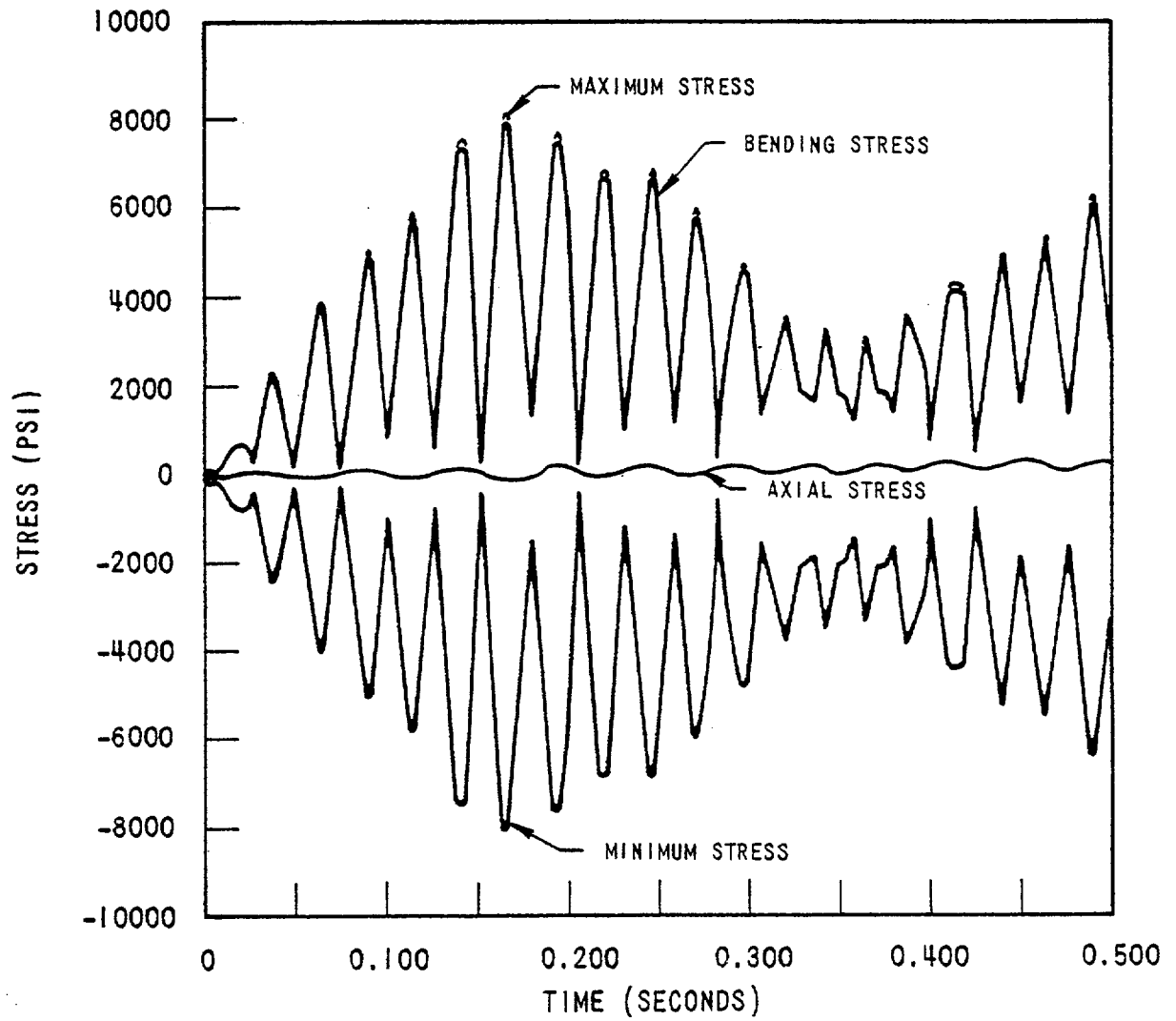


Figure 3.1-48 Stresses at Node Location 7 Due to LOCA Displacement History on Steam Generator. Wall Thickness = .026"

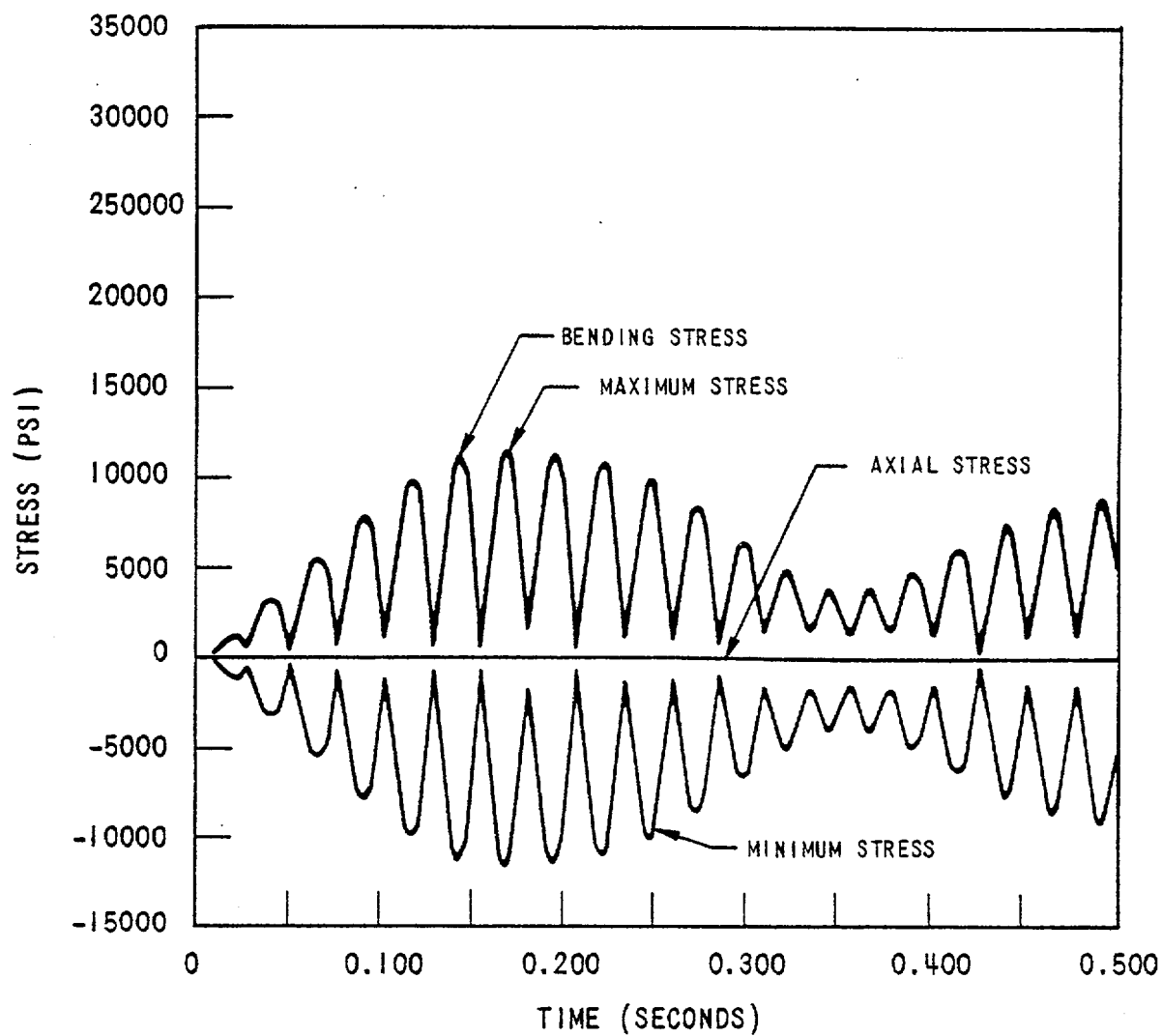


Figure 3.1-49 Stresses at Node Location 10 due to LOCA Displacement History on Steam Generator. Wall Thickness = .026"

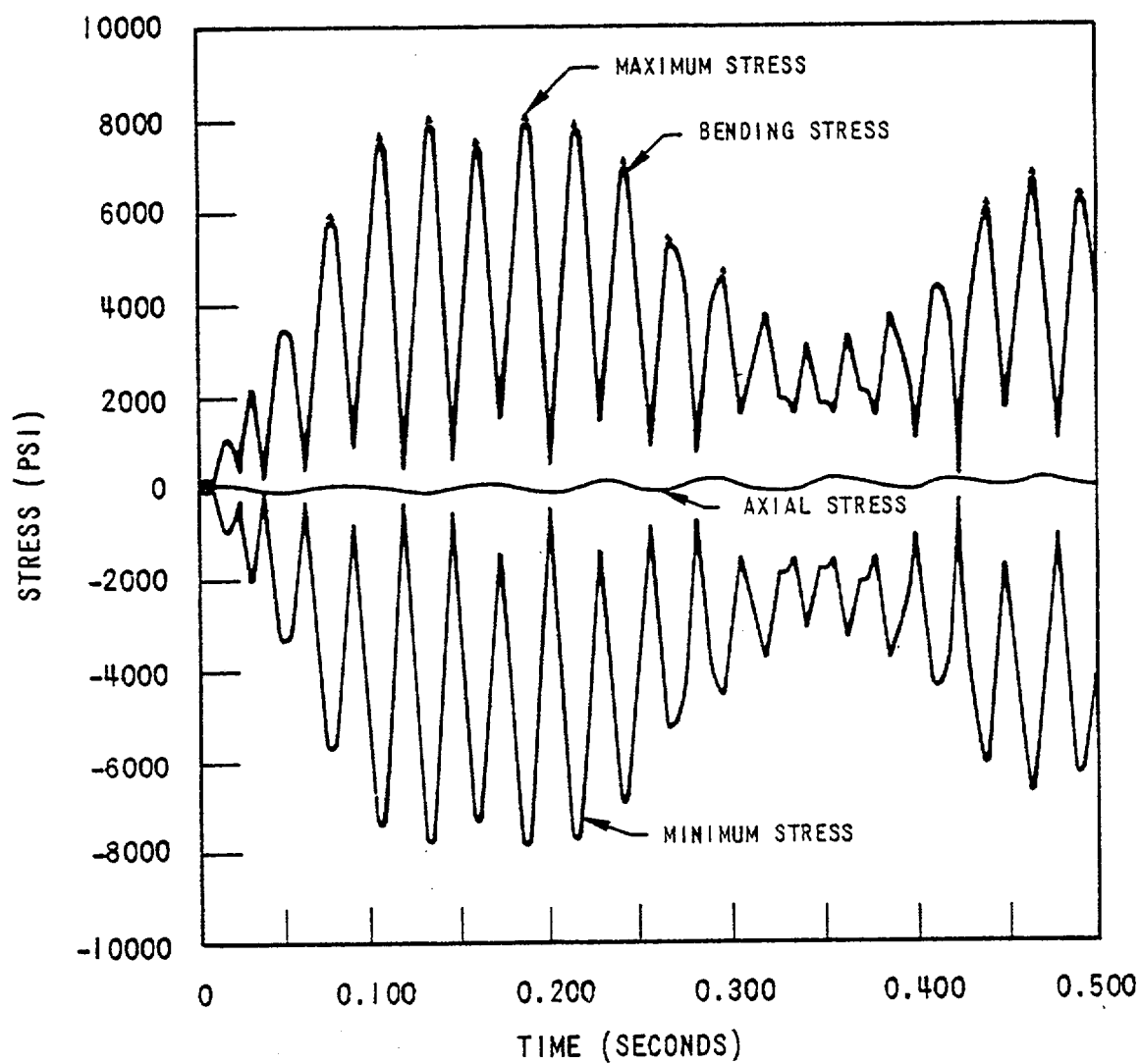


Figure 3.1-50

Stresses at Node Location 13 Due to LOCA
Displacement History on Steam Generator.
Wall Thickness = .026"

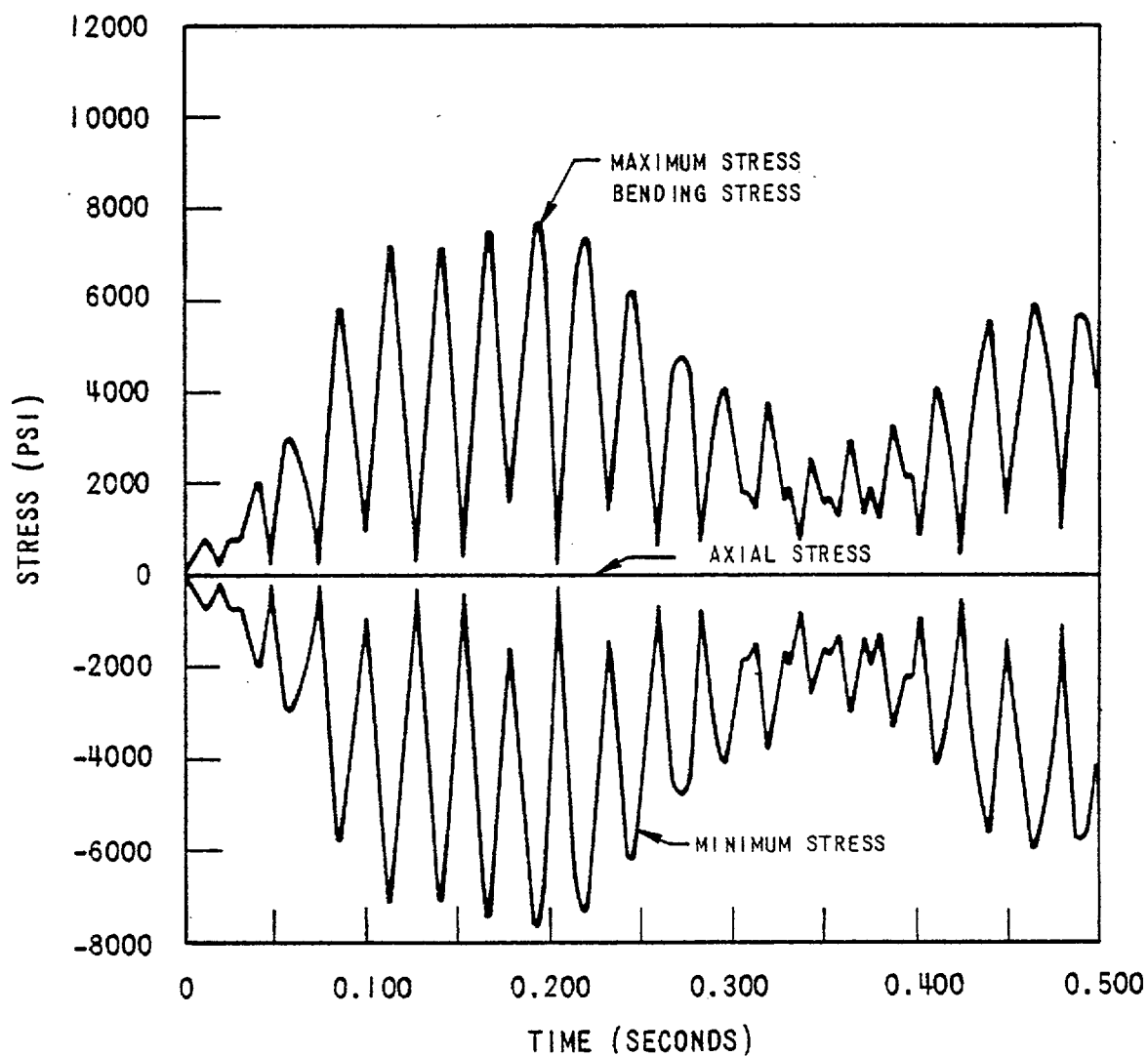


Figure 3.1-51 Stresses at Node Location 16 due to LOCA Displacement History on Steam Generator. Wall Thickness = .026"

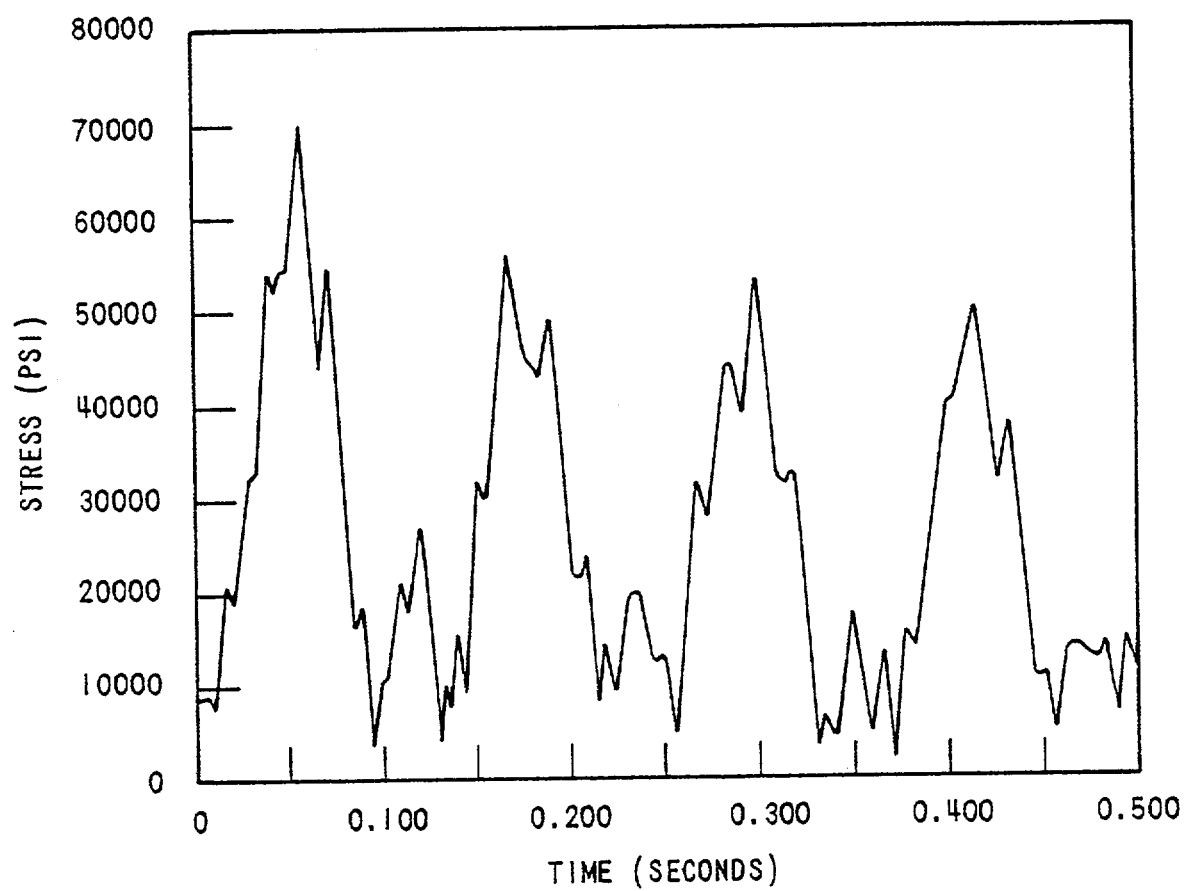


Figure 3.1-52 Maximum Stress Intensity on Tube Outer Wall at Node Location 16. Total LOCA Effects Vs. Time. Wall Thickness = .026"